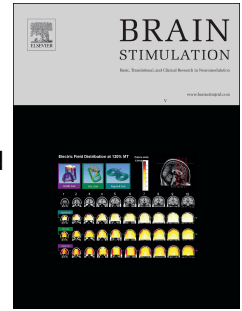


# Journal Pre-proof



TMS combined with EEG: Recommendations and open issues for data collection and analysis

Julio C. Hernandez-Pavon, Domenica Veniero, Til Ole Bergmann, Paolo Belardinelli, Marta Bortoletto, Silvia Casarotto, Elias P. Casula, Faranak Farzan, Matteo Fecchio, Petro Julkunen, Elisa Kallioniemi, Pantelis Lioumis, Johanna Metsomaa, Carlo Miniussi, Tuomas P. Mutanen, Lorenzo Rocchi, Nigel C. Rogasch, Mouhsin M. Shafi, Hartwig R. Siebner, Gregor Thut, Christoph Zrenner, Ulf Ziemann, Risto J. Ilmoniemi

PII: S1935-861X(23)01696-0

DOI: <https://doi.org/10.1016/j.brs.2023.02.009>

Reference: BRS 2333

To appear in: *Brain Stimulation*

Received Date: 20 July 2022

Revised Date: 10 February 2023

Accepted Date: 19 February 2023

Please cite this article as: Hernandez-Pavon JC, Veniero D, Bergmann TO, Belardinelli P, Bortoletto M, Casarotto S, Casula EP, Farzan F, Fecchio M, Julkunen P, Kallioniemi E, Lioumis P, Metsomaa J, Miniussi C, Mutanen TP, Rocchi L, Rogasch NC, Shafi MM, Siebner HR, Thut G, Zrenner C, Ziemann U, Ilmoniemi RJ, TMS combined with EEG: Recommendations and open issues for data collection and analysis, *Brain Stimulation* (2023), doi: <https://doi.org/10.1016/j.brs.2023.02.009>.

This is a PDF file of an article that has undergone enhancements after acceptance, such as the addition of a cover page and metadata, and formatting for readability, but it is not yet the definitive version of record. This version will undergo additional copyediting, typesetting and review before it is published in its final form, but we are providing this version to give early visibility of the article. Please note that, during the production process, errors may be discovered which could affect the content, and all legal disclaimers that apply to the journal pertain.

© 2023 Published by Elsevier Inc.

# TMS Combined with EEG: Recommendations and Open Issues for Data Collection and Analysis

Julio C. Hernandez-Pavon<sup>1,2,3\*</sup>, Domenica Veniero<sup>4\*</sup>, Til Ole Bergmann<sup>5,6</sup>, Paolo Belardinelli<sup>7,8</sup>, Marta Bortoletto<sup>9</sup>, Silvia Casarotto<sup>10,11</sup>, Elias P. Casula<sup>12</sup>, Faranak Farzan<sup>13</sup>, Matteo Fecchio<sup>14</sup>, Petro Julkunen<sup>15</sup>, Elisa Kallioniemi<sup>16</sup>, Pantelis Lioumis<sup>17,18</sup>, Johanna Metsomaa<sup>17,18</sup>, Carlo Miniussi<sup>7</sup>, Tuomas P. Mutanen<sup>17,18</sup>, Lorenzo Rocchi<sup>19,20</sup>, Nigel C. Rogasch<sup>21,22,23</sup>, Mouhsin M. Shafi<sup>24</sup>, Hartwig R. Siebner<sup>25,26,27</sup>, Gregor Thut<sup>28</sup>, Christoph Zrenner<sup>8,29,30,31</sup>, Ulf Ziemann<sup>8,30</sup>, Risto J. Ilmoniemi<sup>17,18</sup>

1. Legs + Walking Lab, Shirley Ryan AbilityLab, Chicago, IL, USA
2. Department of Physical Medicine and Rehabilitation, Feinberg School of Medicine, Northwestern University, Chicago, IL, USA
3. Center for Brain Stimulation, Shirley Ryan AbilityLab, Chicago, IL, USA.
4. School of Psychology, University of Nottingham
5. Neuroimaging Center (NIC), Focus Program Translational Neuroscience (FTN), Johannes Gutenberg University Medical Center
6. Leibniz Institute for Resilience Research (LIR), Mainz, Germany
7. Center for Mind/Brain Sciences - CIMEC, University of Trento, Rovereto, TN, Italy.
8. Department of Neurology & Stroke, University of Tübingen, Tübingen, Germany.
9. Neurophysiology Lab, IRCCS Istituto Centro San Giovanni di Dio Fatebenefratelli, Brescia, Italy.
10. Department of Biomedical and Clinical Sciences, University of Milan, Milan, Italy.
11. IRCCS Fondazione Don Carlo Gnocchi ONLUS, Milan, Italy.
12. Department of Systems Medicine, University of Tor Vergata, Rome, Italy.
13. Simon Fraser University, School of Mechatronic Systems Engineering, Surrey, British Columbia, Canada
14. Center for Neurotechnology and Neurorecovery, Department of Neurology, Massachusetts General Hospital, Boston, MA, USA.
15. Department of Technical Physics, University of Eastern Finland / Department of Clinical Neurophysiology, Kuopio University Hospital, Finland.
16. Department of Biomedical Engineering, New Jersey Institute of Technology, Newark, NJ, USA.
17. Department of Neuroscience and Biomedical Engineering, Aalto University, Espoo, Finland.
18. BioMag Laboratory, HUS Medical Imaging Center, Helsinki University Hospital, Helsinki University and Aalto University School of Science, Helsinki, Finland
19. Department of Clinical and Movement Neurosciences, UCL Queen Square Institute of Neurology, University College London, London, United Kingdom.
20. Department of Medical Sciences and Public Health, University of Cagliari, Cagliari, Italy.
21. University of Adelaide, Adelaide, Australia
22. South Australian Health and Medical Research Institute, Adelaide, Australia
23. Monash University, Melbourne Australia.
24. Berenson-Allen Center for Noninvasive Brain Stimulation, Department of Neurology, Beth Israel Deaconess Medical Center / Harvard Medical School, Boston, MA, USA.
25. Danish Research Centre for Magnetic Resonance, Centre for Functional and Diagnostic Imaging and Research, Copenhagen University Hospital - Amager and Hvidovre, Copenhagen, Denmark.
26. Department of Neurology, Copenhagen University Hospital Bispebjerg and Frederiksberg, Copenhagen, Denmark.
27. Department of Clinical Medicine, Faculty of Health and Medical Sciences, University of Copenhagen, Copenhagen, Denmark.
28. University of Glasgow, United Kingdom.

29. Temerty Centre for Therapeutic Brain Intervention, Centre for Addiction and Mental Health, Toronto, Canada.
30. Hertie Institute for Clinical Brain Research, University of Tübingen, Tübingen, Germany.
31. Department of Psychiatry, University of Toronto, Toronto, Canada.

\* These authors have equally contributed to this work.

†Corresponding author:

Julio C. Hernandez-Pavon (jpavon@sralab.org; julio.hpavon@gmail.com)

Legs + Walking Lab, Shirley Ryan AbilityLab (Formerly, The Rehabilitation Institute of Chicago), 355 E  
Erie St, 60611, Chicago, IL, USA

## 1 **Abstract**

2 Transcranial magnetic stimulation (TMS) evokes neuronal activity in the targeted cortex and  
3 connected brain regions. The evoked brain response can be measured with  
4 electroencephalography (EEG). TMS combined with simultaneous EEG (TMS–EEG) is widely  
5 used for studying cortical reactivity and connectivity at high spatiotemporal resolution.  
6 Methodologically, the combination of TMS with EEG is challenging, and there are many open  
7 questions in the field. Different TMS–EEG equipment and approaches for data collection and  
8 analysis are used. The lack of standardization may affect reproducibility and limit the  
9 comparability of results produced in different research laboratories. In addition, there is  
10 controversy about the extent to which auditory and somatosensory inputs contribute to  
11 transcranially evoked EEG. This review provides a guide for researchers who wish to use  
12 TMS–EEG to study the reactivity of the human cortex. A worldwide panel of experts working on  
13 TMS–EEG covered all aspects that should be considered in TMS–EEG experiments, providing  
14 methodological recommendations (when possible) for effective TMS–EEG recordings and  
15 analysis. The panel identified and discussed the challenges of the technique, particularly  
16 regarding recording procedures, artifact correction, analysis, and interpretation of the transcranial  
17 evoked potentials (TEPs). Therefore, this work offers an extensive overview of TMS–EEG  
18 methodology and thus may promote standardization of experimental and computational  
19 procedures across groups.

20

21 **Keywords:** Transcranial magnetic stimulation; Electroencephalography; Recommendations;  
22 TMS–EEG preparation; TMS–EEG data analysis pipelines; TMS–EEG; TEPs; Artifacts.

23

24

## 25 **1. Introduction**

26 Transcranial magnetic stimulation (TMS) has proven to be an effective, non-invasive tool for  
27 probing the human brain [1]. The first effort to combine TMS with electroencephalography  
28 (TMS–EEG) was reported in 1989 by Cracco and colleagues [2] and later by Amassian and  
29 colleagues [3]. However, the technique was not yet ready for broader use as the recorded cortical  
30 response was obscured by the TMS-induced electromagnetic artifact. A few years had to pass  
31 before the electromagnetic artifact problem was partially solved. In 1996, the first successful  
32 TMS–EEG study (published by Ilmoniemi et al. [4]) demonstrated the feasibility of the  
33 combination to record cortical excitability and connectivity. After these first successful  
34 recordings, the interest in using EEG to measure brain activation elicited by TMS has steadily  
35 increased. Consequently, this has opened new possibilities in basic and clinical research as noted  
36 in a recent review [5].

37

38 More than two decades after the first successful TMS–EEG combination [4], multiple  
39 approaches to recording and analyzing the TMS–EEG data have been developed, and there is  
40 still no consensus on how to standardize the procedures for TMS–EEG preparation, data  
41 acquisition, and analysis. This article aims to review the state of the art in the field and provide,  
42 when possible, recommendations for successful TMS–EEG studies to eventually improve the  
43 reproducibility of experimental and analysis procedures across laboratories. We aim to share our  
44 expertise with the community, based on published data and personal experience. We have  
45 gathered several leading TMS–EEG experts, hoping to promote clarification of concepts,  
46 improvement of our practices, guidance for newcomers, and identification and addressing of  
47 open questions in the field.

48

### 49 **1.1. Electrophysiological aspects of TMS–EEG**

#### 50 ***TMS***

51 TMS excites axons in the brain via inductive electromagnetic stimulation. A strong, very brief,  
52 magnetic field is delivered to the brain via a transducing coil. The changing magnetic field  
53 induces a time-varying electric field (E-field) in the cortex. Depending on the orientation of the  
54 E-field with respect to the geometry of the cortex and cortical neurons, the E-field leads to a  
55 depolarization of axons in the stimulated brain area. Depending on the level of depolarization,

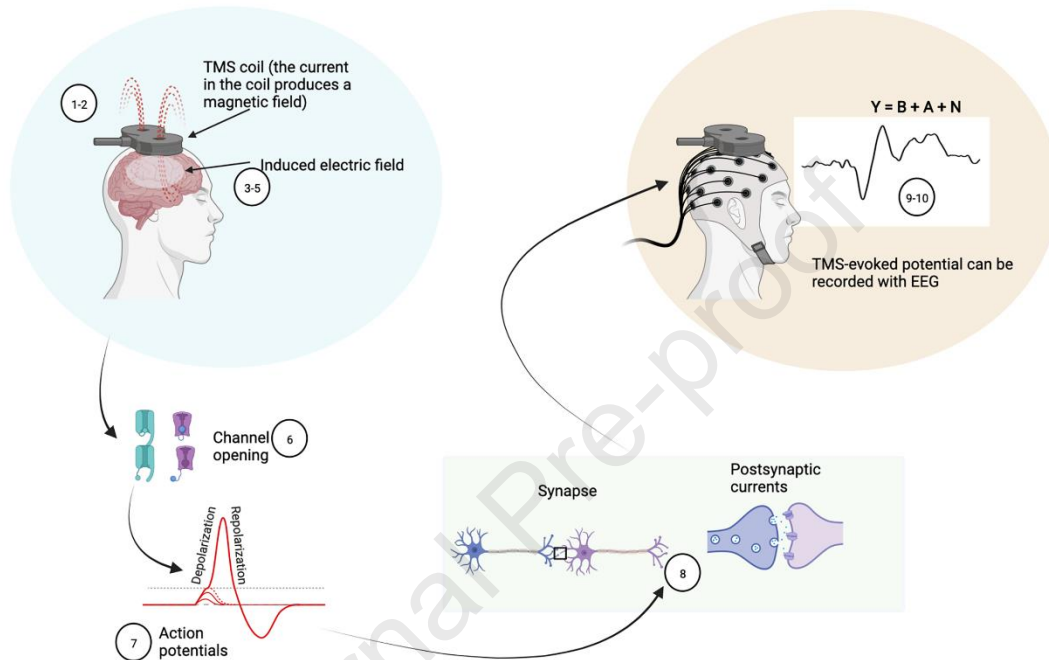
56 action potentials may be triggered [6, 7] which travel orthodromically (towards the axon  
57 terminal) and antidromically (towards the cell body) along the axons [8]. Trans-synaptic  
58 activation of neurons on which the excited axons impinge will induce postsynaptic currents in  
59 the dendritic arbor of cortical pyramidal neurons at the target site. Postsynaptic potentials are  
60 subject to summation spatially and/or temporally. If the summation is large enough and involves  
61 a sufficiently large area of the cortex, the postsynaptic currents will result in a measurable EEG  
62 signal. At the same time, the spread of activation along pyramidal neurons causes a secondary  
63 excitation or inhibition of connected subcortical structures and cortical brain regions. The  
64 temporospatial summation of postsynaptic currents in the dendritic arbor of pyramidal or other  
65 cells in connected cortical areas may also cause a measurable EEG signal, contributing to the  
66 transcranially evoked EEG response.

67

68 TMS is based on electromagnetic induction, described by Faraday's law. A TMS pulse is  
69 initiated by flowing an intense current ( $\sim 5\text{kA}$ ) through the TMS coil windings. This current  
70 produces a time-varying magnetic field that penetrates the scalp and skull unimpeded, inducing  
71 an E-field. The brain is a conductor; therefore, eddy currents (i.e., currents that circulate in  
72 closed loops and in opposite directions than the currents in the TMS coil) are induced in the  
73 brain that can depolarize neurons, producing neuronal firing. TMS is thought to activate cortical  
74 neurons that have axonal bends or other geometrical inhomogeneities or endings in the induced  
75 E-field, as the E-field along neurites changes most rapidly at these locations [9, 10]. The strength  
76 of the magnetic pulse is in the order of 2–3 T, with a rise time of about 50–100  $\mu\text{s}$ . Because of  
77 the short pulse duration, the temporal resolution of TMS is sub-milliseconds, which allows for  
78 real-time modulation of the brain. The spatial extent of the cortical area stimulated by TMS  
79 depends on the coil geometry, stimulus intensity, target area, and, therefore, coil-to-cortex  
80 distance [11-13]. As magnetic fields attenuate rapidly with distance and as the induced E-field  
81 approaches zero at the center of the head, TMS stimulates superficial cortical layers more  
82 strongly than deeper layers. However, the induced neuronal activity depends also on other  
83 aspects (like the position and orientation of neuronal structures and membrane characteristics). In  
84 summary, besides stimulating the target area and surrounding tissues, TMS indirectly activates  
85 synaptically interconnected sites, a feature exploited in brain connectivity studies [4]. When the  
86 stimulation intensity (SI) is adequate, locally evoked action potentials may propagate along

87 anatomical connections across cortical layers within the same cortical column and to other  
 88 cortical and subcortical regions (e.g., [14]), and may result in the activation of an entire network  
 89 [15]. The cascade of events that accompanies TMS (Ilmoniemi et al., 1999a) is described in **Fig.**  
 90 **1.**

91



92

93

94

95 **Fig. 1. Chain of events triggered by the TMS pulse.** (1-2) A current pulse flows through the TMS coil (max  $I \sim 5$   
 96 kA) and produces a brief ( $\sim 100 \mu\text{s}$ ) but strong magnetic field (max  $B \sim 1-3 \text{ T}$ ). (3) The changing magnetic field  
 97 induces an E-field ( $\sim 50-100 \text{ V/m}$ ) in the brain which in turn (4) produces a flow of electric current in the tissue ( $\sim$   
 98  $0.1 \text{ mA/mm}^2$ ). (5) The flow of current (i.e., ions) produces local membrane depolarization ( $> \sim 10 \text{ mV}$ ). (6) Voltage-  
 99 gated ion channels are opened and (7) action potentials are generated in axons where depolarization reaches the  
 100 firing threshold. (8) Neurotransmitters are released in the synaptic cleft. (9) Postsynaptic currents are generated,  
 101 which lead to postsynaptic excitatory (and inhibitory) potentials that in turn lead to action potential generation if the  
 102 firing threshold is exceeded. This transsynaptic activation represents the activation of networks. The potential  
 103 differences (E-fields), resulting from postsynaptic currents, drive volume currents inside the head and the scalp [16].  
 104 (10) The TMS-induced activation can be recorded with EEG. Note that the EEG signal can be described with a  
 105 linear model,  $Y=B+A+N$  (see Section 6.1). Figure created with BioRender.com.

106

107

108

109 The brain activity evoked by TMS can be recorded with different neuroimaging techniques such  
110 as EEG, functional magnetic resonance imaging (fMRI), near-infrared spectroscopy and positron  
111 emission tomography (for a review see [17-19]). However, the most successful and thus  
112 commonly used combination has been with EEG because it is a widespread method, is less  
113 expensive than other neuroimaging techniques, and is technically the least complicated to be  
114 combined online with TMS.

115

### 116 *EEG*

117 Despite developments in measurement technology, the basic principles of EEG remain  
118 unchanged from Berger's time [20]. EEG, with its millisecond temporal resolution and a spatial  
119 resolution of centimeters, is widely used for non-invasively studying the electrophysiological  
120 dynamics of the brain [21, 22]. EEG measures electrical potential differences between pairs of  
121 electrodes placed on the scalp. The recorded signal is a linear mixture of source-current  
122 amplitudes, and the signals in neighboring electrodes commonly correlate [23]. The EEG signal  
123 is primarily due to the synchrony of postsynaptic potentials rather than action potentials [24].  
124 Action potentials have a short duration compared to postsynaptic potentials; for this reason,  
125 action potentials do not overlap as much in time and synchronize much less than postsynaptic  
126 potentials. Furthermore, due to their symmetric current distribution, the E-field generated by  
127 action potentials decays faster with distance than that of postsynaptic currents [16, 22, 23, 25,  
128 26]. Postsynaptic potentials are primarily confined to the dendrites and cell bodies. When a  
129 sufficient number of neurons – several thousand or more – with similar overall orientation  
130 produce synchronous postsynaptic currents, the resulting E-field and volume currents summate,  
131 making it possible to record the cortical EEG response at the scalp level.

132

### 133 *TMS-EEG*

134 The combination of TMS with EEG has been relevant for addressing fundamental neuroscientific  
135 questions in new ways. In particular, the two techniques complement each other, in that causal  
136 information provided by TMS overcomes the correlational nature of EEG data, whereas the  
137 ability to record from the whole scalp provides a global picture of the brain activity generated by  
138 the E-field. One of the main advantages of using TMS-EEG is that outcome measures, derived  
139 from EEG responses to TMS (i.e., evoked potentials or brain oscillations) can be used as a



140 neurophysiological marker of excitability or connectivity for any brain area, including the  
141 regions where TMS does not generate a proxy of cortical/cortico-spinal excitability, such as  
142 motor evoked potentials (MEPs) or phosphenes [4, 27]. Although TMS–EEG data can be  
143 analyzed in the time and frequency domains, so far, most studies have focused on the former, the  
144 so-called TMS-evoked potentials (TEPs).

145

#### 146 *TEPs and TMS-triggered oscillations*

147 TEPs are brain potentials time-locked to the TMS pulse [27, 28]. To study TEPs, the signal is  
148 averaged across trials. The initial TMS-evoked response is presumably produced by the  
149 activation of neurons concentrated in the targeted area followed by the activation of axonally  
150 interconnected areas [4, 29]. Different methods on how to measure the TEPs have been reviewed  
151 elsewhere [5, 30].

152

153 The TEPs consist of positive (P) and negative (N) deflections that reflect a spatio-temporal  
154 superposition of excitatory and inhibitory postsynaptic potentials, like the so-called event-related  
155 potentials (ERPs) [31]. Although the neurophysiological underpinnings of TEPs remain to be  
156 completely elucidated, they are considered a genuine, reproducible measure of cortical reactivity  
157 [32-34]. TMS of the primary motor cortex (M1) evokes several peaks, described at  
158 approximately 15 (N15), 30 (P30), 45 (N45), 60 (P60), 100 (N100), and 180 (P180) milliseconds  
159 [28, 32, 35, 36]. However, recently it has been shown that later peaks (>~ 80ms) such as N100  
160 and P180 may be contaminated by sensory-evoked responses (see **Sections 3.5, 4.2.3, and 4.2.4**),  
161 while very early peaks, such as the N15, can be contaminated by cranial muscle responses (see  
162 **Section 4.2.2**).

163

164 TEPs are detectable up to 400–500 ms around the stimulation area as well as in distant inter-  
165 connected brain areas [4, 32, 37]. Accordingly, for some TEP components, the maximal  
166 amplitude is recorded by the electrodes close to the stimulation site, while others may be more  
167 prominent over distant electrodes, e.g., over the contralateral hemisphere [38]. There is evidence  
168 that TEPs are associated to varying degrees with different neurotransmitters (e.g., [39]). TEP  
169 peaks and time courses depend on the stimulated area, coil orientation [37], and functional state  
170 of the underlying cortex; the latter may be dependent on factors such as behavior [40], level of

171 consciousness (e.g., [41, 42]), and neuropsychiatric diseases (e.g., [43]). In addition, TEP  
172 amplitudes are influenced by the applied TMS pulse strength (e.g., [44, 45]).

173

174 TMS effects on brain activity can be further investigated in the frequency domain. When a  
175 cortical area is perturbed by TMS, the neuronal response as measured by EEG tends to oscillate  
176 at a specific natural frequency [46-48]. Part of this response may be explained by the phase  
177 alignment of ongoing local brain oscillations through the effect of the TMS pulse on the targeted  
178 cortex [49]. Therefore, TMS-EEG can be used to manipulate and investigate brain rhythms by  
179 measuring the impact of a TMS pulse on EEG and associated behavioral effects [50]. The same  
180 methods used to study EEG oscillations can be used in TMS-triggered oscillations [51-53]. Since  
181 this topic is out of the scope of this paper and has been widely discussed elsewhere, we refer the  
182 reader to previous literature (e.g., [5, 53]). However, researchers should carefully distinguish  
183 between TMS-evoked responses (i.e., signals that are phase-locked and thus survive averaging of  
184 single trials) and TMS-induced responses (i.e., signals that are not phase-locked and thus cancel  
185 out during averaging; e.g., [54]). The latter requires the calculation of time-frequency  
186 representations (TFR) at the single-trial level with subsequent averaging to preserve the  
187 oscillatory activity that is related to but not phase-locked to the TMS pulse. Notably, this  
188 measure, which can also involve certain baseline normalization operations and is sometimes  
189 referred to as TMS-related spectral perturbation (TRSP), reveals a mixture of phase-locked and  
190 non-phase-locked responses that are difficult to disentangle [52].

191

192 Throughout this paper, we will mostly refer to TEPs when describing EEG responses to TMS,  
193 but the same considerations apply to TMS evoked and TMS-induced oscillatory activity, except  
194 where otherwise stated.

195

196

## 197 **2. TMS-EEG instrumentation**

198

199 This section aims to provide a comprehensive overview of the equipment currently available to  
200 acquire TMS-EEG data and to discuss how different settings/parameters affect the quality of the

201 recordings. To do so, we reviewed published evidence, reported practices, and experiences  
202 documented by different laboratories.

203

204 The instrumentation to acquire TMS–EEG data typically includes a) TMS device and coils, b)  
205 TMS-compatible EEG amplifier, and c) TMS-compatible electrodes. The integration of a  
206 neuronavigation system is highly recommended to keep the TMS coil on the desired target with  
207 the same orientation and angulation throughout the session and across visits in the case of  
208 longitudinal measurements [32, 33, 55]. In addition, the use of a neuronavigation system is  
209 mandatory in studies involving patients with structural brain lesions, since stimulation of  
210 severely damaged areas does not elicit any EEG response [56]. In the following sections, we  
211 describe each component.

212

### 213 **2.1. TMS stimulators**

214 Currently, there are several TMS stimulators available on the market. When performing  
215 TMS–EEG studies, the following properties can be useful:

216 1. Option to control the recharge delay: a change in the potential of the coil during the  
217 capacitor recharging can cause electrical artifacts in the EEG recording. Since the  
218 recharging typically occurs in a time window overlapping with the relevant signal, it is  
219 crucial to set the time of recharge outside the temporal window of interest (i.e., the  
220 recharge delay should not overlap with the relevant post-TMS signal). To meet this  
221 requirement, most of the stimulators currently available on the market (for instance, some  
222 versions of MagVenture, Nexstim, Magstim, and Deymed stimulators) include a recharge  
223 delay option that allows one to choose the recharge time (see **Section 4** for more details  
224 on this artifact).

225 2. Generation of different pulse waveforms: the most used are monophasic and biphasic  
226 waveforms, although available stimulators can generate other waveforms, such as half-  
227 sine and trapezoidal.

228 3. Some stimulators can change the induced current direction in the coil: this may be  
229 relevant to studying the effect of the induced E-field direction on brain activity.

230 4. Compatibility with different TMS coil sizes/shapes. For example, this can be helpful to  
231 perform multi-site TMS–EEG studies where 2 or more coils are placed on the head.

- 232 5. Cooling system to run long protocols: to improve the signal-to-noise ratio (SNR) of  
233 TMS–EEG data, it is generally recommended to average a sufficient number of trials.  
234 During stimulation, the TMS coil heats up at a rate that depends on stimulation intensity  
235 (SI) and may need to stop working upon reaching a specific temperature because of  
236 safety issues. Liquid- or air-cooled coils reduce coil heating.
- 237 6. Triggering signal communication between TMS stimulator, EEG, and neuronavigation:  
238 the communication between hardware is crucial, i.e., controlling properties of the  
239 stimulator (like SI, inter stimulus interval/randomization) via an external device or, e.g., a  
240 navigation system.

241

## 242 **2.2. TMS coils**

243 Currently, there are many different types of TMS coils [57]. Overall, the coil choice depends on  
244 the TMS protocol to be performed. Their shape, size, and winding determine the induced E-field  
245 and, therefore, the focality and depth of penetration, which impact the brain volume stimulated  
246 [58] and, consequently, the TMS-related EEG responses. The most common TMS coil is the  
247 figure-of-eight coil [4, 59], but so far, there is no systematic study of the effect of the TMS coils  
248 on TMS-related EEG responses. In addition, the type of coil may also determine to what extent  
249 cranial muscles near the area of interest will be stimulated, affecting the EEG recordings.  
250 Therefore, one should be aware of scalp, facial, and neck muscle activations; for instance, the  
251 double-cone coil may trigger strong muscle twitches affecting the EEG recordings, e.g., [60]. Of  
252 note, a novel brain stimulation approach has recently been introduced, the multi-locus TMS  
253 (mTMS) [61-63], allowing electronically controlled stimulation of multiple brain areas at  
254 different times and intensities, (for an example of TMS–EEG and mTMS see [64]).

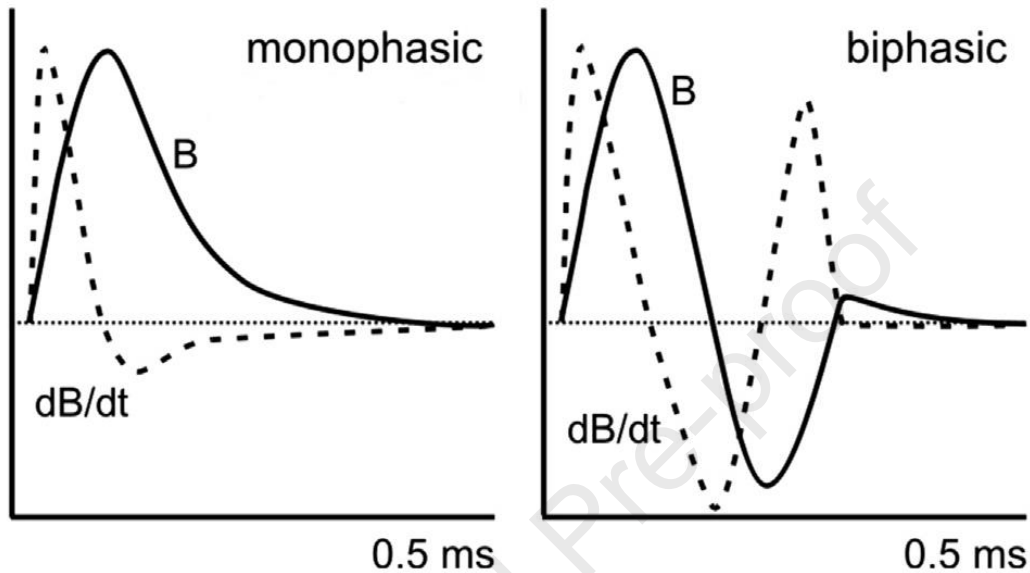
## 255 **2.3. Effect of TMS pulse waveform**

256 In this section, we will briefly outline our current knowledge about the two most common pulse  
257 shapes, in TMS–EEG recordings, i.e., monophasic and biphasic waveforms [65, 66].

258 Monophasic and biphasic pulses are defined by the amplitude ratio of the first and second phases  
259 of the E-field waveform. Monophasic pulses are shorter (usually around 100  $\mu$ s) and consist of a  
260 steep initial current flow in the coil, which is responsible for neuronal depolarization. A switch  
261 or a diode in the stimulator prevents the coil current from flowing in the reverse direction (**Fig.**  
262 **2**). Nevertheless, when the coil current (and the consequent magnetic field) returns to zero, an

263 induced current in the brain in the opposite direction is always present. However, this current in  
 264 the opposite direction only ends the depolarization phase, it will not trigger any action potentials;  
 265 therefore, the biologically relevant current is monodirectional [67-69].

266



267

268 **Fig. 2.** Comparison of monophasic and biphasic pulses. The monophasic pulse (left panel) consists of a steep initial  
 269 current flow, whereas the biphasic pulse (right panel) consists of two half-cycles of opposite polarity (see text for a  
 270 detailed description). The figure shows the time course of monophasic and biphasic magnetic pulse with magnetic  
 271 field strength  $B$  (solid line) and its rate of change  $dB/dt$  (dashed line), which correlates with induced electric field  
 272 strength. Reproduced with permission from Funke [70].

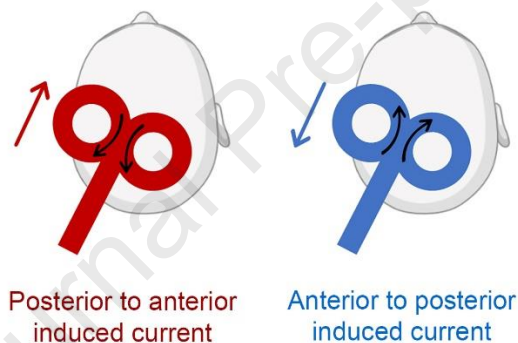
273

274 Biphasic pulses are longer (up to several hundreds of  $\mu s$ ) and usually consist of at least two half-  
 275 cycles of opposite polarity but similar amplitude (thus, with an amplitude ratio close to 1), and a  
 276 shape that is slightly variable across stimulators. In contrast to monophasic pulses, each coil  
 277 current phase can effectively stimulate the cortex ([67, 69], although the second phase  
 278 contributes to most TMS effects due to its larger change of amplitude and duration [71]. In other  
 279 words, for a monophasic pulse, the first phase is more relevant for exciting cortical neurons,  
 280 whereas, for a biphasic pulse, the second phase is more effective. Because of this difference, the  
 281 monophasic pulse is preferred when investigating the effects of current direction, which are less  
 282 pronounced with the biphasic pulse [67].

283

284 *Pulse direction:* On a practical note, the pulse waveform and the stimulator brand determine the  
 285 direction of the current induced in the brain [72]. For example, the optimal current direction of  
 286 monophasic pulses in the brain tissue for M1 stimulation is posterior to anterior and lateral to  
 287 medial [73]. To produce this current (by a current changing in the opposite direction in the coil)  
 288 with Magstim devices, the handle of the coil should point backward for monophasic pulses and  
 289 forward for biphasic pulses [74]. For MagVenture (MagPro), the optimal current for M1  
 290 stimulation with default settings is generated with the handle pointing forward for monophasic  
 291 pulses and backward for biphasic pulses. The difference between Magstim and MagVenture  
 292 stimulators is determined by the current direction in the coil, which goes from the handle towards  
 293 the end of the coil for MagVenture and vice-versa for Magstim (see **Fig. 3**).

294



295

296 **Fig. 3.** Example of induced current direction by two different stimulators. In Magstim stimulators (left figure) the  
 297 current in the coil flows from the top to the handle as indicated by the curved arrows. The current induced in the  
 298 brain flows in the opposite direction and is therefore defined as posterior to anterior as depicted by the straight  
 299 arrow. In other stimulators, such as MagVenture (right figure), the opposite is true. The current in the coil flows  
 300 from the handle to the top as shown by the curved arrows and therefore the induced current in the brain flows  
 301 from the front to the back, i.e., it is an anterior to-posterior current.

302

303 Monophasic and biphasic pulses present unique advantages and disadvantages; the choice will  
 304 therefore depend on the research question. Previous studies [65] have shown that biphasic  
 305 waveforms are more effective, i.e., require lower magnetic fields to stimulate the cortex (e.g.,  
 306 lower resting motor threshold) and, therefore, may be preferred for TMS–EEG experiments,

307 given that the severity of many TMS-related artifacts increases with the SI (e.g., muscle artifacts)  
308 [75]. Lower intensities will also minimize participants' discomfort.

309 Different waveforms have been reported to affect the amplitude of the initial TMS artifact but  
310 not its duration [76, 77]. Following the stimulation of a dummy head, two independent studies  
311 reported that monophasic pulses induced a larger artifact compared to biphasic pulses, but the  
312 EEG signal returned to the baseline levels within 5 ms after the pulse delivery regardless of the  
313 waveform type. It is worth noting that, while these results indicate that the artifact duration does  
314 not depend on the waveform, the 5 ms interval hinges on the EEG equipment and recording  
315 parameters (**Section 2.4**). Furthermore, while the duration of the initial artifact was found to be  
316 similar, this does not rule out effects on later artifacts (some of the authors of this paper have  
317 indeed reported that the monophasic waveform causes an offset that slows the return of the EEG  
318 signal to the baseline).

319 The effect of the TMS pulse waveform on brain activity has been recently investigated by Casula  
320 and colleagues [78] using TEPs. The authors found that TEPs between 50 and 200 ms were  
321 characterized by a larger amplitude when evoked by monophasic compared to biphasic pulses  
322 [78]. However, the effect of pulse shape on the TEPs has not been systematically investigated  
323 and more studies are needed.

324

#### 325 **2.4. EEG amplifiers**

326 The first methodological challenge associated with recording EEG during TMS is the strong E-  
327 field generated by the magnetic pulse, which can saturate the recording amplifiers for several  
328 seconds. To overcome this problem, a sample-and-hold circuit was introduced to control the  
329 recording apparatus and lock the EEG signal [79]. The circuit held the EEG acquisition for a few  
330 milliseconds following TMS delivery [79-81], thereby avoiding saturation of the recording  
331 amplifiers and allowing one to record the response generated by the stimulation after the hold  
332 period. In more recent years, a different generation of amplifiers has gained popularity and has  
333 replaced the sample-and-hold circuit approach. These amplifiers have been designed to work in  
334 high time-varying magnetic fields, thus avoiding saturation, and have in principle the advantage  
335 of allowing the EEG to be acquired continuously. However, the stimulus artifact covers a small  
336 amount of signal, possibly including the initial response of the directly stimulated cortical target,

337 that cannot be recovered with current preprocessing methods (see **Section 4**). For an overview of  
338 different TMS-compatible EEG systems, see **Supplementary Materials (Table S1 and**  
339 **questionnaires)**.

340  
341 Despite the lack of systematic investigations, we know that some recording parameters are more  
342 effective than others in limiting the impact of the initial electrical artifact, which is a high-  
343 amplitude and high-frequency signal. As shown in Fig. 8 in Freche et al. [82] [see also 83], and  
344 as recommended by many manufacturers (**Table S1 Supplementary Materials**), an adequate  
345 sampling rate must be selected, together with a corresponding low-pass cutoff. The lower the  
346 low-pass is, the longer the ripples created by the interaction of the filter with the TMS pulse  
347 artifact last. If sampled at very high rates, the pulse artifact lasts only as long as the actual TMS  
348 pulse and also reflects the pulse shape. With lower sampling rates (and thus lower anti-aliasing  
349 low-pass filters), filter ripples increase in amplitude and duration, and longer pulse artifacts arise.  
350 For example, with the same amplifiers and experimental setting, Veniero et al. [77] reported an  
351 artifact duration of 5 ms with a sampling rate of 5 kHz, whereas Bonato et al. [37] reported a 10  
352 ms artifact with a sampling rate of 1 kHz.

353  
354 As reported in **Table S1 (Supplementary Materials)**, all TMS-compatible EEG amplifiers can  
355 record data with a high sampling rate. It is worth mentioning that some companies report that  
356 with a sampling rate of ~20 kHz, the artifact duration is below 2 ms or even below 1 ms when  
357 sampling at 80 kHz (in line with Freche et al., [82]). However, the definite end of the pulse-  
358 ripple artifact can be difficult to determine objectively [but see 77].

359  
360 To avoid further rippling, additional low-pass filters must be avoided where possible or carefully  
361 chosen. While low-pass filters reduce the pulse artifact amplitude, they increase its duration.  
362 Since the EEG signal covered by the pulse artifact cannot be recovered and is later removed, its  
363 amplitude and clipping can be ignored, and one should aim to reduce its duration as much as  
364 possible. For similar reasons, DC amplifiers are to be preferred over AC amplifiers, since high-  
365 pass filters also interact with the pulse artifact and introduce artificial trends/drift in the signal  
366 around the TMS pulse [for a detailed discussion on high-pass filters effects, see 84]. Of note,  
367 high-pass filters can also tamper with later artifacts and TEPs. For DC amplifiers, either no high-



368 pass filters or a very low one (e.g., 0.016 Hz, i.e., 10 s time constant) should be used to  
369 prevent/reduce such trends.

370

371 For a list of available TMS-compatible EEG systems see **Supplementary Materials**, where we  
372 report the results from a questionnaire, we have asked several manufacturers to fill out with  
373 general information about each system.

374

## 375 **2.5. EEG electrodes**

376 In standard EEG, four types of electrodes can be used: passive, active, dry, and sponge.  
377 However, conventional EEG electrodes cannot be used with TMS [28, 85] because the magnetic  
378 pulse induces eddy currents (i.e., currents that circulate in closed loops) and causes electrode  
379 heating. These issues can be reduced using sintered Ag/AgCl pellet or C-ring electrodes (i.e.,  
380 ring electrodes with a slit to prevent current induction in a closed ring), which have been used in  
381 most TMS–EEG studies. A disadvantage of pellet electrodes is the considerable amount of  
382 preparation time required to reduce the impedances to acceptable values (5 k $\Omega$  or less). The so-  
383 called *Multitrodes* (EasyCap) are C-ring electrodes in which the Ag/AgCl coating is located on  
384 the inner instead of the lower surface of the C-ring. Since the contact surface is larger and more  
385 easily accessible, many authors of this paper have reported that impedances can be lowered more  
386 quickly. C-electrodes are usually preferred because they reduce eddy currents induced by TMS,  
387 which may contribute to the decay artifacts (see **Section 4.1.3**).

388

### 389 *Active vs. passive electrodes*

390 Active electrodes (AEs) have been introduced in electrophysiology only in recent years.  
391 Compared to traditional passive electrodes (PEs), which act as simple recording sites, AEs entail  
392 preamplification of the signal directly at the electrode stage. When recording standard EEG, this  
393 feature provides several advantages, such as the reduction of electrical line noise and the  
394 recording of a better signal at higher electrode impedance levels. In addition, the ease of montage  
395 and the fast preparation of AE recordings result in shorter experimental sessions and a reduction  
396 of discomfort for participants.

397

398 Recently, a few studies have used AE with new active amplifiers to record EEG during TMS [38,  
399 86-88]. One of these studies directly compared the performance of AE and PE by looking at  
400 TEPs [86] and revealed no significant difference in amplitude or scalp topography. However,  
401 some AE users have observed an increase in the decay artifact (see **Section 4.1.3**) duration that  
402 should be further investigated. Moreover, while AEs reduce the preparation time, their larger  
403 thickness increases the coil-to-cortex distance and requires higher TMS intensity, which might  
404 impair the EEG signal quality and lower the spatial specificity of the stimulation. This also  
405 unfavorably affects the activation threshold and should be acknowledged when reporting and  
406 comparing threshold values between studies [89]. Overall, while AEs seem a useful addition to  
407 the TMS–EEG field, more studies are needed to assess their performance in different  
408 experimental settings. shou

409

#### 410 **2.5.1. How many electrodes do we need to record acceptable EEG responses?**

411 A common question in the field is how many electrodes should be used. The original  
412 International 10–20 system was devised with the intention that each electrode would inform  
413 about brain activity in the underlying cerebral structure [90]. The electrode potentials were  
414 usually measured with respect to the same reference electrode, resulting in controversial  
415 discussions about the proper reference electrode location. Currently, as we understand the  
416 sensitivity patterns of the EEG signals, we do not need to worry about the reference electrode  
417 “problem”. Referencing is a linear data transformation therefore the data can be re-referenced  
418 offline. Unless the reference position is particularly prone to local artifacts (from movement,  
419 sweating, TMS, etc), a later re-referencing to the common average (or any other preferred linear  
420 recombination) allows recovering the reference signal, so that the referencing during recording is  
421 arbitrary.

422 Each electrode derivation measures the difference between two scalp potentials, informing us  
423 about one dimension of the source current distribution in the brain. This dimension, described by  
424 the sensitivity pattern or lead field of the derivation, depends on the placement of the electrodes  
425 as well as the details of the conductivity distribution of the head. When the number of electrodes  
426 is increased after the first few dozen, the marginal benefit of each new recording channel  
427 diminishes quickly because nearby electrodes sense nearly the same potential [91]. It has been  
428 found that the rank of the data obtained with a large electrode set is typically 30–50, meaning

429 that with optimal placement on the scalp, 30–50 electrodes would be enough to gather the spatial  
430 information that is available to EEG [92-94]. Because the electrode placement is usually not  
431 optimized, about 60 electrodes (in practice often 64) is sufficient to obtain almost all signal  
432 components available from scalp recordings [92].

433 However, a couple of advantages *are offered by a larger number* of electrodes. First, if an  
434 electrode channel becomes noisy or non-functional in a 256-channel system, virtually no spatial  
435 dimension is lost, since the redundant channels can provide the lost information. Second, if one  
436 can assume that the noise in neighboring electrode channels is statistically independent (as it is if  
437 the noise is mainly from the electrode contact and the amplifiers), the overall SNR is increased;  
438 in effect, signals from neighboring channels will be effectively averaged in the course of data  
439 analysis. Thus, because the source-level SNR is in principle approximately proportional to the  
440 square root of the number of channels with uncorrelated noise, increasing the number of  
441 electrodes from 64 to 256 could double the source-level SNR [95]. In fact, some data-cleaning  
442 methods, such as the source-estimate-utilizing noise-discarding algorithm (SOUND) algorithm  
443 (see **Section 6.3.3** for details), utilize cross-validation between channels to detect the channel-  
444 specific noise. For these methods, “oversampling” the EEG spatially is beneficial when  
445 estimating the noise distribution. However, SNR improvements can be obtained also by  
446 improving electrode contacts and by lowering the noise level in amplifiers. Third, artifacts due to  
447 the activation of cranial muscles could be more accurately pinpointed with additional electrodes.  
448 Since TMS activates muscles only under the coil, in some experiments it would suffice to add  
449 just a few muscle-activity-detecting electrodes over the TMS target area. The extra electrodes  
450 would enable one to measure and model the spatial pattern of the electrical activity of the muscle  
451 so that the artifact could be removed from the rest of the data.

452  
453  
454

## 2.6. Neuronavigation

455 Neuronavigation has become increasingly important in TMS research, as it increases stimulation  
456 accuracy and efficacy [96, 97]. With navigated TMS (nTMS), the coil position and orientation  
457 can be monitored in real-time, ensuring appropriate stimulation of the target area throughout the  
458 experimental session [28, 98, 99]. This reduces possible inter-trial variability in the TMS–EEG  
459 recordings due to coil movement and increases accuracy by reducing the risk of stimulating a

460 slightly different area [100]. As neuronavigation systems can store information on the coil  
461 position and orientation, they also ensure comparable targeting across multiple sessions and  
462 result reproducibility [55, 101, 102]. Some systems can mark EEG trials when displacements  
463 from the target occur.

464

465 Advanced neuronavigation systems compute the induced E-field in the brain, which enables  
466 precise anatomical stimulus targeting; the strength of the E-field serves also as a stimulation  
467 intensity that is independent of coil or stimulator type (see **Section 3.2**). Using nTMS to align the  
468 direction of induced current relative to the underlying gyral pattern is furthermore expected to  
469 increase TMS effectiveness. The strength of stimulation is enhanced when the current is  
470 perpendicular to the target gyrus relative to when it is parallel (for modeling see [103]; for an  
471 application including parallel currents as control, see [104]) (see also **Section 3.4**). Existing  
472 nTMS systems estimate the induced E-field using spherical conductor models to take into  
473 account the local curvature of the skull [105] and display the results on the individual anatomical  
474 MRI to assist with the coil positioning [98, 99]. Another approach to improve targeting and  
475 accuracy consists of using realistically shaped boundary element head models [106, 107]. While  
476 TMS–EEG studies may benefit from using neuronavigation systems based on realistic head  
477 models, such models have not yet been implemented online due to the computational cost [106].

478

479 Robotized nTMS has also been used in combination with EEG to assess the effect of coil  
480 position accuracy on TEPs [108] and to map EEG responses of several brain areas [109]. The  
481 idea is that automatic positioning allows us to target many cortical areas in a reasonable amount  
482 of time with high precision. A caveat of robot-navigated TMS–EEG, however, can be increased  
483 levels of line noise in the EEG data from the electronics of the robot, which may require a  
484 spacer-mediated gap between the TMS coil and EEG cap and/or additional grounding measures.

485

### 486 **3. General aspects of TMS–EEG**

#### 487 **3.1. Number of trials (Signal-to-noise ratio)**

488 One of the most common questions people in the EEG and TMS–EEG community ask is “How  
489 many trials do I need to acquire in my experiments to obtain meaningful TEPs or oscillations?”.

490 Although these are simple questions, they do not have a simple answer.

491 The number of trials depends on the meaningful signal in relation to the noise content, i.e., the  
492 SNR. The SNR depends on the square root of the number of trials [110], provided that the  
493 meaningful signal and noise remain similar from trial to trial. In more detail, let  $S$  be the size of  
494 the signal,  $N$  the size of the noise on a single trial, and  $T$  the number of trials. The SNR on a  
495 single trial is defined as  $S/N$  (the signal divided by the noise). The total SNR of averaged  
496 responses, such as TEPs, is then equal to  $(S/N) * \text{sqrt}(T)$  (the single-trial SNR multiplied by the  
497 square root of the number of trials). The closer the meaningful signal level gets to the level of  
498 noise, the more trials are required. However, if the meaningful signal is below the noise level in a  
499 single trial, even more trials are required. The required number of trials also depends on the set  
500 quality criterion, i.e., the required SNR. Suppose the required SNR is known and the single-trial  
501 signal level and noise levels are known. In that case, the required number of trials can be  
502 calculated. As noted above, the increase in SNR is not linear; therefore, doubling the number of  
503 trials does not double the SNR. For instance, to double the SNR from 100 trials, one needs to  
504 measure 400 trials. This means that, after a certain point, increasing the SNR further would lead  
505 to very lengthy experiments without significant benefit. The power law of SNR has additional  
506 positive implications. When a sufficient number of trials have been recorded, one should not be  
507 too concerned to reject contaminated epochs, as this will have only a minor impact on the  
508 potential maximal SNR. For instance, after recording 300 trials, one can reject 30 trials and  
509 decrease the theoretical maximal SNR by only 5%.

510

511 When TEPs are the signals of interest, a good starting point to set the number of trials could be  
512 looking at studies that have investigated test-retest reliability and reproducibility ([32, 33, 86, 87,  
513 111, 112]). Many of these studies suggest that around 100 *clean trials* (note: clean refers to the  
514 number of trials after exclusion of artifactual epochs) are sufficient to have reliable TEPs.  
515 However, most studies have been performed on motor areas and therefore, this conclusion might  
516 not apply to other areas. Additionally, weak cortical responses tend to require more trials than  
517 strong cortical responses. For example, it has been reported that the reliability of the TEP peaks  
518 is dependent on the investigated component, and the concordance between trials plateaus after 60  
519 trials, while the smallest detectable difference continues to improve with added trials [33].

520

521 Since the amplitude of the cortical responses is related to the applied SI, low intensities tend to  
522 require more trials [45]. Rosanova et al. [113] suggested that the number of trials needed for a  
523 high SNR range between 150 and 300, depending on the intensity of stimulation (as an empirical  
524 rule, the higher the intensity, the lower the number of trials). While this is a good approach, care  
525 should be taken since the strength of the cortical response varies from one location to another  
526 [32, 33, 55, 114], and increasing the SI may also have an impact on TMS-induced activation of  
527 cranial muscle, voltage decay, and sensory evoked potentials. Therefore, different target regions  
528 might require a different number of stimuli. For instance, stimulation of frontal areas is more  
529 prone to artifacts than motor areas and a larger number of trials may be required since there is a  
530 higher likelihood of rejecting bad trials due to artifacts (e.g., eye- blinks and muscle  
531 contractions). However, following good practice during TMS–EEG preparation and recordings  
532 might help to decrease noise and get better SNR (see **Section 5**) with a reasonable number of  
533 trials.

534

535 The number of trials should also be chosen considering the type of outcome measure we are  
536 interested in. Therefore, we recommend referring to the relevant EEG literature to define the  
537 number of trials. As an example, indexes related to the frequency domain, such as pre-stimulus  
538 phase estimation are known to depend strongly on the number of trials [for a review see 115].  
539 TMS–EEG data do not constitute an exception, as demonstrated by Schaworonkow et al. [116],  
540 who confirmed that if the measure of interest is the phase of the EEG signal immediately  
541 preceding the TMS pulse, the phase-estimation algorithm depends strongly on SNR.

542

### 543 **3.2. TMS threshold determination**

544 There are several ways to determine the TMS SI or threshold, which depend on the outcome  
545 measure of choice and a somewhat arbitrarily defined criterion. Thresholds can be determined by  
546 measuring motor responses, phosphene perception, in principle also the amplitude of TEPs, or  
547 estimated by simulations of the induced E-field.

548

549 **Motor responses:** The most common way to determine the SI is to measure the motor threshold  
550 (MT) in a resting muscle. This is done by first mapping the M1 cortical representation for the  
551 target muscle and then finding the optimal position and coil orientation, for that muscle, thereby

552 maximizing the E-field at the cortical representation area (“hotspot”) of the muscle. The MT is  
553 measured by directing the E-field to the hotspot and is typically defined as the minimum TMS  
554 intensity able to evoke MEPs of at least 50  $\mu$ V peak-to-peak in the contralateral muscle of  
555 interest (to the stimulated hemisphere) in 5 out of 10 consecutive trials [e.g., 117, 118]. Of note,  
556 due to TMS-induced E-field spreading and overlapping cortical representations, MEPs are also  
557 elicited in muscles adjacent to the one examined [119]. The interstimulus interval (ISI) between  
558 consecutive TMS-pulses should be set sufficiently long to avoid cumulative effects (e.g., [120,  
559 121]); evidence exists that ISIs of 5 s or longer increase the reliability of MEP measurements  
560 [122, 123]. It is also beneficial to jitter the ISI to avoid any expectation and habituation effects  
561 [123, 124]. If the SI for TMS–EEG measurements is based on the MT, one should consider using  
562 the same ISI and jitter for threshold estimation and TMS–EEG protocols.

563  
564 Although the MT is measured from M1, it is commonly used to set the SI in non-motor areas as  
565 it is simple, fast (depending on the exact MT determination method), it can be reliably  
566 determined with a number of pulses as low as 17 [125], and provides a highly replicable  
567 measurement [126, 127]. The limitation of this approach lies in the assumption that sensitivity to  
568 TMS for non-motor areas is similar or correlated to that of M1. This does not seem to be the  
569 case, for example, see Stewart et al. [128] for a comparison between phosphene and MT [but see  
570 129]. In addition, TMS–EEG studies support different responsiveness to stimulation for different  
571 cortical areas [32, 35, 55]. Unique cytoarchitectonic features could affect how a brain region  
572 reacts to TMS. Also, simple anatomical features such as variations in scalp-to-cortex and,  
573 therefore, coil-to-cortex distance have to be taken into account; this is automatically done in  
574 navigation systems where the cortical E-field is computed (see below). In TMS, the magnetic  
575 field decreases with the square-distance; therefore, the farther the coil-to-cortex distance, the  
576 weaker the magnetic field and the induced E-field in the cortex. As the coil-to-cortex distance  
577 varies between brain areas/targets, it is challenging to know which percentage of MT should be  
578 used for other areas, and practices on how to adjust the TMS intensity vary substantially between  
579 research laboratories [for a simple metric to account for coil-cortex distance see 130].  
580 Instead of recording motor responses with the EMG, some groups determine the TMS threshold  
581 by visually observing muscle twitches. However, this approach overestimates the MT and is not  
582 considered suitable for reproducible measurements [131] and standardizing methods across

583 users. Visual observation of muscle twitches can be useful to ensure that the recorded MEPs  
584 mainly reflect the target muscle of interest.

585  
586 **Phosphenes perception:** In visual areas, the SI can be based on the phosphenes threshold (PT).  
587 Phosphenes are illusory percepts, often described as visual flashes perceived immediately after  
588 the TMS-pulse, thought to occur from the direct activation of the visual cortex [132-134] or fiber  
589 tracts such as the optic radiation projecting into the visual cortex [135]. The PT is calculated  
590 similarly to MT, but rather than relying on objectively measurable responses (i.e., MEPs), it  
591 depends on the participants' subjective report (they are asked to indicate the presence/absence of  
592 phosphenes). As the relevant parts of the visual cortex may be located deeper than the primary  
593 motor cortex, the PT is typically higher than the MT [128, 129, 136]. An additional limitation is  
594 that phosphenes can only be elicited in around 60% of participants [137, 138] and, therefore, MT  
595 is sometimes used to set the TMS intensity if no consistent phosphenes can be obtained [104,  
596 137].

597  
598 **Induced E-field:** Another way to determine the SI is to calculate the induced E-field at the target  
599 and select the TMS intensity that generates the desired E-field [98, 99, 139, 140]. Inherently, and  
600 ideally, this method is not dependent on the coil-to-cortex distance [141] and can be used for any  
601 cortical area. One limitation is that this technique requires the use of advanced neuronavigation  
602 and participants' MRIs (see **Section 2.6**), which might not always be available. Furthermore, the  
603 online E-field calculation is only available in a few TMS/Navigation systems (for which the  
604 underlying algorithms for E-field estimation are not openly available). However, open-source  
605 software, which takes into account the subject-specific anatomy, for offline E-field modeling is  
606 available (e.g., [www.simnibs.org](http://www.simnibs.org); [107]) and is now widely used in the field of transcranial  
607 electrical and magnetic stimulation. In contrast to accurate finite-element calculators, such as  
608 Simnibs, commercial online E-field estimators are based on computational simplifications. For  
609 instance, one such neuronavigation system is based on computing the E-field inside a sphere,  
610 fitted to the local subject-specific geometry. The computational differences between different  
611 systems can lead to discrepancies in the E-field estimations across different studies. Thus, online  
612 E-field monitoring might be most useful to normalize the TMS dose within a cohort and to  
613 ensure test-re-test reliability within a subject.



614 Finally, the relationship between the TMS-induced E-field and the activation of the target site  
615 has to be further investigated. Factors influencing neuronal excitability such as axonal geometry  
616 may affect the required E-field in a way that is difficult to predict based on a priori information,  
617 i.e., we do not know the intensity and orientation of the E-field that should be applied to  
618 effectively stimulate the cortex. Previous studies have shown that when stimulating the visual  
619 cortex: a) with E-field intensities below 50 V/m, post-stimulation activity is indistinguishable  
620 from baseline EEG activity (i.e., no TEPs could be elicited); b) TEP amplitudes progressively  
621 increase with the intensity of the induced E-field; c) at 120 V/m there is a substantial activation  
622 of the target area [142] with the same intensity, there is a clear differentiation in the TEP  
623 frequency content across stimulation sites [46] Importantly, E-field estimates do not consider the  
624 possible effects of other factors such as the TMS pulse waveform and duration or the spatial  
625 extent of the E-field with a certain intensity, which may contribute to the temporal and spatial  
626 summation of the induced activations and thus to the ability of a TMS pulse to evoke action  
627 potentials in cortical neurons.

628  
629 **TEP amplitude:** The SI can also be determined by searching stimulus parameters that maximize  
630 TEP amplitudes. In analogy with the motor hotspot search, the position, orientation, and intensity  
631 of the TMS can be adjusted to optimize the impact of the stimulation on the underlying neuronal  
632 circuits while minimizing artifacts at the same time. This approach relies on the visual inspection  
633 of the data in real-time during the recording (rt-TEP software, [34]). At first, visualization of  
634 single-trial data allows to immediately assess the presence of evoked muscle activity or other  
635 TMS-related artifacts; if the cortical target is not too close to cranial muscles, small adjustments  
636 of coil orientation and/or position are often enough to reduce the impact of these artifacts on the  
637 EEG signal [75]. Subsequently, the effectiveness of the stimulation can be evaluated by  
638 measuring peak-to-peak amplitude of average TEPs (re-referenced to the average reference)  
639 obtained after a limited number of pulses (e.g., 20-trial average) in the first 50 ms after TMS in  
640 the channels closest to the stimulation site. Specifically, EEG responses to TMS are expected to  
641 show larger amplitude a) in the channels close to the stimulation site compared to distant  
642 channels, b) at early latencies compared to late latencies, and c) in the channels of the stimulated  
643 hemisphere compared to the contralateral ones. Based on these TEP features, the peak-to-peak  
644 amplitude of the largest component measured in the first 50 ms in the channel closest to the

645 stimulation site represents a readout of the impact of TMS on the cortex. The reliability can be  
646 further enhanced by combining multiple EEG channels into linear combinations that enhance the  
647 sensitivity of the readout to the region of interest.

648 The peak-to-peak amplitude of the early and local EEG response to TMS after averaging 20  
649 trials correlates with the signal-to-noise ratio of a full session in which 80–100 trials are  
650 averaged and depend on the amplitude and variability of spontaneous (see Supplementary results  
651 in [34]). Although it is not possible to set an absolute value for the ideal peak-to-peak amplitude,  
652 in principle it could be possible to estimate a reasonable endpoint based on the number of trials  
653 to be collected and on the amplitude of ongoing EEG activity.

654  
655 This approach implies that the effects of TMS parameters (intensity, site, orientation) are  
656 assessed in real-time and adjusted (if needed) to minimize muscle artifacts and maximize the  
657 strength of the initial cortical activation; thus, it may imply a deviation from precise targeting  
658 requirements (e.g., while stimulating over cortical sites associated with a certain assumed  
659 function or dysfunction), for improving data quality. In conclusion, relying on a real-time EEG  
660 readout during the experiment provides immediate control over undesired artifacts. This  
661 approach is most effective while stimulating cortical structures close to the midline where cranial  
662 muscle activation can be reduced by small adjustment of TMS parameters and becomes more  
663 challenging when more lateral cortical areas are targeted [75].

664  
665 **3.3. Required/optimal TMS intensity to induce brain activity**

666 The SI will have an impact on whether only local TEP components are evoked or a wider  
667 network is activated, for instance by transcallosal pathways [143-147]. Several studies have  
668 described the input-output characteristics of TMS–EEG responses, i.e., how they change as a  
669 function of the SI, and they mostly indicate a linear relationship at typical SIs, at least on M1 and  
670 prefrontal cortex (e.g., [45, 148], but see [138] for non-linear intensity–amplitude relationship in  
671 visual areas). In other cases, SI may be defined through known behavioral effects from the  
672 literature, hence ensuring suprathreshold SI. For instance, in a recent series of TMS–EEG  
673 experiments on Frontal Eye Fields (FEF)-control over posterior brain signals, Veniero et al. [50]  
674 used a fixed SI of 65% of maximum stimulator output (MSO), which was defined based on prior  
675 studies revealing that exactly this intensity effectively activates FEF and its projections as

676 inferred from behavioral TMS effects on visual attention tasks [149-151] and perception tasks  
677 [152]. In the study by Veniero et al. [50], FEF-TMS at this suprathreshold SI (relative to  
678 behavioral effects) led to changes in intrinsic brain oscillations at occipital sites, i.e., in remote  
679 connected areas. Besides suprathreshold SI, there is also evidence that subthreshold SI (with  
680 respect to MT) can be sufficient to induce TMS–EEG responses, albeit likely confined to the  
681 local level. It has been shown that stimulation of the left and right M1 and prefrontal cortices at  
682 60% MT is sufficient to evoke measurable brain activity [35, 148], and E-fields of around 40  
683 V/m in the targeted neuronal tissue may be sufficient to produce neuronal excitation [144, 147].  
684 In M1, this E-field strength can induce visible TMS–EEG peaks, but these SIs (commonly less  
685 than 50% of MT) may not be enough to activate the whole motor network [144]. There is also  
686 some evidence that the excitation threshold may depend on neuron types and local neuronal  
687 circuits (e.g., [13]).

688

689 The question about the SI necessary to activate transcallosal and other long-range pathways, as  
690 detected with TMS–EEG, is still open and will also depend on the population under investigation  
691 (e.g., brain responses of patients with major depression are altered when compared to healthy  
692 volunteers (e.g., [153])).

693

#### 694 **3.4. The effect of coil location and orientation**

695 It is well-known that coil location and orientation affect the MEPs [73, 154]. These parameters  
696 also influence TEPs [32, 37, 55]. However, in TEPs these effects have not been studied as  
697 extensively as in MEPs, as the impact of only a few coil orientations and locations has been  
698 tested. Different coil orientations influence TEP polarities [78] and amplitudes [55], although not  
699 all components are equally affected [37, 78, 108]. In some participants, varying the coil location  
700 near the hotspot slightly influences TEP amplitudes, whereas, in others, it also affects the TEP  
701 waveform [108]. Coil orientation also influences brain oscillations, as reported in a study by  
702 Thut et al. [104], where the magnitude of the entrained alpha oscillations was at its maximum  
703 when the coil was oriented to induce currents perpendicular to the target gyrus [103].

704

#### 705 **3.5. How to deal with the EEG responses caused by co-stimulation of peripheral** 706 **structures of the nervous system**

707 TMS typically causes somatosensory and auditory sensations because it might not only activate  
708 cortical neurons, but also nerves innervating the face, jaw, and neck muscles. Even when no  
709 muscles are activated, the pulse causes scalp sensations due to the excitation of afferent nerves  
710 (e.g., trigeminal nerve) or to mechanical stimulation of the skin by coil vibrations (e.g., a tapping  
711 sensation). In addition, a clicking sound is produced by the coil wires when the pulse is  
712 discharged and can activate auditory pathways through air and bone conduction. These sensory  
713 inputs may lead to peripherally evoked EEG responses which contaminate transcranially evoked  
714 EEG responses that result from direct cortical activation. The peripherally evoked potentials may  
715 not only contaminate transcranially evoked EEG responses but may also modulate them through  
716 neurophysiological interactions.

717 Recently, a few articles have triggered an intense discussion in the TMS–EEG community,  
718 opening a debate about the extent to which EEG responses to TMS are caused by direct cortical  
719 stimulation or include potentials elicited by sensory input associated with TMS [155-157].  
720 Therefore, more attention has been paid to the use of control and sham stimulation during TMS–  
721 EEG experimentation. In the following, we will discuss strategies that can be used to control for  
722 peripherally evoked EEG responses, the most suitable depending on the experimental design and  
723 aim of the study [158].

724 Several procedures have been proposed to deal with the auditory stimulation that accompanies  
725 the TMS pulse delivery. Some strategies assume the linear summation of the activity generated  
726 by TMS and the auditory activation. Here, TEPs are recorded without the presence of masking  
727 noise, and the auditory evoked potential is mathematically removed either with the use of  
728 independent component analysis (ICA)-based approaches or by recording an additional auditory  
729 sham session that will be subtracted from, or at least compared to, the contaminated TEPs.  
730 Another strategy consists of controlling for auditory stimulation by playing a continuous noise to  
731 mask the coil click, such as white noise, colored noise, or a noise adapted to the spectral  
732 characteristics of the click itself and tailored in real-time based on participants' perception [41].  
733 Recently, Russo and colleagues [159] developed and shared a tool to easily implement the latter  
734 solution with any type of coil and stimulator and to manipulate the standard noises in both time  
735 and frequency domains. Crucially, the use of this tool and the generated customized noise has  
736 been demonstrated to be effective at lower volume intensities (quantified by sound pressure level

737 measurements) compared to the standard noises. It should be noted though that noise-masking  
738 may introduce a change in functional resting-state brain connectivity similar to the effect induced  
739 by scanner noise during fMRI [160]. This change in “brain state” might alter the brain’s  
740 responsiveness to TMS.

741 While there is reasonable evidence that air-conducted auditory evoked responses can be  
742 suppressed by masking noise, at least under certain experimental conditions [38, 41, 56, 161], the  
743 TMS click may still elicit auditory responses through bone conduction [162, 163]. Furthermore,  
744 as suggested in some cognitive studies, somatosensory evoked potentials (SEP) might be  
745 modulated by the white noise [164]. Studies are warranted to systematically assess whether or  
746 how concurrent noise exposure shapes the TEPs. Instead of masking the coil click with  
747 additional noise, one may try to reduce the coil click as much as possible. Recently, a TMS coil  
748 with substantially reduced acoustic noise has been developed by attaching the windings to a  
749 surrounding damping casing separated by an air gap [165]. The acoustic noise of the coil click  
750 was reduced by 18–41 dB. However, this coil has not been tested in TMS–EEG experiments yet.

751 Complementing the efforts to mask or minimize auditory and somatosensory co-stimulation,  
752 several groups have used “realistic sham stimulation” to replicate the coil click and the sensation  
753 of a real magnetic stimulation without significantly stimulating the brain tissue [166]. However,  
754 establishing an effective sham stimulation procedure is a longstanding issue in the TMS  
755 literature and remains problematic [167]. In TMS–EEG experiments, one option that has been  
756 explored is complementing TMS with cutaneous electrical stimulation. The TMS coil is used to  
757 reproduce the clicking noise, whereas electrodes attached to the scalp [38, 156, 167] or to the  
758 coil itself [60] are used to apply electric stimuli intended to mimic the somatosensory input  
759 associated with real TMS [168]. Despite all efforts to develop a realistic multisensory sham  
760 stimulation, none of the reported procedures have been able to perfectly match the peripheral co-  
761 stimulation of real TMS (see, for instance, [38, 167]). This is mainly because the somatosensory  
762 percept related to TMS and electrical stimulation are qualitatively different and can be  
763 distinguished by the subjects [38, 156, 167].

764

765 A different way of dealing with spurious activations is to implement a comparative strategy as is  
766 typically done in fMRI experiments [169], that permits isolation of the effect of interest. If the

767 study aims to evaluate the effects of an experimental manipulation (e.g., learning), a pre/post-test  
768 design offers the advantage of testing the same participant at different timepoints, i.e., before and  
769 after the intervention, with the same TMS parameters. Likewise, studies that aim at testing the  
770 task-dependent modulations of TEPs may include recordings with the same TMS parameters in  
771 different task conditions. If this is the case, the sensory stimulation will be the same across time  
772 points or conditions, and differences in EEG can be attributed to direct cortical stimulation,  
773 provided that the experimental manipulation does not change the processing of sensory input.  
774 This strategy has been used in several TMS–EEG studies (e.g., [170-174]). The “comparative  
775 strategy” assumes that the interventional protocol does not change the peripherally evoked EEG  
776 response elicited by TMS. Although this might not always be the case it should be controlled  
777 when needed for the research question and protocol. Participants might habituate or become  
778 sensitized to peripheral co-stimulation, introducing order effects on peripherally evoked EEG  
779 responses in TMS–EEG experiments. The intervention itself may directly modulate the  
780 peripherally evoked EEG responses or indirectly by changing the arousing or attentional effects  
781 of peripheral co-stimulation on the TEP.

782  
783 A similar comparative strategy has been applied in studies aiming at characterizing excitability  
784 and connectivity of a brain area in different states or during a task. In this case, the experimental  
785 design should include conditions that can be compared to answer the research question. Not  
786 many studies have used TMS–EEG during a cognitive task, but in this case, having a control task  
787 while keeping the stimulation parameter constant would ensure equal sensory stimulation. As an  
788 example, Morishima et al. [175] traced FEF connectivity in a face discrimination task and  
789 compared it to the same measure obtained in a motion discrimination task (note that faces and  
790 moving dots were presented simultaneously). Another approach entails the use of TMS pulses  
791 delivered at different intervals from an event of interest (e.g., movement onset, visual stimulus).  
792 The comparison of TEPs evoked during different “tasks”, “task epochs”, or “states” can still be  
793 influenced by task-specific, epoch-specific or state-specific modulations of the central processing  
794 caused by peripheral co-stimulation (e.g., resulting in gating or attentional shifts).

795  
796 In TMS studies without EEG, a control site is often used to control for unspecific effects and  
797 establish site-specificity. However, the stimulation of different sites may induce distinct scalp

798 sensations and muscle activation [75, 176]. Others have explored the possibility of applying  
799 TMS controls over the same site but changing coil orientation from a more effective orientation  
800 (E-field induced perpendicular to the target gyrus) to a less effective orientation (E-field parallel  
801 to the gyrus) [104]. This should keep peripheral activation similar across conditions (e.g., from  
802 sounds), although differences in somatosensation due to different muscle fibers being activated  
803 by the two coil orientations cannot be excluded.

804  
805 Therefore, many approaches have been explored but no consensus has been reached yet on the  
806 best approach. It is important to consider EEG responses caused by co-stimulation of peripheral  
807 structures when designing a study and apply the solution that is most reasonable for the purpose  
808 of the study.

809

810

### 811 **3.6. Triggering of TMS based on EEG features “open- and closed-loop”**

812 Resting TMS–EEG can provide valuable information about the general excitability state or  
813 connectivity of the cortex. However, the information obtained about the causal role of specific  
814 brain phenomena, such as cortical oscillations, is limited, because there is no obvious way to  
815 control these activities. Triggering TMS based on the current brain state can directly probe the  
816 role of different cortical functions. There has been some confusion regarding the terminology  
817 when it comes to brain-state-dependent *vs.* -independent and closed- *vs.* open-loop TMS (for a  
818 recent discussion see [177]). Triggering TMS in real-time, based on particular EEG features  
819 (e.g., oscillatory phase and amplitude of specific frequency bands), allows brain-state-dependent  
820 TMS as compared to brain state-independent TMS. The latter is when TMS is applied through  
821 some predefined sequence (e.g., with a certain ISI  $\pm$  some jitter) and therefore disregarding the  
822 current brain state. Beyond brain-state-dependent stimulation, closed-loop operation requires that  
823 a particular parameter of a system is monitored continuously and that TMS parameters (control  
824 signals) are adjusted (e.g., intensity and timing of TMS) accordingly to achieve, maintain, or  
825 change the monitored parameter as desired (e.g., aiming at a particular kind of brain state). The  
826 prime example of a closed-loop is a thermostat that measures the temperature and modifies the  
827 flow of hot water to a radiator to reach and maintain a preset temperature value. However, if the  
828 control signal does not change the monitored parameter (e.g., if TMS does not change the

829 monitored brain state), and if this change does not feed back to the stimulation parameters, the  
830 loop remains open [178]. All studies published so far, therefore, represent at best open-loop brain  
831 state-dependent TMS–EEG since TMS-related EEG artifacts and peripheral co-stimulation  
832 evoked/induced responses currently still prevent continuous EEG monitoring in real-time.

833

834 An open-loop real-time approach is represented by the TMS pulse to the brain delivered at a  
835 predefined brain state (e.g., phase), implying that the induced brain response (e.g., TEPs) does  
836 not influence the characteristics of the next TMS pulse. In essence, the state of the brain is used  
837 to guide the TMS, delivered based on a parameter decided a priori, allowing an improvement in  
838 testing the brain response in specific conditions. The other approach is defining a closed-loop,  
839 which implies controlling the brain state via TMS to reach and maintain the TMS-induced  
840 response within a predefined range. In this condition, the induced brain response provides  
841 feedback for adjusting the TMS parameters via a feedback loop [179].

842 In this context, EEG–TMS (i.e., TMS guided by EEG) can be used to characterize the  
843 physiology of endogenous oscillations, both in terms of phase-dependent excitability (e.g., which  
844 phase of the sensorimotor  $\mu$ -rhythm corresponds to maximum corticospinal excitability) [180-  
845 183] but also phase-dependent plasticity [181, 184]. The promise of such EEG-triggered TMS  
846 protocols is not only that a stronger and more reliable plastic response may be achieved at the  
847 site of stimulation, but also that specific neural pathways may be modulated, when synchronizing  
848 the stimulation with EEG-derived brain connectivity states.

849 In terms of signal processing, whereas the pre-stimulus EEG period is unaffected by the TMS  
850 artifact, averaging cannot be used in the same way to remove random noise. Since each trial must  
851 be considered individually, signal quality issues (baseline fluctuations, eye blinks, periods of low  
852 amplitude in the oscillation of interest, etc.) are critical. Especially slow drifts caused by the  
853 previous TMS pulse when recording in DC mode can be problematic; this needs to be considered  
854 in the preparation and online signal processing pipeline.

855 When using oscillatory brain activity as a “state marker” to trigger TMS, the state effects will  
856 critically depend on the method used to capture the ongoing oscillatory activity [183]. Due to the  
857 limited spatial resolution of EEG, the oscillatory activity at the sensor level may reflect a mixture



858 of activity from various cortical regions rather than being generated locally in the cortex targeted  
859 by TMS [185].

860

#### 861 **4. The artifact problem in TMS–EEG: non-physiological and physiological signals**

862 The TMS pulse can induce different artifacts, which can be of non-physiological or physiological  
863 nature. These artifacts can be time-locked or non-time-locked to the TMS-pulse. Both have been  
864 described in several publications [27, 28, 85, 186-188]. In this section, we review known EEG  
865 artifacts generated by TMS, clarify their nature and present possible solutions to deal with them.

866

##### 867 **4.1. Non-physiological artifacts**

868 Non-physiological artifacts are induced by the TMS pulse, and their origin is electromagnetic or  
869 mechanical.

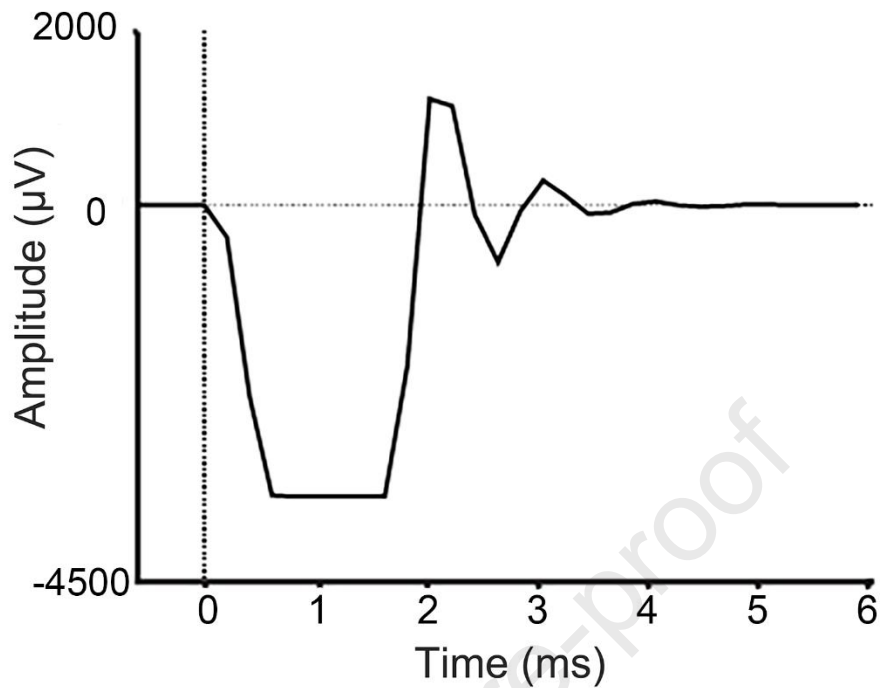
870

##### 871 **4.1.1. Pulse artifact or electromagnetic artifact**

872 This is the largest artifact generated by the TMS pulse (**Fig. 4**). It is electromagnetic in nature  
873 and is produced by the electromotive force induced in the loops formed by EEG electrode leads.  
874 It can be up to several volts, masking the brain signals and saturating EEG amplifiers, limiting  
875 the use of simultaneous TMS–EEG.

876

877 *Solution:* this artifact cannot be avoided; however, TMS-compatible EEG amplifiers have been  
878 developed, allowing one to handle this artifact (see **Supplementary Materials** for a list of  
879 TMS–compatible EEG systems). The best strategy we have is to reduce the pulse artifact  
880 duration to its minimum. As explained before, a sufficient dynamic range, adequate sampling  
881 frequency, and high-enough cut-off frequency for the anti-aliasing low-pass filters can reduce the  
882 artifact duration significantly.

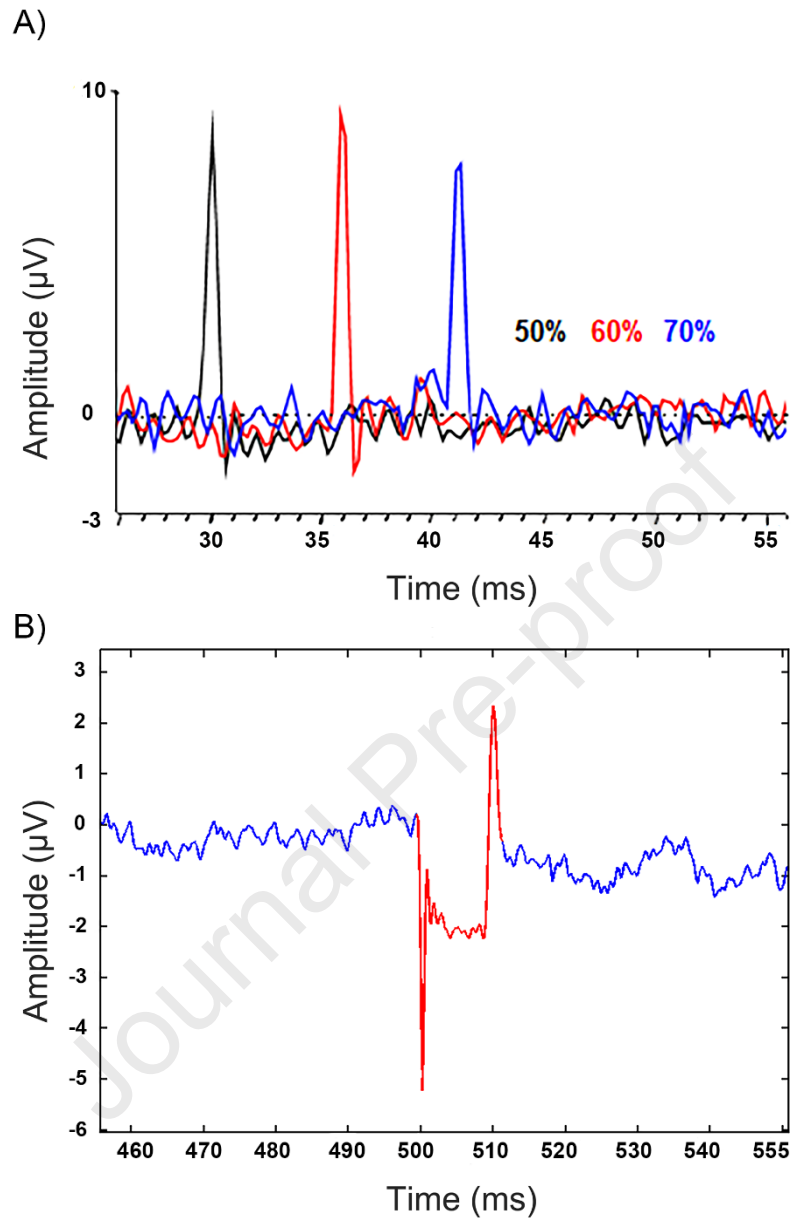


883  
 884 **Fig. 4.** TMS pulse artifact recorded using a sampling rate of 5 kHz and an anti-aliasing low-pass filter of 1 kHz  
 885 (resulting in filter ripples or ‘ringing’). In addition, signal saturation can be observed for the first large negative  
 886 deflection around 1 ms.

887

#### 888 4.1.2. TMS Recharge artifacts

889 This artifact is produced when the capacitors, which store the electric charge required for TMS,  
 890 are recharged. The recharge artifact can look like a spike, an abrupt signal jump, an exponential  
 891 decay, or a waning high-frequency discharge, depending on the TMS device used (**Fig. 5**). This  
 892 artifact can corrupt the EEG recordings and be mistakenly interpreted as a brain signal,  
 893 particularly if low-pass filtering is applied or TFRs are calculated before inspecting the data.



894

895

896 **Fig. 5.** Example of recharge artifact. A) When the recharge delay is not set by the experimenter, the Magstim  
 897 Standard Rapid<sup>2</sup> generates a recharge artifact that peaks at different latencies depending on the stimulation intensity.  
 898 In this example, the artifact peaked at 30, 36, and 42 ms after the pulse delivery at an intensity of 50, 60, and 70% of  
 899 MSO respectively. Note that the amplitude of the artifact does not change with the intensity. B) Recharge artifact  
 900 caused by the MagVenture MagPro X100 when the recharge delay is set at 500 ms from the pulse delivery  
 901 (Modified from [https://www.fieldtriptoolbox.org/assets/img/tutorial/tms-eeg/art\\_recharge\\_2.png](https://www.fieldtriptoolbox.org/assets/img/tutorial/tms-eeg/art_recharge_2.png)).

902

903 *Solution:* in newer TMS stimulators, the timing of the capacitor recharge can be manually  
 904 adjusted; therefore, the recharge artifact can be delayed and set to occur outside of the time

905 window of interest. When the stimulator does not allow us to adjust the delay, it is important to  
906 determine the exact onset of the recharging from the manufacturer or by performing phantom  
907 recordings [77] to facilitate the offline removal and interpolation of uncorrupted signals. It is  
908 important to note that, in some TMS systems, the recharge delay may vary depending on the SI,  
909 although there would be a consistent latency at a given SI [77].

910 Additionally, in some devices, brief (few ms) low amplitude spikes may be visible, which are not  
911 time-locked to the TMS pulse but reflect maintenance recharging of the capacitors while idling  
912 (this can be observed in some MagVenture stimulators). Custom modifications of the device  
913 allow to transiently prevent maintenance recharging for time windows of interest. Alternatively,  
914 moving median filters (width of a few ms) allows for post-hoc removal.

#### 915 **4.1.3. Decay artifact**

916 Different authors have referred to this artifact as decay artifact, discharge artifact, or electrode  
917 polarization artifact [28, 34, 186, 187, 189]. In many cases, the electrode–skin interface can be  
918 polarized by electric currents between the electrolyte gel and the recording electrode. When an  
919 electrode is polarized, it might take hundreds of milliseconds after the TMS pulse for the charges  
920 to return to equilibrium. This typically leads to an exponentially decaying charge, the decaying  
921 current being proportional to the remaining polarization voltage [82]. Note that the artifact can  
922 consist of several different decaying components with different time constants.

923  
924 *Solution:* polarization artifacts can be minimized by choosing non-polarizable electrode materials  
925 and electrolyte, as well as by low contact impedance. By ensuring the best possible conductance  
926 between the scalp and the electrode, one can shorten the time constant of the capacitive behavior  
927 of the electrode–skin connection, thus shortening the lifetime of the artifact. Low impedances  
928 (that can be further minimized by mini-punctures of the skin) have been shown to reduce the size  
929 of the pulse and decay artifacts [190]. Decreasing the impedance of the skin dramatically reduces  
930 skin potentials [191]; this is relevant because skin potentials are slow shifts that can lead to an  
931 increase in low frequencies that affect the EEG recordings. Finally, minimizing the impedance of  
932 the skin–electrode interface decreases the thermal voltage noise [192, 193].

933  
934

#### 935 **4.1.4. Electrode motion artifacts**

936 This artifact is very common [194] and is of mechanical origin. It is caused by the movement of  
937 the electrode against the electrolyte gel and of the latter against the skin. This artifact may occur  
938 for several reasons: a) it may result from the vibration of the TMS coil transmitted to the  
939 electrodes via direct contact, as well as repelling magnetic force caused by the electric current  
940 induced in electrode and wires by the magnetic pulse [79, 195]; b) muscle twitch/head  
941 movements induced by the TMS pulse; c) the coil or operator touches the electrodes; d)  
942 movement-related skin stretching causing skin potential shifts [196]. The motion artifacts that  
943 are induced by the pulse delivery either directly (a) or indirectly (b) usually occur within the first  
944 ~10 ms after the TMS pulse and are usually masked by the pulse artifact, the cranial muscle  
945 response, and the decay artifact. As an exception, artifacts generated by skin-stretching resulting  
946 from cranial muscle contractions can last longer [196]. However, as recently reported [197],  
947 artifacts can simply result from the contact between TMS coil and EEG electrodes and affect  
948 both pre- and post-pulse EEG activity.

949  
950 *Solution:* the electrode motion artifact and in general, contact artifacts, can be reduced by placing  
951 a thin layer of foam between the coil and electrodes and wrapping the EEG cap with a  
952 cellophane layer (this is done in some labs, although one should make sure that no additional  
953 artifacts are induced by sweating) and/or an elastic net bandage. 3D printable spacers for  
954 separating the TMS coil from the electrodes to prevent electrode movement have been designed  
955 and tested [197].

#### 956 957 **4.2. Physiological artifacts (TMS-locked)**

958 Eye blinks, cranial muscle twitch, auditory responses to the coil click, and SEPs, are all  
959 physiological but unwanted signals that can be induced by the TMS pulse. These responses are  
960 true physiological signals that can confound the true TEPs, i.e., the neuronal response to the  
961 transcranial stimulation of the brain tissue, and complicate their interpretation (see **Section 3.5**).

#### 962 963 964 **4.2.1. Eye blinks and eye movements artifacts**

965 Eye blinks artifacts occur spontaneously and are very common in traditional EEG recordings.  
966 They result from a strong dipole consisting of positive and negative poles at the front and back of  
967 the eye, respectively. The dipole maintains a strong and stationary electrical field potential,  
968 which extends to the surrounding parts of the head, the field falling off gradually toward the back  
969 of the head [198, 199]. Eye movements slightly modulate the dipole, causing a substantial  
970 deflection in the EEG. Ocular artifacts can be induced by TMS as part of a startle reflex due to  
971 the coil click.

972

973 *Solution:* training of the subject can help decrease TMS-elicited startle-related eye-blink  
974 artifacts. Spontaneous eye movements (not triggered by TMS) are less severe than the TMS-  
975 induced ocular artifacts as the former are not time-locked to the TMS pulse and therefore  
976 statistically independent of TMS-evoked activity and thus easier to remove from the data using  
977 techniques such as ICA. To prevent spontaneous eye movements (not triggered by TMS) during  
978 recordings, a fixation cross could be provided for the subject (if no behavioral task is used).

979

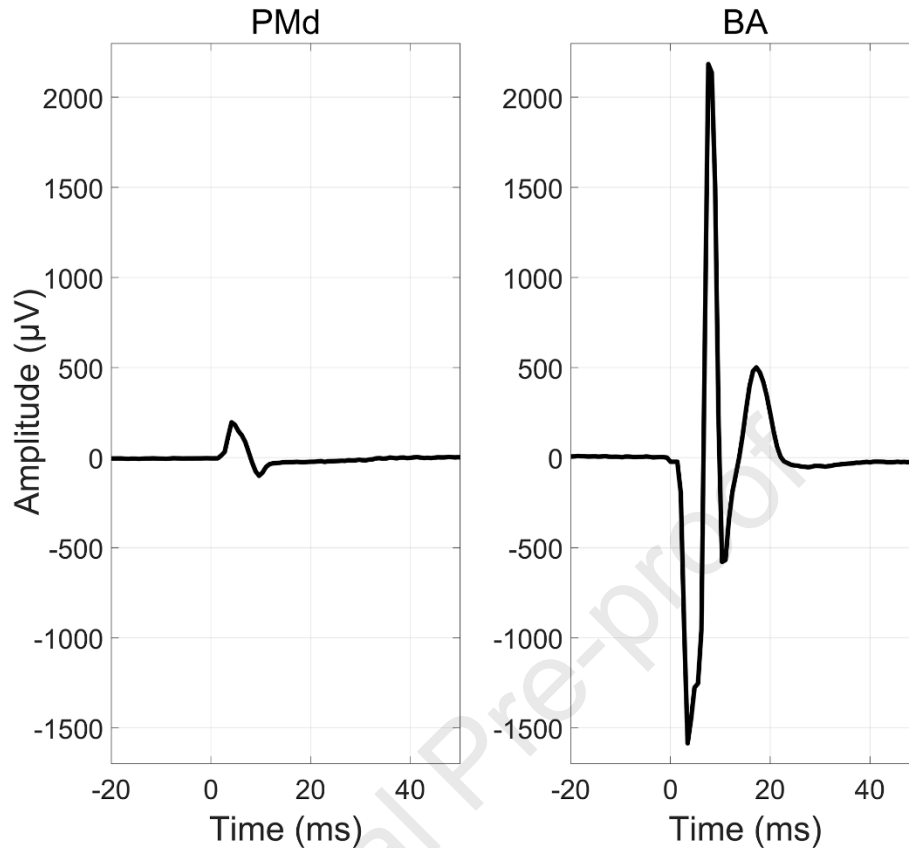
#### 980 **4.2.2. Cranial muscle artifact**

981 These artifacts can be induced by the TMS pulse when muscles innervating the head/face are  
982 stimulated and can strongly contaminate the EEG. They are thus time-locked responses and not  
983 to be confused with the typical muscle artifacts observable in EEG-only recordings, originating  
984 from tonic muscle activity or spontaneous movements. The TMS-evoked muscle artifacts are  
985 often biphasic deflections and up to 3 orders of magnitude stronger ( $\sim$  mV) than the neuronal  
986 responses ( $\mu$ V) with a variable duration that depends on the activated muscle ( $\sim$ 10–30 ms  
987 possibly followed by a slow return to baseline, **Fig. 6**). Muscle artifacts peak within milliseconds  
988 after the pulse delivery, thus heavily affecting the early responses to TMS [75, 200]. These  
989 artifacts may result either from depolarization of intramuscular motor nerve endings or from  
990 activation of cranial motor nerves, such as the facial trigeminal nerves [201]. Therefore, they  
991 represent compound muscle action potentials (just like those in hand muscles when applying  
992 TMS to the median nerve). Most likely to be activated are neck, facial [202], frontal, temporal,  
993 or masseter muscles, depending on the placement of the TMS coil [75, 76]. Consequently, large  
994 artifacts are likely to be elicited depending on the proximity of the TMS target to lateral aspects  
995 of the head [75], language areas such as Broca's and Wernicke's areas (by activation of temporal

996 muscles, e.g., masseter muscle) [200, 203], and dorsolateral prefrontal cortex (by activation of  
997 frontal and orbicularis oculi muscles) [36]. Note that cranial muscle contractions can lead to  
998 electrode movements and stretch the overlying skin, which leads to related disturbances in the  
999 electrode–electrolyte–skin interfaces and electrode motion artifacts, respectively. Consequently,  
1000 the topography of decay and muscle artifacts is often coupled, with particularly large/long decays  
1001 for electrodes overlying cranial muscles.

1002  
1003 *Solution:* one practical solution to reduce muscle artifacts is to move the location or change the  
1004 orientation of the TMS coil. However, this may not be always possible if the target coordinates  
1005 or research questions are strictly constrained. Reduction of the TMS intensity or use of smaller,  
1006 more focal coils can also be beneficial to decrease muscle artifacts (**Section 3**). However, when  
1007 the muscle artifacts cannot be avoided during TMS–EEG data acquisition, certain artifact  
1008 removal methods can be used offline to remove or suppress the muscle artifacts (see **Section**  
1009 **6.3**).

1010  
1011  
1012  
1013



1014

1015

1016 **Fig. 6.** Muscle artifacts. Waveforms after stimulating the dorsal premotor cortex (PMd), and Broca's area (BA) in a  
 1017 representative subject. Those signals correspond to the responses recorded with electrodes near the respective  
 1018 stimulation sites. The artifacts in both PMd and BA are much larger than the brain signal. The amplitude of the  
 1019 artifacts in BA is about 2500  $\mu\text{V}$ . The artifacts that arise after stimulating lateral brain areas mask the brain signals  
 1020 because they can be several orders of magnitude larger than the brain signals and last for tens of milliseconds.

1021

### 1022 4.2.3. Auditory artifacts

1023 The magnetic field generated by the TMS coil produces strong forces on the currents in the coil  
 1024 windings, which results in a loud click. This sound has been shown to produce an auditory  
 1025 evoked potential. These responses are maximally expressed at the vertex, in a time window  
 1026 approximately from 100 to 200 ms, and can confound TMS-evoked brain activity analysis [38,  
 1027 156, 163, 167, 204]. Also, general arousal due to TMS or auditory inter-sensory facilitation by  
 1028 the coil click might be present.

1029



1030 *Solution:* auditory responses can be dampened by combining noise masking with hearing  
1031 protection so that the coil click becomes attenuated or imperceptible [38, 41, 173]. Part of the  
1032 sound is still transmitted to the inner ear through bone conduction [162, 163], but this can be  
1033 attenuated using a piece of foam between the coil and the scalp [142]( but see [205] for less  
1034 convincing effects of foam padding). The effectiveness of the auditory dampening/masking  
1035 procedure should be validated empirically for each study. Different set-ups have been previously  
1036 used: a) Masking composed of white noise mixed with specific time-varying frequencies of the  
1037 TMS click (e.g.,[49]), with a specific procedure now available as an open-source toolbox [159].  
1038 b) Earphones playing continuous white noise, where the white noise is always kept below 90 dB  
1039 [142, 206]. c) Earplugs plus ear defenders. d) Earphones playing continuous white noise plus ear  
1040 defenders on top of the earplugs [38, 205]. Another approach to control for auditory confounds is  
1041 to introduce a realistic sham condition and/or comparative strategies (see **Section 3.5**). It is worth  
1042 noting that some of the authors are currently unsure as to whether noise-masking procedures  
1043 themselves affect TEPs (see for example [164, 207]). Finally, new solutions have been  
1044 developed to produce quieter coils [61, 208].

1045

#### 1046 **4.2.4. Somatosensory responses**

1047 TMS may cause somatosensory peripheral co-stimulation via several mechanisms: a) the coil  
1048 vibration can activate mechanoreceptors in the skin, b) the pulse may directly activate local  
1049 peripheral sensory axons, c) entire sensory cranial nerve bundles may be activated (e.g., branches  
1050 of facial, trigeminal, occipital nerves), d) cranial muscle twitch induced by TMS (see previous  
1051 sections) can result in afferent volleys from muscle afferent fibers. This peripheral co-stimulation  
1052 may induce unwanted SEPs and oscillatory responses that are not triggered by the transcranial  
1053 activation of the cortex. However, SEPs have not been fully characterized in the TMS–EEG  
1054 literature, due to difficulties in reproducing the somatosensory stimulation induced by TMS  
1055 independently from cortical activation.

1056

1057 *Solution:* there is no agreed-upon solution to this unwanted signal because the best strategy will  
1058 depend on the aim of the study. As previously pointed out, a foam layer between coil and skin  
1059 can reduce bone-conducted auditory input [163] and might decrease somatosensory activation

1060 induced by coil vibration as well. If compatible with the study design, small changes in TMS coil  
1061 position/orientation may reduce the peripheral co-stimulation of nerve trunks, but in most cases  
1062 do not remove it completely. Additional strategies can include a so-called realistic sham [156,  
1063 167, 209] and/or active control conditions (e.g., [175]) that control for somatosensory confounds  
1064 by experimental design (but see **Section 3.5** for a discussion on the limitations of the different  
1065 approaches).

1066

### 1067 **4.3. Other artifacts**

#### 1068 **4.3.1. Artifacts unrelated to TMS**

1069 In addition to TMS-induced artifacts, other events may disturb the EEG recordings. These  
1070 include electrical interference from radio broadcasts, mobile phones, computer monitors, line-  
1071 frequency currents, pumps, air conditioning, elevators, etc. Therefore, nearby electrical  
1072 equipment can interfere directly with the EEG system, especially if grounding arrangements in  
1073 the laboratory have not been done correctly, for example if there are ground loops. Physiological  
1074 artifacts, such as electrocardiographic and respiratory signals, tonic and phasic muscle activity,  
1075 spontaneous movements (including blinking and swallowing), and sweating, can also  
1076 contaminate the EEG recordings. EEG can also suffer from skin potentials and thermal noise  
1077 (see **Section 4.1.3**).

1078

1079 *Solution:* some of these artifacts can be removed by using electrically shielded rooms or offline  
1080 filtering, the latter *only after the TMS artifact has been removed* (**Section 6.2**). The main  
1081 recommendation is to keep any devices that cause noise far from the EEG cap and to instruct the  
1082 subjects to delay any form of voluntary motor activity outside the time windows of interest.  
1083 Reducing the contact impedance between the skin and the electrode also helps to remove the  
1084 common mode accurately to suppress the amount of line noise coupled to the EEG leads [210].  
1085 In addition, if a laptop is used to record EEG data, some authors recommend unplugging the  
1086 laptop during the recording. However, this has not been systematically tested and might depend  
1087 on the EEG system. Also, using notch filtering during data preprocessing can significantly  
1088 reduce electrical noise, but see Section 6.2 (Temporal filtering) for filters-related issues.

#### 1089 **4.3.2. Filtering artifacts**

1090 Typically, the filters applied to EEG are designed to attenuate noisy and uninteresting  
1091 frequencies. For example, low-pass filtering is used to remove high-frequency signals from the  
1092 data. Filter design is often based on the assumption that the target signal power and phase  
1093 content are stationary. When the assumption is violated, for example when the signal presents  
1094 sudden changes, such as steps, peaks, or deflections, artificial oscillatory activity in the data  
1095 around these phenomena may be caused; this is often termed ringing [211]. One can  
1096 unintentionally interpret such oscillations as brain-produced EEG activity. In TMS-EEG,  
1097 filtering over the pulse artifact and the evoked EEG signal can induce ringing around the short-  
1098 term events. This also applies to any residual artifacts or discontinuities that might be introduced  
1099 in the signal during data analysis. For example, filtering of the EEG signal after interpolation  
1100 used to remove the pulse artifact can induce ringing if the timepoint post pulse is not at baseline  
1101 level (see **Section 6.2**) because of cranial muscle or decay artifact.

1102

1103 *Solution:* during data acquisition, any unnecessary low-pass filters should be avoided and the  
1104 cut-off of the (often implicitly applied) anti-aliasing low-pass filter increased by using  
1105 appropriate sampling frequencies. During data analysis, both finite-impulse response (FIR) and  
1106 infinite-impulse response (IIR) filters may induce ringing, but in general, IIR filters are more  
1107 vulnerable to rapid events than FIR filters, and higher-order filters are more sensitive than those  
1108 of lower-order. It is noteworthy that any downsampling requires anti-aliasing low-pass filtering.  
1109 Thus, downsampling should be avoided before the abrupt high-amplitude artifacts are removed  
1110 from the data.

1111

1112 There are also filtering techniques specifically tailored for discontinuous/non-stationary data.  
1113 Robust detrending [212] applies polynomial fitting for trend detection after excluding the poorly  
1114 fitting data (with spikes/steps, etc.). This type of detrending is applicable for TEPs as well. To  
1115 diminish the amplitude of ripple (rapidly changing noise) signal in single-trial TEPs, Wiener-  
1116 estimation-based filtering can also be used [213].

1117

1118 It should be critically considered whether filtering is required to answer the research question at  
1119 hand. If so, before temporal filtering, spatial filtering or other techniques must be used to remove  
1120 the TMS-related artifacts. After filtering, it is good practice to visually verify that the filtered and

1121 original signals are aligning sensibly, as residual artifacts or signal discontinuities can produce  
1122 considerable ringing if filtered.

1123

## 1124 **5. TMS–EEG preparation**

1125 *The best way to deal with artifacts is to avoid them* [186]. Therefore, the first step to recording  
1126 good quality data is to perform high-quality experiments. While many steps for standard EEG  
1127 preparation can be applied to TMS–EEG (for a comprehensive guide to record EEG data see  
1128 [214]), additional steps are required to minimize the impact of confounding factors and artifacts  
1129 introduced by TMS. In **Section 4**, we described these artifacts and have already reported some  
1130 specific requirements for TMS–EEG preparation, e.g., very low impedances ( $< 5 \text{ k}\Omega$ ),  
1131 positioning of reference and ground electrodes far from the stimulation target, proper selection of  
1132 the EEG amplifier settings (hardware filtering bandwidth, sampling rate, amplitude resolution).  
1133 In this section, we present a summary of the procedures carried out across different laboratories  
1134 and describe several steps that can be considered to improve data. Tips reported in this section  
1135 are based on a short survey carried out among the authors of the paper (full results can be found  
1136 in the **Supplementary Materials**).

1137

### 1138 *EEG Preparation*

- 1139 1) Before placing the EEG cap, cleaning the forehead, the skin around the eyes, and  
1140 locations where the reference and ground will be placed with an isopropyl alcohol pad  
1141 will help lower the impedance. For the reference and ground electrodes, some of the  
1142 authors gently abrade the skin with sandpaper or abrasive gel after (or before) the area  
1143 has been prepped with an alcohol pad (see question 4 in the survey).
- 1144 2) As for any EEG study, it is important that the EEG cap tightly fits the participant's head.  
1145 It may be helpful to measure the size of the head before the recording as described by  
1146 Farrens et al. [214]. If the 10–20 system is used for reporting electrode locations, the Cz  
1147 electrode should fall exactly halfway between nasion and inion and halfway between the  
1148 left and right preauricular points, the central line should be straight and on the midline.  
1149 Importantly, always check the EEG cap condition (e.g., dirty/broken channels, etc.).
- 1150 3) The placement of ground and reference varies across laboratories and depends on the  
1151 stimulation site, the amplifiers, and on whether the available EEG system allows

- 1152 choosing their position (see survey for a brief overview). Placing the reference far from  
1153 the TMS coil is advisable to reduce interference and to avoid spreading high-amplitude,  
1154 TMS-locked artifacts to all channels [77]; this seems to be a popular choice (survey  
1155 question 22). For instance, if the TMS pulse is delivered to the left M1: a) the reference  
1156 electrode can be placed on the right mastoid and the ground electrode over the right  
1157 cheekbone; b) the reference electrode to the right mastoid and the ground electrode next  
1158 to it. c) reference and ground electrodes on the forehead. In any case, ensure that a stable  
1159 signal can be obtained from the reference electrode. Central midline channels are often  
1160 used as a reference in EEG research to achieve a tight fit, little movement, no underlying  
1161 muscles, etc.
- 1162 4) Additional electrodes can be used to record electrooculogram (EOG), cardiac, and  
1163 muscular responses. Electrodes for horizontal and vertical EOGs can be placed as  
1164 described by Farrens et al. [214]. The required number of electrodes depends on the aim  
1165 of the study (questions 7, 8).
- 1166 5) Preparing cap-electrode contacts is a standard procedure in EEG experiments. This can  
1167 be done using abrasive electrode paste and/or conductive gel (question 9).
- 1168 6) Electrode impedances are crucial in TMS–EEG studies. There seems to be a consensus  
1169 on keeping this value  $\leq 5 \text{ k}\Omega$  (survey question 12).
- 1170 7) Once all the electrodes have been prepared, an additional check is to ensure the EEG  
1171 system is recording the signal. Standard practice is to ask the subject to blink and tense  
1172 the jaw muscles to check that the signals are visible. If all electrodes are noisy, the  
1173 reference and ground could be the problem or external devices might be interfering. In  
1174 addition, some researchers ask the participant to close their eyes to see if the alpha  
1175 rhythm is increased over the occipital electrodes to test that EEG works as expected.
- 1176 8) We can then move to neuronavigation, if available, and perform all the associated  
1177 procedures, such as fixating the head tracker, and registration of landmarks. *Optional:*  
1178 For source analysis, electrode digitization/registration is recommended to construct an  
1179 accurate subject-specific EEG head model.
- 1180 9) A practice performed in some laboratories is to place a thin piece of foam between the  
1181 TMS coil and the scalp to reduce somatosensory and bone-conducted auditory evoked  
1182 responses and electrode motion artifacts. This should be done already when determining

1183 the optimal coil placement and MT, to avoid biasing the SI due to the added thickness of  
1184 the foam ([215]; see survey questions 19, 20).

1185 10) Provide hearing protection to the participant (e.g., earplugs plus ear defenders) and carry  
1186 out the navigation to find the hot spot (see **Section 4.2.3**).

1187 11) Find the SI (**Section 3.2**). It is worth mentioning that if masking noise is used, it might be  
1188 appropriate to calculate the SI while playing the noise.

1189

### 1190 **5.1. Online/pseudo-online monitoring of TMS-evoked EEG**

1191 Once the EEG and neuronavigation have been prepared, and the TMS target (hot spot) and SI  
1192 set, a recommendable step before starting TMS–EEG recordings consists of "*online or pseudo-*  
1193 *online monitoring for data quality*".

1194 1) Some EEG systems have online interfaces to monitor the quality of the TEPs, in other  
1195 cases, a simple MATLAB or Python script can be implemented to look at the data offline,  
1196 or real-time TEPs visualization toolboxes can be used [34, 216].

1197 2) At this point, noise-masking can be provided if necessary (see **Section 4.2.3** for  
1198 alternative solutions to control for the auditory artifact). White noise with ear defenders  
1199 or earplugs plus ear defenders can be used. Note that the defenders or headphones may  
1200 interfere with the coil positioning, depending on the area being stimulated.

1201 If white noise is used, this should be adjusted to mask the coil click. This can be done by  
1202 increasing the volume of the noise until participants can no longer hear the click. If  
1203 responses are present, then adjust the masking noise parameters and do the step again.  
1204 Details on this procedure can be found in the recent work of Casarotto et al. [34] and  
1205 Russo et al. [159]. However, depending on SI and the particulars of the individual  
1206 subject, some may not be able to tolerate the noise-masking at volumes sufficient to  
1207 completely mask the TMS pulse stimulus.

1208 3) Changing the electrode wire arrangement to minimize the effective areas of loops formed  
1209 by electrode wires (and the head) can reduce the TMS-induced artifacts [217]. While  
1210 optimal cable positions may not be achievable due to the complex shape of the magnetic  
1211 field and the geometry of the human head, it may be worth optimizing cable locations for

1212 the most crucial electrodes (i.e., those at the stimulation site, and reference, and ground;  
1213 see survey questions 16, 17).

1214 4) An online or offline graphical user interface (GUI) can be used to monitor the quality of  
1215 the EEG signals [159, 216]. For example, one could deliver 10–20 TMS pulses and look  
1216 at the average responses to check the EEG quality. Then, if needed, cable orientation can  
1217 be changed as well as small adjustments in coil position and/or orientation, if this does  
1218 not affect the study protocol. Looking at average responses allows us to evaluate whether  
1219 the impact of TMS on the cortex is strong enough to elicit a measurable response. For the  
1220 online approach before looking at average signals, it is necessary to look at single-trial  
1221 data and possibly reduce muscle artifacts. This procedure has been fully described in  
1222 Casarotto et al. [34].

1223 5) Once the artifacts have been reduced and the TMS–EEG responses are acceptable, some  
1224 experiments may benefit from placing a plastic wrap and/or a net bandage around the  
1225 cap. The plastic wrap prevents the electrodes from drying out during very long  
1226 recordings, direct electrical contact between TMS coil and gel, and gel smearing by coil  
1227 movements. Of note, avoid moving or touching the navigation tracker; you can make a  
1228 hole in the plastic film to go through the tracker. The wrap and the elastic net also keep  
1229 cables in place (as artifact shape can change when wires are moved, impeding proper  
1230 post-hoc artifact removal). They also slightly press the electrodes against the scalp and  
1231 ensure that proper contact is maintained throughout the recording.

1232

## 1233 6. TMS–EEG data analysis

### 1234 6.1. Linear model in EEG

1235 The linear model that relates the recorded electrical signals (EEG) to neuronal events can be  
1236 described by equation (1).

$$1237 \mathbf{Y} = \mathbf{B} + \mathbf{A} + \mathbf{N}, \quad (1)$$

1238 Here,  $\mathbf{Y}$  is the EEG recorded signal,  $\mathbf{B}$  the brain signals of interest,  $\mathbf{A}$  the sum of the artifacts  
1239 (e.g., TMS-induced artifacts), and  $\mathbf{N}$  is the noise (e.g., background signal) that contaminates the  
1240 recorded data [213, 218].  $\mathbf{Y}$  is a signal matrix whose entry  $Y_{i,t}$  contains the measured value of  
1241 channel  $i$  at time  $t$ . The brain responses,  $\mathbf{B}$ , can be represented as a product of two matrices  $\mathbf{B} =$   
1242  $\mathbf{LS}$ , where  $\mathbf{L}$  is the *lead-field* or *mixing matrix* whose entry  $L_{i,j}$  determines the sensitivity of

1243 channel  $i$  to the source  $j$ , and  $\mathbf{S}$  is the source matrix whose entry  $S_{j,t}$  denotes the *amplitude* of the  
 1244 source  $j$  at a time  $t$  (*the  $j^{\text{th}}$  row  $S_j$  contains the whole-time courses of source  $j$* ). Similarly, the  
 1245 elements  $A_{i,t}$  and  $N_{i,t}$  of matrices  $\mathbf{A}$  and  $\mathbf{N}$  add artifacts and noise to the recorded signal  $Y_{i,t}$ .

1246  
 1247  $\mathbf{L}$  is in general restricted to be sensitive to only those sources that are expected *a priori* to be  
 1248 responsible for the measured signal. Therefore,  $\mathbf{L}$  is made zero in areas where neuronal sources  
 1249 are not assumed to be situated (such as the skull, outside the head, or the white matter). Typically  
 1250 for EEG, the signal is assumed to be produced by postsynaptic currents in the cortex, modeled  
 1251 with a dense grid of discrete current dipoles (typical cortical model consisting of 1000–10000  
 1252 dipoles) [16, 219]. Often, a further assumption is made that, due to their geometrical  
 1253 organization, mainly the pyramidal neuron populations are responsible for the detected EEG  
 1254 signals [23, 219]. Thus,  $\mathbf{L}$  is often defined such that it maps only postsynaptic currents that are  
 1255 orthogonal to the cortical surface. The column vectors of  $\mathbf{L}$  hold the EEG topographies of the  
 1256 possible intracranial postsynaptic sources, whereas a row of  $\mathbf{L}$  describes the sensitivity profile of  
 1257 an EEG channel to all the brain sources.

1258  
 1259 Equation (1) can be further written as

$$1260 \quad \mathbf{Y} = \mathbf{L}\mathbf{S} + \mathbf{L}_A\mathbf{S}_A + \mathbf{L}_N\mathbf{S}_N, \quad (2)$$

1261 where  $\mathbf{L}_A$ ,  $\mathbf{S}_A$ ,  $\mathbf{L}_N$ , and  $\mathbf{S}_N$  are the artifact-mixing-, artifact-signal-, noise-mixing-, and noise-  
 1262 signal matrices, respectively. The columns of mixing matrices define the EEG topographies of  
 1263 different artifact and noise components, whereas the rows of signal matrices contain the time  
 1264 courses of the corresponding components. **Section 6.3** describes the different analysis strategies  
 1265 to separate the recording  $\mathbf{Y}$  into the unknown source, artifact, and noise components present in  
 1266 equation (2).

## 1267 1268 **6.2. TMS–EEG pipelines for analysis**

1269  
 1270 Analyzing the data is another major challenge in TMS–EEG experiments because different  
 1271 experimental arrangements (e.g., EEG amplifiers, electrodes, TMS coils and their positions,  
 1272 TMS electronics, etc.) can result in different artifact profiles. Thus, it is not always possible to  
 1273 use the same pipeline for analyzing data collected with different setups. Furthermore, the



1274 question of which pipeline is most effective in preserving the neuronal signals of interest while  
1275 minimizing artifacts is extremely difficult to answer without ground truth, especially for data  
1276 containing high-amplitude artifacts like TMS-evoked muscle activity, (for a recent review see  
1277 [213, 220]). Nevertheless, some steps are similar across laboratories and should always be  
1278 performed independently of the experimental arrangement. The EEG signals are a linear  
1279 combination of multiple sources (as discussed in **Section 6.1**) and can be explained with methods  
1280 of linear algebra. However, the problem again arises due to the TMS pulse which can produce  
1281 different artifacts complicating this linear relationship. Therefore, TMS–EEG and standard EEG  
1282 analysis differ mainly because we need to change the order of some of the steps. Furthermore,  
1283 once a pipeline has been selected, even changing the order of the steps within the same pipeline  
1284 could change the amplitude and topography of the TEPs [112, 220]. For these reasons, as  
1285 mentioned in **Section 5**, it is crucial to minimize the presence of artifacts during the recording  
1286 session.

1287  
1288 In this Section, we describe commonly used processing steps for TMS–EEG data and outline  
1289 some considerations for each of these steps. The order in which they should be used is out of the  
1290 scope of this paper and has been discussed to some extent in previous papers [112, 213, 220].  
1291 *Here we do not provide or recommend any pipeline for TMS–EEG data analysis.* The different  
1292 offline methods for removing TMS artifacts are discussed in **Section 6.3**.

1293  
1294 The benefits of any signal-processing method depend on the validity of the underlying  
1295 assumptions or knowledge. For example, removing line frequency interference with a narrow  
1296 band-stop filter will not be successful if the suppressed frequency band is not correct. Also, and  
1297 this is particularly important for TMS–EEG, ICA may incorrectly divide the signal into  
1298 components if the underlying components are not sufficiently independent. Here, statistical  
1299 independence means that observation of features of one signal does not provide any information  
1300 about features of the other signal. If TMS elicits both a brain signal and an artifact signal, these  
1301 signals are not independent, because the observation of, say, a TMS artifact informs us about the  
1302 fact that TMS was administered, from which one knows that a brain signal may have been  
1303 elicited as well. In such a case, the benefits of ICA are not guaranteed.

1304

1305 *1. Epoching data around the TMS pulse*

1306 A common early step in processing TMS–EEG data is to epoch the data around the TMS pulse,  
1307 like other event-related EEG paradigms. The amount of data required before and after the TMS  
1308 pulse depends on the intended analysis. For time-domain analysis, sufficient long segments of  
1309 signals are required before the pulse to allow baseline correction and after the pulse to capture  
1310 the TEPs, which can last up to 400–500 ms after TMS. For frequency-domain analysis, enough  
1311 data are required to allow for sliding-window time-frequency decomposition, which needs a  
1312 certain length of data before and after any given time point. For time-domain analysis, epoching  
1313 the data from –500 to 500 ms around the TMS pulse is reasonable, whereas for the frequency  
1314 domain the exact length depends on the frequency of interest and analysis parameters (for  
1315 example, the number of cycles included in the wavelet and frequency of interest).

1316

1317 Another important aspect to consider is “when” epoching is performed. Temporal filtering is  
1318 often applied after epoching and removal of the pulse artifact to avoid ringing around the pulse.  
1319 However, applying filters across epoch boundaries (i.e., the start and end of the epoch) can result  
1320 in additional artifacts due to zero-padding, especially for high-pass filtering. One approach to  
1321 minimize this issue is to include enough data before and after the pulse so that these boundary  
1322 artifacts have time to recover and do not impact data of interest (e.g., the baseline period or the  
1323 TEPs). This could be done by initially having a longer epoch and then redefining the trials after  
1324 high-pass filtering or by ‘mirroring’ the epoch (i.e., flip and concatenate the data at either end of  
1325 the epoch). Alternatively, a solution is to remove the pulse artifact and apply high-pass filtering  
1326 to continuous recordings before epoching [159]. In any case, no high-pass filtering is to be  
1327 applied before the TMS pulse and other high amplitude artifacts have been removed from the  
1328 data.

1329

1330 *2. Removing bad channels/trials:* A common strategy for minimizing noise is to remove the  
1331 affected data from the signal. For example, channels can be removed from the data if they have  
1332 become disconnected during recording, or if they show persistent artifactual activity due to poor  
1333 contact, ongoing muscle activity, or contact with the TMS coil. In addition, individual  
1334 epochs/trials can be removed if they are affected by artifacts such as excessive muscle activity  
1335 (e.g., due to jaw clenching, swallowing, or activation of facial muscles), large blinks or eye

1336 movements, and other movement artifacts (e.g., if the participant moved or scratched their head).  
1337 Strategies for selecting which channels/trials to remove vary from manual methods in which the  
1338 experimenter visually assesses the data and decides which channels/trials to remove, to  
1339 automated methods which use features of the signal and statistical approaches to identify  
1340 artifactual data for removal, to combined automated/manual approaches.

1341

1342 While removing affected data is a highly effective strategy for reducing noise, it also comes at a  
1343 cost. For example, if an artifact is present across many channels/trials, then a large amount of  
1344 data will be removed, leaving little data containing the signal of interest. This can pose a  
1345 particular problem for TMS–EEG signals which often contain many contaminated channels in  
1346 the vicinity of the stimulation target, which often also overlay the region of interest on the cortex.  
1347 Removing (or topographically interpolating) channels also reduces the rank of the signal, which  
1348 can impact subsequent processing steps such as ICA. Furthermore, removing channels often  
1349 results in an unbalanced montage across the scalp, which invalidates the assumptions of average  
1350 re-referencing and therefore requires additional processing steps to interpolate the missing data,  
1351 see Section *interpolate removed channels*. Also, many types of artifacts can effectively be  
1352 removed using ICA (e.g., eye blinks, muscle noise, etc.), and removing entire trials or channels  
1353 beforehand may unnecessarily sacrifice those data. On the other hand, ICA may be occupied by  
1354 single bad electrodes or trials, reducing the ICA’s capacity for capturing other, more relevant  
1355 artifacts. Therefore, sometimes a tedious iterative process of artifact rejection and ICA  
1356 application may be required,

1357

1358

### 1359 *3. Removing and interpolating the TMS pulse artifact*

1360 The time-varying magnetic field of TMS results in a high-amplitude pulse artifact in EEG  
1361 recordings. The most common approach to deal with TMS pulse artifacts is to remove and  
1362 replace the affected data. There is no consensus on the time window to be interpolated, as the  
1363 pulse artifact duration depends on the EEG system and set-up, in particular the sampling rate and  
1364 related anti-aliasing low-pass filter, but usually, the interpolation starts 1–2 ms before the pulse  
1365 and lasts up to 5–10 ms after the pulse, either on epoched or continuous data. This step is not  
1366 required in EEG systems that use sample-and-hold circuits (e.g., the Nexstim EEG system).

1367

1368 To avoid additional artifacts, it is crucial to replace the removed data with cubic interpolation  
1369 rather than linear interpolation [187, 221]. As the EEG signal in the first milliseconds after the  
1370 TMS pulse may not be at baseline level when early-latency artifacts are present (e.g., electrode  
1371 polarization/decay artifacts, TMS-evoked muscle artifacts, etc.), linear interpolation can generate  
1372 a transient in the data and result in ringing artifacts or spurious power in TFRs following  
1373 temporal filtering. Replacing the missing data with interpolated data generated using a cubic  
1374 (instead of a linear) function can help minimize this effect by smoothing the transition between  
1375 the real and interpolated data.

1376

1377 In any case, the smoothness of the data should be carefully inspected after interpolation to ensure  
1378 that no residual artifacts, step responses, and signal discontinuities exist. If necessary,  
1379 interpolation duration needs to be extended or its method changed to obtain better results. If  
1380 spatial filters or other artifact removal techniques follow, interpolation may be repeated/refined  
1381 thereafter, when the removal of muscle/decay artifacts may have minimized the vertical offset of  
1382 the interpolation endpoint in the post-TMS period.

1383

1384 It is noteworthy that the interpolated data segment must not be used as input for ICA or principal  
1385 component analysis (PCA). As interpolated data is artificially generated, it can also affect these  
1386 statistical methods in unpredictable ways. It is thus good practice to simply cut out the  
1387 interpolated data windows before feeding data into a spatial filtering method and use them only  
1388 for visualization or when required for temporal filtering.

1389

#### 1390 *4. Re-referencing the data (mean reference/average reference)*

1391 As for EEG recordings, data are usually recorded against a single reference electrode and are  
1392 often re-referenced against either the common average of all cephalic electrodes or a non-  
1393 cephalic reference (such as linked mastoids or earlobes) to allow topographical interpretation of  
1394 the signals. Note that the common average reference is most widely used, but artifacts from bad  
1395 channels might thereby spread to all other channels, and these must be removed (or excluded)  
1396 beforehand; also note that the removal of bad channels may result in an asymmetry of the  
1397 common average reference. Therefore, interpolation of removed channels may be necessary

1398 before common average reference. The use of a common average reference is also useful to  
1399 compare data across laboratories since the positioning of the physical reference may vary (for a  
1400 comprehensive discussion about referencing see [219]).

1401

#### 1402 *5. Baseline correction*

1403 Another common step in TMS–EEG analysis is to ‘zero’ or ‘baseline correct’ the data by  
1404 subtracting a given value from all data points, thereby centering the voltage from each electrode  
1405 around a common reference value. For TMS–EEG data, the baseline correction should be in a  
1406 time window that does not contain the TMS pulse (for instance, –500 to –10 ms). Baseline  
1407 correction is necessary because factors such as skin hydration and static charges in the electrodes  
1408 may cause an offset in the EEG recordings. Furthermore, this step can be quite important as  
1409 TMS–EEG data are often collected without a high-pass filter (i.e., with amplifiers in direct  
1410 current or DC mode), meaning that the ‘baseline’ voltage can differ substantially between  
1411 electrodes and their signals are often not at 0 V. The most common approach for removing  
1412 offsets in the data is to subtract the average of the baseline period before the TMS pulse (baseline  
1413 correction), however, other approaches include subtracting the average of the entire epoch  
1414 (demeaning the data), subtracting a linear or polynomial function fit from the epoch (detrending  
1415 the data), or applying a high-pass filter to remove the low-frequency aspects of the data including  
1416 any offsets. While demeaning and detrending based on the full trial are advisable before  
1417 calculating time-frequency representations to prevent power from slow frequencies and DC  
1418 offsets ‘bleed’ into other frequency bins [218], they are typically discouraged for ERP and  
1419 therefore TEP analyses. Care should also be taken when demeaning or detrending the data if the  
1420 TMS pulse/muscle/motion artifact is still present as the large amplitude deflections can influence  
1421 the average, or the model fit to the data. In addition, the TEPs can be asymmetric and DC offsets  
1422 may be introduced by the TMS pulse, so detrending may introduce spurious trends in the post-  
1423 TMS period.

1424

#### 1425 *6. Dealing with large amplitude artifacts*

1426 High-amplitude artifacts can have a detrimental effect on temporal filters, by generating ringing  
1427 artifacts; and on blind source separation approaches like ICA, by biasing the spatial weightings  
1428 of neuronal components.

1429 Several approaches have been developed to suppress electrode polarization, decay, and TMS-  
1430 evoked muscle artifacts, and to recover the underlying neuronal signals [209]. One approach is to  
1431 fit a model representing the artifact to the signal and then subtract the best fit of the model from  
1432 the data. To fit the decay artifact, linear models, single and double exponential models, adaptive  
1433 algorithms which select the best fit between linear and exponential models, and biophysical  
1434 models of the skin/electrode interface (second-order power-law) have been used [81, 152, 185,  
1435 219]. Another approach is to use blind source separation algorithms such as ICA or PCA to  
1436 separate the EEG signal into different components based on temporal or statistical relationships  
1437 within the data. The signal is then reconstructed after removing components thought to represent  
1438 the artifacts. As the amplitude, time-locked nature, and spatial overlap of these artifacts can  
1439 violate (or at least weaken) some of the assumptions of common ICA and PCA methods, several  
1440 approaches have been suggested specifically for TMS–EEG data. Some examples include the  
1441 enhanced deflation method (EDM) of ICA [196], PCA suppression [199], mean-subtracted ICA,  
1442 momentary-uncorrelated component analysis (MUCA) [220], signal space projection [221],  
1443 signal space projection with source informed reconstruction (SSP-SIR) [214], the SOUND [217],  
1444 etc. See **Section 6.3** for a complete list of artifact removal methods.

1445  
1446 One of the debated questions in the field is whether ICA or PCA should be used to clean the  
1447 data. In PCA, the components are set to be uncorrelated, but the decomposition by  
1448 uncorrelatedness is not unique, so the PCA solution is to some extent arbitrary. ICA on the  
1449 contrary aims to decompose the EEG data into unique components (artifactual and neural) that  
1450 are independent. In practice, PCA is useful in giving a set of topographies defining a subspace  
1451 within which the artifacts are estimated to lie. However, this same subspace also contains neural  
1452 data, and PCA does not provide any spatial filters that can differentiate the pure artifact signals  
1453 from the whole data. ICA does yield spatial filters in the form of the demixing matrix, which  
1454 could give ICA an advantage over PCA. The downside is that the ICA assumptions are rather  
1455 strict: in addition to independence, the data should be stationary (non-time-dependent), the  
1456 number of components should stay small (in practice, the same or lower as the data  
1457 dimensionality, often around 30-40), and the physical component-generation for each component  
1458 should stay the same for producing a fixed topography. These assumptions are violated by many  
1459 TMS-evoked artifacts, which can bias the ICA results. Of note, to date we do not know which

1460 artifacts are compatible with the ICA assumptions. A significant practical problem is that,  
1461 currently, we have no tools to test for the goodness of either ICA or PCA in cleaning TEPs, i.e.,  
1462 we lack the ground truth to assess to what extent neural responses are preserved and artifactual  
1463 signals removed. These assumptions are violated by many TMS-evoked artifacts, which can bias  
1464 the ICA results. A significant practical problem is that currently, we have no tools to test for the  
1465 goodness of either ICA or PCA in cleaning TEPs, i.e., we have no ground truth to assess to what  
1466 extent neural responses are preserved and artifactual signals removed.

1467

### 1468 *7. Dealing with auditory and somatosensory evoked responses (Peripheral-evoked potentials-* 1469 *PEPs) in the TMS–EEG*

1470 Some of the offline approaches presented in the previous section have been suggested for dealing  
1471 with PEPs, which include both somatosensory and auditory responses. These approaches include  
1472 subtracting or regressing a sensory control condition from the TEPs [209], removing components  
1473 representing PEPs using ICA (at least for the auditory component, [36, 222]), and using a variant  
1474 of SSP-SIR with a sensory control condition [223] (see **Section 3.5** for a full discussion on these  
1475 issues).

1476

1477 Some of these methods can be applied within the TMS–EEG cleaning pipeline (e.g., ICA), while  
1478 others necessitate a separate step after the cleaning pipeline and may also require the acquisition  
1479 of data for an experimental control condition.

1480

### 1481 *8. Temporal filtering*

1482 Temporal filters (low-pass, band-pass, and band-stop “Notch” filters) should be used only after  
1483 removing the TMS pulse, decay, and muscle artifacts [187, 211, 213]. High-pass, low-pass,  
1484 band-pass, and band-stop filters are often used to remove low-frequency drifts, high-frequency  
1485 noise, and residual line noise from the EEG signal, respectively. Using standard temporal  
1486 filtering to remove the TMS-elicited artifacts is not recommended because short-lasting peaks  
1487 consist of multiple frequencies, making the conventional frequency-based filters inefficient. For  
1488 instance, using a low-pass filter may attenuate the artifact amplitude, but it simultaneously  
1489 spreads lower-than-cutoff frequency oscillations around the peak, which is termed ringing [211].  
1490 High-pass filtering in the presence of the TMS pulse is also problematic and can lead to slow

1491 ringing artifacts around the pulse. Therefore, temporal filtering should only be applied once the  
1492 TMS pulse artifact has been removed.

1493

#### 1494 *9. Interpolate removed channels*

1495 When bad channels are removed, a common practice is to interpolate them. Some approaches  
1496 consist of using spline interpolation of surrounding channels or related methods. The source-  
1497 informed reconstruction (SIR) allows for interpolation of the channels based on the cortical  
1498 current estimates based on the non-contaminated channels [218, 224]. Channels can be removed  
1499 and interpolated from individual trials as opposed to the entire recording, thereby minimizing  
1500 data loss. Of note, removing or replacing bad channels reduces the dimensionality of the data,  
1501 which may impact further analysis, for instance, ICA and source analysis.

1502

#### 1503 *10. Averaging across trials*

1504 The TMS-evoked EEG data are aligned to the time-locking event, and the voltages from all EEG  
1505 trials at a given time point are averaged. In other words, the single-trial EEG waveforms are  
1506 summed and then divided by the number of trials.

1507

#### 1508 *11. Downsampling the data*

1509 TMS-EEG data is often collected at high sampling rates ( $\geq 5,000$  Hz) to minimize interactions  
1510 between low-pass filters and the TMS pulse artifact. While this approach helps to reduce the  
1511 length of the TMS pulse artifact, the data files are often large (in the order of GB, although this  
1512 depends on the length of the recording) causing issues with data storage and processing speeds.  
1513 Furthermore, such high sampling rates often greatly exceed those required to capture the TEPs  
1514 which are typically  $< 100$  Hz in frequency, thereby requiring a minimum sampling frequency of  
1515 only 400 Hz to adequately characterize the signal. To reduce file sizes, TMS-EEG data are often  
1516 ‘downsampled’ to a lower sampling frequency (e.g., 500 or 1,000 Hz). An important  
1517 preprocessing step prior to downsampling is to apply a low-pass filter at  $\frac{1}{4}$  of the target sampling  
1518 frequency to avoid aliasing artifacts. Anti-aliasing filters are often automatically applied in  
1519 downsampling functions (e.g., `pop_resample.m` in EEGLAB) and can cause ringing artifacts if  
1520 large deflections are present in the data, such as the TMS pulse artifact. Therefore,



1521 downsampling should be applied only after TMS pulse and other large-amplitude artifacts have  
1522 been minimized/removed from the data.

1523

1524 *What is the optimal order for performing the above steps when processing TMS–EEG data?*

1525 To answer this question, a systematic analysis should be performed where real and simulated  
1526 “ground-truth” data are used. As we have discussed, every step should be applied with caution.  
1527 Perhaps, the most important advice is to make sure the next step in the analysis is not *negatively*  
1528 affected by the previous steps. It is also good practice to check the intermediate results of the  
1529 data processing before drawing any conclusions.

1530

### 1531 **6.3. Methods for removing artifacts from TMS-evoked EEG**

1532 In Section 4, we described the nature of different artifacts and outlined some solutions to avoid  
1533 or reduce them. Unfortunately, following best practices during TMS–EEG preparation and data  
1534 acquisition are not always sufficient to deal with the TMS-evoked artifacts. This issue has led to  
1535 the development of numerous advanced offline artifact removal methods, some of which may  
1536 also be implemented online. However, many publications lack details about the methods, and in  
1537 many cases, the methods are difficult to implement. In this section, we review some artifact  
1538 removal methods. For a more detailed explanation and mathematical framework of these  
1539 approaches, we refer the readers to the work by Hernandez-Pavon et al. [213].

1540

#### 1541 **What is the best artifact removal method?**

1542 This is a key topic in the TMS–EEG field that has led to the development of several artifact  
1543 removal procedures. While we do not have an answer to this question, all methods are efficient  
1544 to remove the artifacts to some extent, no artifact removal method works perfectly in all  
1545 situations. In the best-case scenario, different methods may be combined to improve their  
1546 performance [213]. While several methods have become widely adopted, it is important to note  
1547 that suppressing high-amplitude artifacts while maintaining the underlying neuronal signal is  
1548 extremely challenging. Currently, we lack empirical data demonstrating the efficacy of these  
1549 approaches in recovering neuronal signals, mainly because we do not have a ground-truth signal  
1550 to benchmark methods against. Therefore, these analytical approaches must be used with  
1551 extreme caution.

### 1552 **6.3.1. Blind source separation**

1553 Blind source separation (BSS) is used to decompose the recorded data into spatial and temporal  
1554 patterns as given by Eq. (2) without using physical modeling of the signal generating processes.  
1555 This differs from source localization where the mixing  $\mathbf{L}$  is derived from modeling the geometry  
1556 and conductivity distribution of the head. Typically, no distinction between source types is made  
1557 within BSS, so we may simply write  $\mathbf{Y} = \mathbf{MS}$ . The sources  $\mathbf{S}$  are referred to as components and  
1558  $\mathbf{M}$  as the mixing matrix. The decomposition is often performed by setting prior assumptions to  $\mathbf{S}$   
1559 by considering the columns in  $\mathbf{S}$  as samples collected from a set of underlying random variables.  
1560 With TMS–EEG, the most often used prior assumptions are the independence and/or  
1561 uncorrelatedness of the components. Other possibilities include, for example, sparsity of the  
1562 components, or finding the smallest number of components capable of explaining the time-  
1563 locked evoked response.

1564  
1565 Since BSS methods do not clarify the origin of the components, after estimating the BSS  
1566 decomposition terms  $\mathbf{M}$  and  $\mathbf{S}$ , the user needs to classify them into relevant categories. This  
1567 classification is based on features of  $\mathbf{S}$ , such as power spectrum, and  $\mathbf{M}$ , such as spatial  
1568 smoothness of the topographies. BSS has proven a practical way of removing artifact  
1569 components from the data. After detecting the artifact components and collecting their mixings  
1570 and waveforms into  $\mathbf{L}$  and  $\mathbf{S}$ , respectively, one can erase them simply by subtracting them from  
1571 the data.

#### 1573 **6.3.1.1. Independent component analysis (ICA)**

1574 ICA is probably the most popular BSS method to remove artifacts from EEG data. ICA has been  
1575 shown to successfully remove a wide variety of artifacts such as blinks, eye movements, muscle  
1576 activity, heartbeats, and electrical line noise [225].

1577  
1578 ICA is a data-driven method that looks for statistically independent components that are non-  
1579 Gaussian [226, 227]. In EEG, the electrodes or sensors record a mixture of electrical responses  
1580 from neuronal sources in the brain and spurious activity such as artifacts. Then ICA, in principle,  
1581 can be used to identify components that represent artifacts based on their topographies, time

1582 courses, and sample distribution. Components representing artifacts can then be subtracted from  
1583 the data [225].

1584

1585 In TMS–EEG, ICA has been widely used to remove artifacts of moderate size [228], and strong  
1586 muscle artifacts after stimulating lateral (e.g., Broca’s and Wernicke’s areas) and frontal areas of  
1587 the brain [200]. One approach is to run a two-step ICA on the TMS-evoked EEG data [36, 222,  
1588 229]. In the two-step ICA approach, the first round of ICA is used to remove electrode  
1589 polarization/TMS-evoked muscle artifacts before a second round of ICA, which is used to  
1590 identify and suppress other artifacts such as blinks/eye movements and tonic muscle activity. The  
1591 rationale behind this approach is to optimize the second round of ICA by first suppressing high-  
1592 amplitude signals, which can result in suboptimal ICA performance, particularly for neuronal  
1593 signals. In contrast, other pipelines use one round of ICA to suppress all artifact types. It remains  
1594 unclear how beneficial the two-step approach is in practice. Of note, the number of ICs cannot be  
1595 higher than the rank of the data matrix because the ICA outcome will not be reliable. This is  
1596 important to consider when using the two-step ICA approach or after bad channels are removed,  
1597 as these steps will lower the rank of the data [213].

1598

#### 1599 **6.3.1.2. Methods based on PCA**

1600 PCA is a method that can be used to reduce the dimensionality of the EEG data, for instance,  
1601 high-dimensional data can be projected to a lower-dimensional subspace by assuming that the  
1602 components that account for a relatively large proportion of variance reflect true signals, whereas  
1603 components that account for relatively little variance reflect artifacts or noise [230].

1604

1605 In TMS–EEG, PCA has been used to remove or suppress TMS-induced artifacts. However, in  
1606 contrast to the belief that components with little variance reflect artifacts, in TMS–EEG data the  
1607 first PCs with larger variance have shown to represent muscle artifacts [200, 203, 231]. Based on  
1608 that finding, one approach consists in rescaling the artifacts to the size of the brain signals by  
1609 suppressing the PCs that represent artifacts [203]. Scaling down the artifact directions rather than  
1610 removing them completely has shown to be beneficial. This method can be applied directly to  
1611 suppress artifacts from TMS–EEG data [232] but also, as a preprocessing step before ICA [203].  
1612 For instance, muscle artifacts are often so large that they may distort the separation of the data to

1613 IC and the neuronal components can be affected. Thus, suppressing the largest PCs before ICA  
1614 can improve ICA performance [203]. Another approach is to use PCA to project out the first PCs  
1615 with a larger variance to remove the magnetic pulse and muscle artifacts [231].

1616

### 1617 **6.3.2. Methods based on signal space projection (SSP)**

1618 Signal-space projection (SSP) is a method for data cleaning in the spatial domain [233]. SSP can  
1619 be used to estimate the artifact topographies and project them out from the data. As seen in Eq.  
1620 (2), both the neuronal and artifact signals consist of time-invariant topographies (the column  
1621 vectors of matrices  $\mathbf{L}$ ) and the corresponding time-varying amplitudes (the row vectors of  
1622 matrices  $\mathbf{S}$ ). Even though the artifactual and neuronal signals might heavily overlap in time and  
1623 frequency domains, there might still be time intervals or frequency ranges that contain only  
1624 artifact signals. The idea of SSP is to utilize these segments of data to estimate the artifact  
1625 topographies to be rejected. For instance, the TMS-evoked muscle artifacts overlap in time and  
1626 frequency with the early cortical responses to TMS. However, muscle activity is seen in EEG  
1627 also at high frequencies (above 100 Hz), which is atypical for neuronal signals. Thus, SSP can  
1628 estimate the muscle-artifact topographies from the high-pass filtered data and project them out  
1629 from the whole TMS–EEG dataset [234]. The key assumption here is that both the high- and  
1630 low-frequency components of muscle artifacts have similar spatial topographies. One  
1631 disadvantage of SSP is its tendency to distort the data spatially. Once the artifact topographies  
1632 are projected out, the rows of the cleaned data do not directly correspond to any of the original  
1633 physical EEG electrodes. Instead, each of the data rows corresponds to virtual EEG channels that  
1634 are sensitive to neuronal EEG signals but insensitive to the suppressed artifacts. In addition,  
1635 projecting out topographies lowers the rank of the data. The distortional effects can be, however,  
1636 taken into account with SIR (see **Section 6.3.5** for details).

1637

1638 In TMS–EEG, SSP has been used to suppress both the TMS-induced muscle artifacts [218, 234]  
1639 and the TMS-pulse related sensory inputs [223]. These approaches have been implemented in the  
1640 open-source TESA toolbox [187, 235].

1641

### 1642 **6.3.3. Source model-based methods**

1643 The neuronal EEG signals have different electromagnetic generators than the various artifact-  
1644 and noise components. Most noise and artifacts originate from extracranial sources and thus can  
1645 show different spatial features. This is depicted by Eq. (2), which shows that each signal  
1646 category has its own lead-field or mixing matrices ( $\mathbf{L}$ ). This characteristic low spatial resolution  
1647 of neuronal signals can also be exploited in TMS–EEG data analysis to separate the neuronal  
1648 components from the various disturbances. With the help of mathematical and numerical tools  
1649 (e.g., [236, 237]), and electromagnetic theory [238], we can forward model the topographies  
1650 generated by different cortical sources and calculate the lead field (Eq. 2). In short, the source-  
1651 model-based methods could be defined as techniques that use the lead field and consecutive  
1652 inverse and forward computation steps to separate artifact signals from the data. One of the first  
1653 attempts was made by Litvak et al. ([189]), who constructed a model matrix containing sets of  
1654 representative artifactual and neuronal topographies, the former being estimated from the data  
1655 and the latter using forward modeling. By solving the inverse problem of the TMS–EEG data  
1656 using the constructed model matrix, the TEPs were separated into neuronal and artifactual  
1657 components. The artifact signals were finally subtracted from the original data.

1658

1659 SSP–SIR belongs to source model-based methods and can be used to project out artifacts and  
1660 interpolate removed channels [218]. SSP–SIR is an extension of the previously described SSP.  
1661 The idea of the SIR step is to extrapolate the removed signal dimensions, and hence recover the  
1662 neuronal topographies distorted by SSP, using consecutive inverse and forward estimations.  
1663 Another method that has proven to be useful for TMS–EEG applications is the SOUND  
1664 algorithm. SOUND finds a spatial filter to cancel out spurious EEG signals such as electrode-  
1665 polarization, line-noise, and electrode-movement artifacts, which are not likely to originate from  
1666 intracranial postsynaptic currents [221]. Recently, SOUND has successfully been tested for real-  
1667 time TMS–EEG data [239]. The spatial filter was updated on a parallel process, while the  
1668 streaming data was cleaned instantaneously with the most recent SOUND filter.

1669

#### 1670 **6.3.4. Modified ICA and BSS**

1671 TMS-evoked EEG signals are time-dependent, which is highlighted by the fact that the averaged  
1672 EEG trials show a time-varying mean. In addition, induced oscillations are known to show  
1673 synchronization (increase in power) or desynchronization (decrease) patterns changing as a

1674 function of time and frequency. In statistical terms, it is said that TMS–EEG data are *non-*  
1675 *stationary* because the statistical properties (e.g., mean and variance) are different at different  
1676 times.

1677  
1678 Commonly, the BSS approaches assume that the input data are stationary and can yield biased  
1679 estimates when this assumption is not met by the data, but it is also possible to design BSS which  
1680 makes use of the changing properties of the data. If components are active at overlapping time  
1681 windows, ICA may not be capable of accurately separating them since they easily become  
1682 correlated and dependent (see [213] for examples). Metsomaa et al. [240] illustrated how simple  
1683 preprocessing of the data makes the data mean-independent, meaning that the mean of the  
1684 underlying components cannot be predicted from other components. Mean-independence is  
1685 sufficient for FastICA and several other ICA methods to separate the signals even if their  
1686 waveforms tend to activate simultaneously [227]. In practice, the artifact amplitude is also  
1687 significantly reduced by mean subtraction [240], which results in numerically stable solutions.  
1688 The requirement is that the average data containing phase-locked activity constitutes roughly the  
1689 same dominant components as the single-trial data.

1690  
1691 Rather than assuming independence, one may make the assumption that the components to be  
1692 separated are uncorrelated. Performing BSS only based on the assumption of uncorrelatedness is  
1693 not a sufficient criterion for getting a unique decomposition. Because of non-stationarity, we can  
1694 set the assumption of uncorrelatedness separately at each time point, which gives us enough  
1695 criteria to perform component separation based on uncorrelatedness only. Metsomaa et al. [241],  
1696 developed MUCA to uncover components that are uncorrelated at each selected time point (or  
1697 time window) after TMS. Additionally, the variances of the components (powers) need to change  
1698 over time points. The benefit of using uncorrelated components rather than independent  
1699 components in BSS is that ICA easily overfits outliers and sparsely occurring activity, making  
1700 the decomposition inaccurate.

1701  
1702 In practice, based on the pre-requisites of MUCA, it is especially suitable for uncovering induced  
1703 oscillations where the power of neuronal oscillators changes with time relative to the TMS onset.  
1704 MUCA does not require filtering, but band-pass filtering may be useful if one is interested in a

1705 particular frequency band. Both MUCA [241] and the mean-subtraction approach [240] are  
1706 suitable for studying trial-to-trial variability in the TEPs/induced oscillations because the  
1707 deterministic (averaged) TEP is not relevant for such interpretations.

1708

## 1709 **7. Toolboxes for TMS–EEG data analysis**

1710 Different toolboxes have been put together to facilitate the analysis of TMS-evoked EEG data:  
1711 FieldTrip [242], TMSEEG [243], TMS–EEG signal analyzer (TESA) [187], Automated aRTifact  
1712 rejection for single-pulse TMS–EEG Data (ARTIST) [244], and The Brain Electrophysiological  
1713 recording and STimulation (BEST) [216]. There has also been an interest in comparing the  
1714 impact of the pipelines used in some of the previous toolboxes on the TMS–EEG signals [112].  
1715 In this section, we present general aspects of different toolboxes and their content.

1716

### 1717 **7.1. FieldTrip**

1718 While the FieldTrip toolbox for MATLAB ([242]; [www.fieldtriptoolbox.org](http://www.fieldtriptoolbox.org)) does not provide a  
1719 GUI nor a fixed predefined pipeline for TMS–EEG analysis, according to its philosophy, a series  
1720 of MATLAB functions accompanied by a detailed tutorial and example datasets are made  
1721 available online ([www.fieldtriptoolbox.org/tutorial/tms-eeg](http://www.fieldtriptoolbox.org/tutorial/tms-eeg)) to support TMS–EEG artifact  
1722 removal (including pulse artifact interpolation and ICA-based removal of muscle/decay artifacts)  
1723 and analyses (TEPs, TFRs, global mean field power, GMFP) according to the pipeline published  
1724 by Herring et al. [49].

1725

### 1726 **7.2. TMSEEG**

1727 The TMSEEG toolbox is a plug-in implemented within EEGLAB on the MATLAB platform  
1728 [243]. This toolbox includes ten steps divided into preprocessing, removing different artifacts  
1729 with two ICA steps, filtering, and data visualization. In particular, the toolbox allows removing  
1730 the TMS artifact by removing the segment of the data where this artifact is present. Then the bad  
1731 channels and trials can be removed, and thereafter two ICA steps can be applied. The first ICA  
1732 step aims to remove the TMS decay artifact, whereas the second step may remove residual TMS  
1733 and general EEG artifacts. TMSEEG makes use of FastICA [227]. The code for TMSEEG is  
1734 available at <http://www.tmseeg.com/downloads/>.

1735

### 1736 7.3. TESA

1737 The TESA toolbox (TMS–EEG signal analyzer) [187] is also a plug-in implemented within the  
1738 popular EEG analysis toolbox EEGLAB [245] on the MATLAB platform. The overarching aim  
1739 of TESA is to provide a standardized library of methods used in TMS–EEG research, thereby  
1740 improving the transparency and reproducibility of TMS–EEG analysis across the field. TESA  
1741 follows the modular format of EEGLAB, allowing the flexible design of analysis pipelines and  
1742 integration with existing EEGLAB functions. As such, TESA does not advocate for any  
1743 particular pipeline but allows users to easily design and compare different analysis approaches.

1744  
1745 TESA includes a broad range of functions coding different analysis steps, including finding the  
1746 TMS pulse artifact; removing and interpolating data around the TMS pulse and recharge  
1747 artifacts; suppressing electrode polarization and TMS-evoked muscle activity artifacts (FastICA,  
1748 EDM, PCA, SSP-SIR, SOUND, linear and exponential models); region-of-interest, peak and  
1749 amplitude analysis of TEPs; and basic TEP visualization [187, 200, 203, 235]. TESA also  
1750 includes heuristic methods for classifying ICA components based on different artifact signal  
1751 features. Each analysis function is represented across two levels: a base function containing the  
1752 relevant analysis code, and a ‘pop’ function that launches a GUI window, allowing users to  
1753 manually modify input parameters without interacting with the MATLAB command line. Users  
1754 can generate the command line function for a given analysis method from the GUI windows  
1755 using the EEGLAB history feature and then use the command line functions to build analysis  
1756 pipelines as MATLAB script files. The GUI implementation of EEGLAB is particularly helpful  
1757 for users not familiar with coding and ensures that methods are available and accessible to all  
1758 members of the TMS–EEG community regardless of their background and skill set.

1759  
1760 The process of converting pipelines to scripts helps to standardize and automate analysis across  
1761 data sets for a given project, minimizing the possibility of errors associated with manual point-  
1762 and-click analysis. Importantly, these pipeline scripts can be published alongside manuscripts  
1763 (e.g., through platforms like GitHub or the open science framework), providing an easy way to  
1764 ensure the reproducibility of published analyses. The code for TESA is available at:  
1765 <https://github.com/nigelrogasch/TESA/releases>. TESA is also supported by an open-access  
1766 online book, the TESA user manual, which details how to use TESA and considerations for



1767 developing TMS–EEG analysis pipelines: <https://nigelrogasch.gitbook.io/tesa-user-manual/>.  
1768 With the help of the TMS–EEG community, it is hoped the TESA library will continue to grow  
1769 as new and improved methods become available.

1770

#### 1771 **7.4. Automated aRTifact rejection for Single-pulse TMS–EEG Data (ARTIST)**

1772 The main difference between ARTIST and the previous toolboxes is that ARTIST is based on a  
1773 fully automated algorithm for single-pulse TMS (spTMS)–EEG artifact rejection [244]. The  
1774 algorithm implemented in ARTIST decomposes the spTMS–EEG data into independent  
1775 components ICs, and then trains a pattern classifier to automatically identify artifact components  
1776 based on knowledge of the spatio-temporal profile of both neuronal and artifactual activities.  
1777 ARTIST consists of three stages, each aimed at removing specific types of artifacts. The first  
1778 stage removes large-amplitude TMS-related artifacts from the continuous data (removes DC  
1779 drift, removes and interpolates the TMS pulse artifact, downsamples, and removes the decay  
1780 artifacts with a one-step ICA). The second stage band-pass filters the continuous data to remove  
1781 the AC line noise and high-frequency noise and then rejects bad epochs and channels from the  
1782 epoched data. The third stage removes the remaining artifacts (for instance, the residual decay  
1783 artifacts, ocular artifacts, ECG artifact, and persistent EMG artifact with a second ICA step) from  
1784 the epoched data after the data are re-referenced to the common average and baseline corrected.  
1785 ARTIST applies a two-step ICA; the ICA algorithm is based on Infomax [226]. The code for  
1786 ARTIST is available at <http://etkinlab.stanford.edu/toolboxes/ARTIST/>.

1787

#### 1788 **7.5. BEST Toolbox**

1789 The Brain Electrophysiological recording and STimulation (BEST) toolbox ([www.best-](http://www.best-toolbox.org)  
1790 [toolbox.org](http://www.best-toolbox.org)) is an open-source MATLAB toolbox with GUI [216], which enables the user to  
1791 easily design, save/load, run, and online analyze multi-protocol/multi-session experiments  
1792 involving a variety of brain stimulation techniques, such as TMS, TES and also transcranial  
1793 ultrasound stimulation. It interfaces with many recording and stimulation devices and can online  
1794 analyze and display the input signals from EMG and EEG and change TMS parameters on the  
1795 fly (via the MAGIC toolbox, [246]), thereby facilitating real-time applications. Besides several  
1796 modules for conducting MEP measurements of all kinds (such as motor hotspot search, threshold  
1797 hunting, MEP measurements, dose-response curves, as well as paired-pulse and double-coil

1798 protocols), the BEST toolbox also supports TEP hotspot search and TEP measurements by  
1799 providing online graphical feedback for re-referenced EEG signals (also lead-fields for arbitrary  
1800 spatial filters can be defined), incremental condition-wise time-locked TEP averages and  
1801 topographical maps of selected TEP components. Future releases are planned to also provide  
1802 real-time artifact rejection methods. The BEST toolbox does not provide a built-in TMS–EEG  
1803 artifact correction pipeline but can interact with all MATLAB-based pipelines or toolboxes. The  
1804 internal data format is based on FieldTrip.

1805

## 1806 **8. Conclusion and future directions**

1807 In this article, we have reviewed the state of the art of TMS–EEG technique. We have covered  
1808 TMS–EEG hardware, preparation, data collection, and analysis. The TMS–EEG field is growing  
1809 rapidly, and we have identified and discussed the challenges of the technique. Our goal is to  
1810 provide a set of recommendations when possible or to provide alternatives for cases where  
1811 standard practices have not been developed. We hope this article will be useful to both  
1812 established TMS–EEG researchers and newcomers in the field and that it will promote the joint  
1813 discussion of key issues and a collaborative effort to find effective solutions.

1814

1815 **Conflicts of Interest:** PJ has received consulting fees and shares a patent with Nexstim Oyj. PL  
1816 has received consulting fees from Nexstim Oyj. Hartwig R. Siebner has received honoraria as  
1817 speaker from Sanofi Genzyme, Denmark, Lundbeck AS, Denmark, and Novartis, Denmark, as  
1818 consultant from Sanofi Genzyme, Denmark, Lophora, Denmark, and Lundbeck AS, Denmark,  
1819 and as editor-in-chief (Neuroimage Clinical) and senior editor (NeuroImage) from Elsevier  
1820 Publishers, Amsterdam, The Netherlands. He has received royalties as book editor from Springer  
1821 Publishers, Stuttgart, Germany and from Gyldendal Publishers, Copenhagen, Denmark. TPM has  
1822 successfully applied for funding for a collaborative research project (project not started at the  
1823 time of the submission) with Bittium Biosignals Oy (Kuopio, Finland).

1824  
1825 **Acknowledgments:** JCHP and RJI want to dedicate this work to the memory of Prof. Jukka  
1826 Sarvas one of the most beautiful minds and humble hearts that have existed in this world.  
1827 Hartwig R. Siebner holds a 5-year professorship in precision medicine at the Faculty of Health  
1828 Sciences and Medicine, University of Copenhagen which is sponsored by the Lundbeck  
1829 Foundation (Grant Nr. R186-2015-2138). TPM has been supported by the Academy of Finland  
1830 (Grant No. 321631).

1831  
1832 **CRedit author contribution statement**

1833 **Julio C. Hernandez-Pavon:** Conceptualization; Data curation; Formal analysis; Investigation;  
1834 Methodology; Project administration; Resources; Supervision; Validation; Visualization;  
1835 Roles/Writing - original draft; Writing - review & editing; **Domenica Veniero:**  
1836 Conceptualization; Data curation; Formal analysis; Investigation; Methodology; Project  
1837 administration; Resources; Supervision; Validation; Visualization; Roles/Writing - original draft;  
1838 Writing - review & editing; **Til Ole Bergmann, Paolo Belardinelli, Marta Bortoletto, Silvia**  
1839 **Casarotto, Elias Casula, Faranak Farzan, Matteo Fecchio, Petro Julkunen, Elisa**  
1840 **Kallioniemi, Pantelis Lioumis, Johanna Metsomaa, Carlo Miniussi, Tuomas P. Mutanen,**  
1841 **Lorenzo Rocchi, Nigel C. Rogasch, Mouhsin M. Shafi, Hartwig R. Siebner, Gregor Thut,**  
1842 **Christoph Zrenner, Ulf Ziemann:** Investigation; Methodology; Writing - review & editing;  
1843 **Risto J. Imoniemi:** Funding acquisition; Investigation; Methodology; Writing - review &  
1844 editing.

1845 **References**

- 1846 [1] Barker A, Jalinous R, Freeston I. Non-invasive magnetic stimulation of human motor cortex.  
1847 *Lancet* 1985;1(8437):1106-7.
- 1848 [2] Cracco R, Amassian V, Maccabee P, Cracco J. Comparison of human transcallosal responses  
1849 evoked by magnetic coil and electrical stimulation. *Electroencephalogr Clin Neurophysiol* 1989;74:417–  
1850 24.
- 1851 [3] Amassian V, Cracco R, Maccabee P, Cracco J. Cerebello-frontal cortical projections in humans  
1852 studied with the magnetic coil. *Electroenceph Clin Neurophysiol* 1992;85(4):265-72.
- 1853 [4] Ilmoniemi R, Virtanen J, Ruohonen J, Karhu J, Aronen H, Näätänen R, et al. Neuronal responses  
1854 to magnetic stimulation reveal cortical reactivity and connectivity. *Neuroreport* 1997;8:3537-40.
- 1855 [5] Tremblay S, Rogasch N, Premoli I, Blumberger D, Casarotto S, Chen R, et al. Clinical utility and  
1856 prospective of TMS–EEG. *Clin Neurophysiol* 2019;130(5):802-44.
- 1857 [6] Ridding M, Rothwell J. Is there a future for therapeutic use of transcranial magnetic stimulation?  
1858 *Nat Rev Neurosci* 2007;8(7):559-67.
- 1859 [7] Ilmoniemi R, Ruohonen J, Virtanen J, Aronen H, Karhu J. EEG responses evoked by transcranial  
1860 magnetic stimulation. *Electroencephalogr Clin Neurophysiol Suppl* 1999;51:22-9.
- 1861 [8] Siebner HR, Funke K, Aberra AS, Antal A, Bestmann S, Chen R, et al. Transcranial magnetic  
1862 stimulation of the brain: What is stimulated? - A consensus and critical position paper. *Clin Neurophysiol*  
1863 2022;140:59-97.
- 1864 [9] Maccabee P, Amassian V, Eberle L, Cracco R. Magnetic coil stimulation of straight and bent  
1865 amphibian and mammalian peripheral nerve in vitro: locus of excitation. *J Physiol* 1993;460:201-19.
- 1866 [10] Ruohonen J. Chapter 1 Background physics for magnetic stimulation. *Supplements to Clinical*  
1867 *Neurophysiology Transcranial Magnetic Stimulation and Transcranial Direct Current Stimulation,*  
1868 *Proceedings of the 2nd International Transcranial Magnetic Stimulation (TMS) and Transcranial Direct*  
1869 *Current Stimulation (tDCS) Symposium 2003;56:3-12.*
- 1870 [11] Deng Z, Lisanby S, Peterchev A. Electric field depth-focality tradeoff in transcranial magnetic  
1871 stimulation: Simulation comparison of 50 coil designs. *Brain Stimul* 2013;6(1):1-13.
- 1872 [12] Ilmoniemi R, Ruohonen J, Karhu J. Transcranial magnetic stimulation--a new tool for functional  
1873 imaging of the brain. *Crit Rev Biomed Eng* 1999;27(3-5):241-84.
- 1874 [13] Romero M, Davare M, Armendariz M, Janssen P. Neural effects of transcranial magnetic  
1875 stimulation at the single-cell level. *Nat Commun* 2019;10(2642):1-11.
- 1876 [14] Di Lazzaro V, Ziemann U. The contribution of transcranial magnetic stimulation in the functional  
1877 evaluation of microcircuits in human motor cortex. *Front Neural Circuits* 2013;7:18.
- 1878 [15] Bergmann TO, Hartwigsen G. Inferring Causality from Noninvasive Brain Stimulation in Cognitive  
1879 Neuroscience. *J Cogn Neurosci* 2021;33(2):195-225.
- 1880 [16] Baillet S, Mosher J, Leahy R. Electromagnetic brain mapping. *IEEE Signal Processing Magazine*  
1881 2001;18(6):14-30.
- 1882 [17] Bergmann T, Karabanov A, Hartwigsen G, Thielscher A, Siebner H. Combining non-invasive  
1883 transcranial brain stimulation with neuroimaging and electrophysiology: Current approaches and future  
1884 perspectives.
- 1885 . *Neuroimage* 2016;140:4-19.
- 1886 [18] Hallett M, Di Iorio R, Rossini P, Park J, Chen R, Celnik P, et al. Contribution of transcranial  
1887 magnetic stimulation to assessment of brain connectivity and networks. *Clin Neurophysiol*  
1888 2017;128(11):2125-39.
- 1889 [19] Siebner H, Bergmann T, Bestmann S, Massimini M, Johansen-Berg H, Mochizuki H, et al.  
1890 Consensus paper: combining transcranial stimulation with neuroimaging. *Brain Stimul* 2009;2(2):58-80.

- 1891 [20] Berger H. Uber das Elektroenkephalogramm des Menschen (On the electroencephalogram of  
1892 man). *Arch Psychiatr Nervenkr* 1929;87:527-70.
- 1893 [21] Cohen M. Where Does EEG Come From and What Does It Mean? *Trends Neurosci*  
1894 2017;40(4):208-18.
- 1895 [22] Schomer D, da Silva F. *Niedermeyer's Electroencephalography: Basic Principles, Clinical*  
1896 *Applications, and Related Fields*. 2018.
- 1897 [23] Ilmoniemi R, Sarvas J. *Brain Signals Physics and Mathematics of MEG and EEG*. The MIT Press  
1898 2019.
- 1899 [24] Okada Y, Wu J, Kyuhou S. Genesis of MEG signals in a mammalian CNS structure.  
1900 *Electroencephalogr Clin Neurophysiol* 1997;103:474-85.
- 1901 [25] de Munck J, Vijn P, Lopez da Silva F. A random dipole model for spontaneous brain activity. *IEEE*  
1902 *Trans Biomed Eng* 1992;39(8):791-804.
- 1903 [26] Ilmoniemi R. *Neuromagnetism : theory, techniques, and measurements* Department of  
1904 *Technical Physics, Helsinki University of Technology, Espoo, Finland; 1985*.
- 1905 [27] Miniussi C, Thut G. Combining TMS and EEG offers new prospects in cognitive neuroscience.  
1906 *Brain Topogr* 2010;22(4):249-56.
- 1907 [28] Ilmoniemi R, Kicić D. Methodology for combined TMS and EEG. *Brain Topogr* 2010;22(4):233-48.
- 1908 [29] Bortoletto M, Bonzano L, Zazio A, Ferrari C, Pedullà L, Gasparotti R, et al. Asymmetric  
1909 transcallosal conduction delay leads to finer bimanual coordination. *Brain Stimul* 2021;14(2):379-88.
- 1910 [30] Kallioniemi E, Saari J, Ferreri F, Määttä S. TMS-EEG responses across the lifespan: Measurement,  
1911 methods for characterisation and identified responses. *J Neurosci Methods* 2022;366(109430):1-19.
- 1912 [31] Luck S. *An Introduction to the Event-Related Potential Technique, Second Edition*. Second  
1913 Edition ed.; 2014.
- 1914 [32] Lioumis P, Kičić D, Savolainen P, Mäkelä J, Kähkönen S. Reproducibility of TMS-Evoked EEG  
1915 responses. *Hum Brain Mapp* 2009;30(4):1387-96.
- 1916 [33] Kerwin L, Keller C, Wu W, Narayan M, Etkin A. Test-retest reliability of transcranial magnetic  
1917 stimulation EEG evoked potentials. *Brain Stimul* 2018;11(3):536-44.
- 1918 [34] Casarotto S, Fecchio M, Rosanova M, Varone G, D'Ambrosio S, Sarasso S, et al. The rt-TPEP tool:  
1919 real-time visualization of TMS-Evoked Potential to maximize cortical activation and minimize artifacts. *J*  
1920 *Neurosci Methods* 2022:109486.
- 1921 [35] Komssi S, Kähkönen S, Ilmoniemi R. The effect of stimulus intensity on brain responses evoked  
1922 by transcranial magnetic stimulation. *Hum Brain Mapp* 2004;21:154-64.
- 1923 [36] Rogasch N, Thomson R, Farzan F, Fitzgibbon B, Bailey N, Hernandez-Pavon J, et al. Removing  
1924 artifacts from TMS-EEG recordings using independent component analysis: importance for assessing  
1925 prefrontal cortex network properties. *NeuroImage* 2014;101:425-39.
- 1926 [37] Bonato C, Miniussi C, Rossini P. Transcranial magnetic stimulation and cortical evoked  
1927 potentials: a TMS/EEG co-registration study. *Clin Neurophysiol* 2006;117(8):1699-707.
- 1928 [38] Rocchi L, Di Santo A, Brown K, Ibáñez J, Casula E, Rawji V, et al. Disentangling EEG responses to  
1929 TMS due to cortical and peripheral activations. *Brain Stimul* 2021;14(1):4-18.
- 1930 [39] Belardinelli P, König F, Liang C, Premoli I, Desideri D, Müller-Dahlhaus F, et al. TMS-EEG  
1931 signatures of glutamatergic neurotransmission in human cortex. *Sci Rep* 2021;11(1):1-14.
- 1932 [40] Nikulin V, Kičić D, Kähkönen S, Ilmoniemi R. Modulation of electroencephalographic responses  
1933 to transcranial magnetic stimulation: evidence for changes in cortical excitability related to movement.  
1934 *Eur J Neurosci* 2003;18(5):1206-12.
- 1935 [41] Massimini M, Ferrarelli F, Huber R, Esser S, Singh H, Tononi G. Breakdown of cortical effective  
1936 connectivity during sleep. *Science* 2005;309(5744):2228-32.

- 1937 [42] Sarasso S, Boly M, Napolitani M, Gosseries O, Charland-Verville V, Casarotto S, et al.  
 1938 Consciousness and Complexity during Unresponsiveness Induced by Propofol, Xenon, and Ketamine.  
 1939 *Curr Biol* 2015;25(23):3099-105.
- 1940 [43] Shafi M, Vernet M, Klooster D, Chu C, Boric K, Barnard M, et al. Physiological consequences of  
 1941 abnormal connectivity in a developmental epilepsy. *Ann Neurol* 2015;77(3):487-503.
- 1942 [44] Fox P, Narayana S, Tandon N, Fox S, Sandoval H, Kochunov P, et al. Intensity modulation of TMS-  
 1943 induced cortical excitation: Primary motor cortex. *Hum Brain Mapp* 2006;27:478-87.
- 1944 [45] Saari J, Kallioniemi E, Tarvainen M, Julkunen P. Oscillatory TMS-EEG-Responses as a Measure of  
 1945 the Cortical Excitability Threshold. *IEEE Trans Neural Syst Rehabil Eng* 2018;26(2):383-91.
- 1946 [46] Rosanova M, Casali A, Bellina V, Resta F, Mariotti M, Massimini M. Natural frequencies of human  
 1947 corticothalamic circuits. *J Neurosci* 2009;29(24):7679-85.
- 1948 [47] Thut G, Miniussi C, Gross J. The functional importance of rhythmic activity in the brain. *Curr Biol*  
 1949 2012;22(16):R658-R63.
- 1950 [48] Vallesi A, Del Felice A, Capizzi M, Tafuro A, Formaggio E, Bisiacchi P, et al. Natural oscillation  
 1951 frequencies in the two lateral prefrontal cortices induced by Transcranial Magnetic Stimulation.  
 1952 *Neuroimage* 2021;227:117655.
- 1953 [49] Herring JD, Thut G, Jensen O, Bergmann TO. Attention Modulates TMS-Locked Alpha Oscillations  
 1954 in the Visual Cortex. *J Neurosci* 2015;35(43):14435-47.
- 1955 [50] Veniero D, Gross J, Morand S, Duecker F, Sack AT, Thut G. Top-down control of visual cortex by  
 1956 the frontal eye fields through oscillatory realignment. *Nat Commun* 2021;12(1):1757.
- 1957 [51] David O, Kiebel S, Harrison L, Mattout J, Kilner J, KJ F. Dynamic causal modeling of evoked  
 1958 responses in EEG and MEG. *Neuroimage* 2006;[Epub ahead of print].
- 1959 [52] Premoli I, Bergmann T, Fecchio M, Rosanova M, Biondi A, Belardinelli P, et al. The impact of  
 1960 GABAergic drugs on TMS-induced brain oscillations in human motor cortex. *Neuroimage* 2017;163:1-12.
- 1961 [53] Thut G, Bergmann TO, Frohlich F, Soekadar SR, Brittain JS, Valero-Cabre A, et al. Guiding  
 1962 transcranial brain stimulation by EEG/MEG to interact with ongoing brain activity and associated  
 1963 functions: A position paper. *Clin Neurophysiol* 2017;128(5):843-57.
- 1964 [54] Pellicciari MC, Veniero D, Miniussi C. Characterizing the Cortical Oscillatory Response to TMS  
 1965 Pulse. *Front Cell Neurosci* 2017;11:38.
- 1966 [55] Casarotto S, Romero Lauro L, Bellina V, Casali A, Rosanova M, Pigorini A, et al. EEG responses to  
 1967 TMS are sensitive to changes in the perturbation parameters and repeatable over time. *PLoS One*  
 1968 2010;5(4):e10281.
- 1969 [56] Gosseries O, Sarasso S, Casarotto S, Boly M, Schnakers C, Napolitani M, et al. On the cerebral  
 1970 origin of EEG responses to TMS: insights from severe cortical lesions. *Brain Stimul* 2015;8(1):142-9.
- 1971 [57] Rossi S, Antal A, Bestmann S, Bikson M, Brewer C, Brockmüller J, et al. Safety and  
 1972 recommendations for TMS use in healthy subjects and patient populations, with updates on training,  
 1973 ethical and regulatory issues: Expert Guidelines. *Clin Neurophysiol* 2021;132(1):269-306.
- 1974 [58] Deng Z, Lisanby S, Peterchev A. Coil design considerations for deep transcranial magnetic  
 1975 stimulation. *Clin Neurophysiol* 2014;125(6):1202-12.
- 1976 [59] Ueno S, Tashiro T, Harada K. Localized stimulation of neural tissue in the brain by means of a  
 1977 paired configuration of time-varying magnetic fields. *J App Phys* 1988;64:5862-4.
- 1978 [60] Fernandez L, Biabani M, Do M, Opie G, Hill A, Barham M, et al. Assessing cerebellar-cortical  
 1979 connectivity using concurrent TMS-EEG: a feasibility study. *J Neurophysiol* 2021;125(5):1768-87.
- 1980 [61] Koponen L, Nieminen J, Ilmoniemi R. Multi-locus transcranial magnetic stimulation-theory and  
 1981 implementation. *Brain Stimul* 2018;11(4):849-55.
- 1982 [62] Nieminen JO, Sinisalo H, Souza VH, Malmi M, Yuryev M, Tervo AE, et al. Multi-locus transcranial  
 1983 magnetic stimulation system for electronically targeted brain stimulation. *Brain Stimul* 2022;15(1):116-  
 1984 24.

- 1985 [63] Souza VH, Nieminen JO, Tugin S, Koponen LM, Baffa O, Ilmoniemi RJ. TMS with fast and accurate  
 1986 electronic control: Measuring the orientation sensitivity of corticomotor pathways. *Brain Stimul*  
 1987 2022;15(2):306-15.
- 1988 [64] Tervo AE, Nieminen JO, Lioumis P, Metsomaa J, Souza VH, Sinisalo H, et al. Closed-loop  
 1989 optimization of transcranial magnetic stimulation with electroencephalography feedback. *Brain Stimul*  
 1990 2022;15(2):523-31.
- 1991 [65] Sommer M, Alfaro A, Rummel M, Speck S, Lang N, Tings T, et al. Half sine, monophasic and  
 1992 biphasic transcranial magnetic stimulation of the human motor cortex. *Clin Neurophysiol*  
 1993 2006;117(4):838-44.
- 1994 [66] Jung N, Delvendahl I, Pechmann A, Gleich B, Gattinger N, Siebner H, et al. Transcranial magnetic  
 1995 stimulation with a half-sine wave pulse elicits direction-specific effects in human motor cortex. *BMC*  
 1996 *Neurosci* 2012;13(139):1-9.
- 1997 [67] Delvendahl I, Gattinger N, Berger T, Gleich B, Siebner H, Mall V. The role of pulse shape in motor  
 1998 cortex transcranial magnetic stimulation using full-sine stimuli. *PLoS One* 2014;9(12):e115247.
- 1999 [68] Delvendahl I, Lindemann H, Jung N, Pechmann A, Siebner H, Mall V. Influence of waveform and  
 2000 current direction on short-interval intracortical facilitation: a paired-pulse TMS study. *Brain Stimul*  
 2001 2014;7(1):49-58.
- 2002 [69] Groppa S, Oliviero A, Eisen A, Quartarone A, Cohen L, Mall V, et al. A practical guide to  
 2003 diagnostic transcranial magnetic stimulation: report of an IFCN committee. *Clin Neurophysiol*  
 2004 2012;23(5):858-582.
- 2005 [70] Funke K. Transcranial Magnetic Stimulation of Rodents: Repetitive Transcranial Magnetic  
 2006 Stimulation—A Noninvasive Way to Induce Neural Plasticity In Vivo and In Vitro. In: Manahan-Vaughan  
 2007 D, editor *Handbook of Behavioral Neuroscience*: Elsevier; 2018, p. 365-87.
- 2008 [71] Rossini P, Burke D, Chen R, Cohen L, Z D, Di Iorio R, et al. Non-invasive electrical and magnetic  
 2009 stimulation of the brain, spinal cord, roots and peripheral nerves: Basic principles and procedures for  
 2010 routine clinical and research application. An updated report from an I.F.C.N. Committee. *Clin*  
 2011 *Neurophysiol* 2015;26(6):1071-107.
- 2012 [72] Kammer T, Beck S, Thielscher A, Laubis-Herrmann U, Topka H. Motor thresholds in humans: a  
 2013 transcranial magnetic stimulation study comparing different pulse waveforms, current directions and  
 2014 stimulator types. *Clin Neurophysiol* 2001;112(2):250-8.
- 2015 [73] Mills K, Boniface S, Schubert M. Magnetic brain stimulation with a double coil: the importance  
 2016 of coil orientation. *Electroencephalogr Clin Neurophysiol* 1992;85:17-21.
- 2017 [74] Corthout E, Barker A, Cowey A. Transcranial magnetic stimulation: Which part of the current  
 2018 waveform causes the stimulation? . *Exp Brain Res* 2001;141(1):128-32.
- 2019 [75] Mutanen T, Mäki H, Ilmoniemi R. The effect of stimulus parameters on TMS-EEG muscle  
 2020 artifacts. *Brain Stimul* 2013;6(3):371-6.
- 2021 [76] Rogasch N, Thomson R, Daskalakis Z, Fitzgerald P. Short-latency artifacts associated with  
 2022 concurrent TMS-EEG. *Brain Stimul* 2013;[Epub ahead of print].
- 2023 [77] Veniero D, Bortoletto M, Miniussi C. TMS-EEG co-registration: on TMS-induced artifact. *Clin*  
 2024 *Neurophysiol* 2009;120(7):1392-9.
- 2025 [78] Casula E, Rocchi L, Hannah R, Rothwell J. Effects of pulse width, waveform and current direction  
 2026 in the cortex: A combined cTMS-EEG study. *Brain Stimul* 2018;11(5):1063-70.
- 2027 [79] Virtanen J, Ruohonen J, Näätänen R, Ilmoniemi R. Instrumentation for the measurement of  
 2028 electric brain responses to transcranial magnetic stimulation. *Med Biol Eng Comput* 1999;37(3):322-6.
- 2029 [80] Iramina I, Maeno T, Nonaka Y, Ueno S. Measurement of evoked electroencephalography  
 2030 induced by transcranial magnetic stimulation. *J Appl Phys* 2003; 93(10):6718 -20.
- 2031 [81] Taylor J, Loo C. Stimulus waveform influences the efficacy of repetitive transcranial magnetic  
 2032 stimulation. *J Affect Disord* 2007;97(1-3):271-6.

- 2033 [82] Freche D, Naim-Feil J, Peled A, Levit-Binnun N, Moses E. A quantitative physical model of the  
 2034 TMS-induced discharge artifacts in EEG. *PLoS Comput Biol* 2018;14(7):1-35.
- 2035 [83] Bae J, MacFall J, Krishnan K, Payne M, Steffens D, Taylor W. Dorsolateral prefrontal cortex and  
 2036 anterior cingulate cortex white matter alterations in late-life depression. *Biol Psychiatry*  
 2037 2006;60(12):1356-63.
- 2038 [84] Tanner D, Norton JJ, Morgan-Short K, Luck SJ. On high-pass filter artifacts (they're real) and  
 2039 baseline correction (it's a good idea) in ERP/ERMF analysis. *J Neurosci Methods* 2016;266:166-70.
- 2040 [85] Varone G, Hussain Z, Sheikh Z, Howard A, Boulila W, Mahmud M, et al. Real-Time Artifacts  
 2041 Reduction during TMS-EEG Co-Registration: A Comprehensive Review on Technologies and Procedures.  
 2042 *Sensors (Basel)* 2021;21(637):1-23.
- 2043 [86] Mancuso M, Sveva V, Cruciani A, Brown K, Ibáñez J, Rawji V, et al. Transcranial Evoked Potentials  
 2044 Can Be Reliably Recorded with Active Electrodes. *Brain Sci* 2021;11(145):1-16.
- 2045 [87] Ozdemir R, Tadayon E, Boucher P, Momi D, Karakhanyan K, Fox M, et al. Individualized  
 2046 perturbation of the human connectome reveals reproducible biomarkers of network dynamics relevant  
 2047 to cognition. *Proc Natl Acad Sci U S A* 2020;117(14):8115-25.
- 2048 [88] Rawji V, Kaczmarczyk I, Rocchi L, Fong PY, Rothwell JC, Sharma N. Preconditioning Stimulus  
 2049 Intensity Alters Paired-Pulse TMS Evoked Potentials. *Brain Sci* 2021;11(3).
- 2050 [89] Julkunen P, Säisänen L, Sarasti M, Könönen M. Effect of electrode cap on measured cortical  
 2051 motor threshold. *J Neurosci Methods* 2009;176(2):225-9.
- 2052 [90] Jasper H. The ten-twenty electrode system of the international federation. *Electroenceph Clin*  
 2053 *Neurophysiol* 1958;10:371-5.
- 2054 [91] Iivanainen J, Makinen AJ, Zetter R, Stenroos M, Ilmoniemi RJ, Parkkonen L. Spatial sampling of  
 2055 MEG and EEG based on generalized spatial-frequency analysis and optimal design. *Neuroimage*  
 2056 2021;245:118747.
- 2057 [92] Ryyanen OR, Hyttinen JA, Laarne PH, Malmivuo JA. Effect of electrode density and  
 2058 measurement noise on the spatial resolution of cortical potential distribution. *IEEE Trans Biomed Eng*  
 2059 2004;51(9):1547-54.
- 2060 [93] Michel CM, Brunet D. EEG Source Imaging: A Practical Review of the Analysis Steps. *Front Neurol*  
 2061 2019;10:325.
- 2062 [94] Sohrabpour A, Lu Y, Kankirawatana P, Blount J, Kim H, He B. Effect of EEG electrode number on  
 2063 epileptic source localization in pediatric patients. *Clin Neurophysiol* 2015;126(3):472-80.
- 2064 [95] Goldenholz DM, Ahlfors SP, Hamalainen MS, Sharon D, Ishitobi M, Vaina LM, et al. Mapping the  
 2065 signal-to-noise-ratios of cortical sources in magnetoencephalography and electroencephalography. *Hum*  
 2066 *Brain Mapp* 2009;30(4):1077-86.
- 2067 [96] Sack A, Kadosh R, Schuhmann T, Moerel M, Walsh V, Goebel R. Optimizing functional accuracy  
 2068 of TMS in cognitive studies: A comparison of methods. *J Cogn Neurosci* 2009;21(2):207-21.
- 2069 [97] Lioumis P, Rosanova M. The role of neuronavigation in TMS-EEG studies: Current applications  
 2070 and future perspectives. *J Neurosci Methods* 2022;380:109677.
- 2071 [98] Ruohonen J, Karhu J. Navigated transcranial magnetic stimulation. *Neurophysiol Clin*  
 2072 2010;40(1):7-17.
- 2073 [99] Hannula H, Ilmoniemi R. Basic Principles of Navigated TMS. In: Krieg S, editor *Navigated*  
 2074 *Transcranial Magnetic Stimulation in Neurosurgery*; Springer; 2017.
- 2075 [100] Bashir S, Edwards D, Pascual-Leone A. Neuronavigation increases the physiologic and behavioral  
 2076 effects of low-frequency rTMS of primary motor cortex in healthy subjects. *Brain Topogr* 2011;24(1):54-  
 2077 64.
- 2078 [101] Cincotta M, Giovannelli F, Borgheresi A, Balestrieri F, Toscani L, Zaccara G, et al. Optically  
 2079 tracked neuronavigation increases the stability of hand-held focal coil positioning: evidence from



- 2080 "transcranial" magnetic stimulation-induced electrical field measurements. *Brain Stimul* 2010;3(2):119-  
2081 23.
- 2082 [102] Julkunen P, Säisänen L, Danner N, Niskanen E, Hukkanen T, Mervaala E, et al. Comparison of  
2083 navigated and non-navigated transcranial magnetic stimulation for motor cortex mapping, motor  
2084 threshold and motor evoked potentials. *Neuroimage* 2009;44(3):790-5.
- 2085 [103] Thielscher A, Opitz A, Windhoff M. Impact of the gyral geometry on the electric field induced by  
2086 transcranial magnetic stimulation. *Neuroimage* 2011;54(1):234-43.
- 2087 [104] Thut G, Veniero D, Romei V, Miniussi C, Schyns P, Gross J. Rhythmic TMS causes local  
2088 entrainment of natural oscillatory signatures. *Curr Biol* 2011;21(14):1176-85.
- 2089 [105] Sarvas J. Basic mathematical and electromagnetic concepts of the biomagnetic inverse problem.  
2090 *Phys Med Biol* 1987;32(1):11-22.
- 2091 [106] Nummenmaa A, Stenroos M, Ilmoniemi R, Okada Y, Hämäläinen M, Raji T. Comparison of  
2092 spherical and anatomically realistic boundary element head models for transcranial magnetic  
2093 stimulation navigation. *Clin Neurophysiol* 2013;124(10):1995-2007.
- 2094 [107] Thielscher A, Antunes A, Saturnino G. Field modeling for transcranial magnetic stimulation: A  
2095 useful tool to understand the physiological effects of TMS? *Annu Int Conf IEEE Eng Med Biol Soc*  
2096 2015:222-5.
- 2097 [108] de Goede A, Ter Braack E, van Putten M. Accurate Coil Positioning is Important for Single and  
2098 Paired Pulse TMS on the Subject Level. *Brain Topogr* 2018;31(6):917-30.
- 2099 [109] Harquel S, Bacle T, Beynel L, Marendaz C, Chauvin A, David O. Mapping dynamical properties of  
2100 cortical microcircuits using robotized TMS and EEG: Towards functional cytoarchitectonics. *Neuroimage*  
2101 2016;135:115-24.
- 2102 [110] Goldenholz D, Ahlfors S, Hämäläinen M, Sharon D, Ishitobi M, Vaina L, et al. Mapping the signal-  
2103 to-noise-ratios of cortical sources in magnetoencephalography and electroencephalography. *Hum Brain*  
2104 *Mapp* 2009;30(4):1077-86.
- 2105 [111] Hui J, Zomorodi R, Lioumis P, Salavati B, Rajji TK, Chen R, et al. Pharmacological mechanisms of  
2106 interhemispheric signal propagation: a TMS-EEG study. *Neuropsychopharmacology* 2020;45(6):932-9.
- 2107 [112] Bertazzoli G, Esposito R, Mutanen T, Ferrari C, Ilmoniemi R, Miniussi C, et al. The impact of  
2108 artifact removal approaches on TMS-EEG signal. *Neuroimage* 2021;239(118272):1-15.
- 2109 [113] Rosanova M, Casarotto S, Pigorini A, Canali P, Casali AG, Massimini M. Combining transcranial  
2110 magnetic stimulation with electroencephalography to study human cortical excitability and effective  
2111 connectivity. 2012.
- 2112 [114] Komssi S, Huttunen J, Aronen H, Ilmoniemi R. EEG minimum-norm estimation compared with  
2113 MEG dipole fitting in the localization of somatosensory sources at S1. *Clin Neurophysiol*  
2114 2004;115(3):534-42.
- 2115 [115] VanRullen R. How to Evaluate Phase Differences between Trial Groups in Ongoing  
2116 Electrophysiological Signals. *Front Neurosci* 2016;10(426):1-22.
- 2117 [116] Schaworonkow N, Caldana Gordon P, Belardinelli P, Ziemann U, Bergmann T, Zrenner C.  $\mu$ -  
2118 Rhythm Extracted With Personalized EEG Filters Correlates With Corticospinal Excitability in Real-Time  
2119 Phase-Triggered EEG-TMS. *Front Neurosci* 2018;12(954):1-6.
- 2120 [117] Rossini P, Barker A, Berardelli A, Caramia M, Caruso G, Cracco R, et al. Non-invasive electrical  
2121 and magnetic stimulation of the brain, spinal cord and roots: basic principles and procedures for routine  
2122 clinical application. Report of an IFCN committee. *Electroencephalogr Clin Neurophysiol* 1994;91(2):79-  
2123 92.
- 2124 [118] Rothwell J, Hallett M, Berardelli A, Eisen A, Rossini P, Paulus W. Magnetic stimulation: motor  
2125 evoked potentials. *The International Federation of Clinical Neurophysiology. Electroencephalogr Clin*  
2126 *Neurophysiol Suppl* 1999;52:97-103.

- 2127 [119] Reijonen J, Pitkänen M, Kallioniemi E, Mohammadi A, Ilmoniemi R, Julkunen P. Spatial extent of  
 2128 cortical motor hotspot in navigated transcranial magnetic stimulation. *J Neurosci Methods*  
 2129 2020;346(108893):1-9.
- 2130 [120] Julkunen P, Säisänen L, Hukkanen T, Danner N, Könönen M. Does second-scale intertrial interval  
 2131 affect motor evoked potentials induced by single-pulse transcranial magnetic stimulation? *Brain Stimul*  
 2132 2012;5(4):526-32.
- 2133 [121] Pellicciari M, Miniussi C, Ferrari C, Koch G, Bortoletto M. Ongoing cumulative effects of single  
 2134 TMS pulses on corticospinal excitability: An intra- and inter-block investigation. *Clin Neurophysiol*  
 2135 2016;127(1):621-8.
- 2136 [122] Hassanzahraee M, Zoghi M, Jaberzadeh S. Longer Transcranial Magnetic Stimulation Intertrial  
 2137 Interval Increases Size, Reduces Variability, and Improves the Reliability of Motor Evoked Potentials.  
 2138 *Brain Connect* 2019;9( 10):770-6.
- 2139 [123] Pitkänen M, Kallioniemi E, Julkunen P. Effect of inter-train interval on the induction of repetition  
 2140 suppression of motor-evoked potentials using transcranial magnetic stimulation. *PLoS One* 2017;12(7):1-  
 2141 10.
- 2142 [124] Tran D, McNair N, Harris J, Livesey E. Expected TMS excites the motor system less effectively  
 2143 than unexpected stimulation. *Neuroimage* 2021;226(117541):1-10.
- 2144 [125] Awiszus F. Fast estimation of transcranial magnetic stimulation motor threshold: is it safe? *Brain*  
 2145 *Stimul* 2011;4(1):58-9.
- 2146 [126] Capozio A, Chakrabarty S, Astill S. The Effect of Sound and Stimulus Expectation on Transcranial  
 2147 Magnetic Stimulation-Elicited Motor Evoked Potentials. *Brain Topogr* 2021;34(6):720-30.
- 2148 [127] Brown KE, Lohse KR, Mayer IMS, Strigaro G, Desikan M, Casula EP, et al. The reliability of  
 2149 commonly used electrophysiology measures. *Brain Stimul* 2017;10(6):1102-11.
- 2150 [128] Stewart L, Walsh V, Rothwell J. Motor and phosphene thresholds: a transcranial magnetic  
 2151 stimulation correlation study. *Neuropsychologia* 2001;39(4):415-9.
- 2152 [129] Deblieck C, Thompson B, Iacoboni M, Wu AD. Correlation between motor and phosphene  
 2153 thresholds: a transcranial magnetic stimulation study. *Hum Brain Mapp* 2008;29(6):662-70.
- 2154 [130] Stokes M, Chambers C, Gould I, Henderson T, Janko N, Allen N, et al. Simple metric for scaling  
 2155 motor threshold based on scalp-cortex distance: application to studies using transcranial magnetic  
 2156 stimulation. *J Neurophysiol* 2005;94(6):4520-7
- 2157
- 2158
- 2159 [131] Westin G, Bassi B, Lisanby S, Luber B. Determination of motor threshold using visual observation  
 2160 overestimates transcranial magnetic stimulation dosage: safety implications. *Clin Neurophysiol*  
 2161 2014;125(1):142-7.
- 2162 [132] Kammer T, Puls K, Strasburger H, Hill N, Wichmann F. Transcranial magnetic stimulation in the  
 2163 visual system. I. The psychophysics of visual suppression. *Exp Brain Res* 2005;160(1):118-28.
- 2164 [133] Kammer T, Puls K, Erb M, Grodd W. Transcranial magnetic stimulation in the visual system. II.  
 2165 Characterization of induced phosphenes and scotomas. *Exp Brain Res* 2005;160(1):129-40.
- 2166 [134] Taylor P, Walsh V, Eimer M. The neural signature of phosphene perception. *Hum Brain Mapp*  
 2167 2010;31(9):1408-17.
- 2168 [135] Marg E, Rudiak D. Phosphenes induced by magnetic stimulation over the occipital brain:  
 2169 description and probable site of stimulation. *Optom Vis Sci* 1994;71(5):301-11.
- 2170 [136] Antal A, Nitsche M, Kincses T, Lampe C, Paulus W. No correlation between moving phosphene  
 2171 and motor thresholds: a transcranial magnetic stimulation study. *Neuroreport* 2004;15(2):297-302.
- 2172 [137] Romei V, Gross J, Thut G. On the role of prestimulus alpha rhythms over occipito-parietal areas  
 2173 in visual input regulation: correlation or causation? *J Neurosci* 2010;30(25):8692-7.

- 2174 [138] Zazio A, Bortoletto M, Ruzzoli M, Miniussi C, Veniero D. Perceptual and Physiological  
 2175 Consequences of Dark Adaptation: A TMS-EEG Study. *Brain Topogr* 2019;32(5):773-82.
- 2176 [139] Janssen A, Oostendorp T, Stegeman D. The coil orientation dependency of the electric field  
 2177 induced by TMS for M1 and other brain areas. *J Neuroeng Rehabil* 2015;12(47):1-13.
- 2178 [140] Janssen A, Oostendorp T, Stegeman D. The effect of local anatomy on the electric field induced  
 2179 by TMS: evaluation at 14 different target sites. *Med Biol Eng Comput* 2014;52(10):873-83.
- 2180 [141] Julkunen P, Saisanen L, Danner N, Awiszus F, Kononen M. Within-subject effect of coil-to-cortex  
 2181 distance on cortical electric field threshold and motor evoked potentials in transcranial magnetic  
 2182 stimulation. *J Neurosci Methods* 2012;206(2):158-64.
- 2183 [142] Casali A, Casarotto S, Rosanova M, Mariotti M, Massimini M. General indices to characterize the  
 2184 electrical response of the cerebral cortex to TMS. *Neuroimage* 2010;49(2):1459-68.
- 2185 [143] Kähkönen S, Wilenius J, Komssi S, Ilmoniemi R. Distinct differences in cortical reactivity of motor  
 2186 and prefrontal cortices to magnetic stimulation. *Clin Neurophysiol* 2004;115(3):583-8.
- 2187 [144] Komssi S, Savolainen P, Heiskala J, Kähkönen S. Excitation threshold of the motor cortex  
 2188 estimated with transcranial magnetic stimulation electroencephalography. *Neuroreport* 2007;18(1):13-  
 2189 6.
- 2190 [145] Raffin E, Harquel S, Passera B, Chauvin A, Bougerol T, David O. Probing regional cortical  
 2191 excitability via input-output properties using transcranial magnetic stimulation and  
 2192 electroencephalography coupling. *Hum Brain Mapp* 2020;41(10):2741-61.
- 2193 [146] Schaworonkow N, Triesch J, Ziemann U, Zrenner C. EEG-triggered TMS reveals stronger brain  
 2194 state-dependent modulation of motor evoked potentials at weaker stimulation intensities. *Brain Stimul*  
 2195 2019;12(1):110-8.
- 2196 [147] Zmeykina E, Mittner M, Paulus W, Turi Z. Weak rTMS-induced electric fields produce neural  
 2197 entrainment in humans. *Sci Rep* 2020;10((1):11994):1-16.
- 2198 [148] Kähkönen S, Komssi S, Wilenius J, Ilmoniemi R. Prefrontal transcranial magnetic stimulation  
 2199 produces intensity-dependent EEG responses in humans. *Neuroimage* 2005;24(4):955-60.
- 2200 [149] Muggleton NG, Juan CH, Cowey A, Walsh V. Human frontal eye fields and visual search. *J*  
 2201 *Neurophysiol* 2003;89(6):3340-3.
- 2202 [150] O'Shea J, Muggleton NG, Cowey A, Walsh V. Timing of target discrimination in human frontal  
 2203 eye fields. *J Cogn Neurosci* 2004;16(6):1060-7.
- 2204 [151] Juan CH, Muggleton NG, Tzeng OJ, Hung DL, Cowey A, Walsh V. Segregation of visual selection  
 2205 and saccades in human frontal eye fields. *Cereb Cortex* 2008;18(10):2410-5.
- 2206 [152] Silvanto J, Lavie N, Walsh V. Stimulation of the human frontal eye fields modulates sensitivity of  
 2207 extrastriate visual cortex. *J Neurophysiol* 2006;96(2):941-5.
- 2208 [153] Voineskos A, Farzan F, Barr M, Lobaugh N, Mulsant B, Chen R, et al. The role of the corpus  
 2209 callosum in transcranial magnetic stimulation induced interhemispheric signal propagation. *Biol*  
 2210 *Psychiatry* 2010;68(9):825-31.
- 2211 [154] Kallioniemi E, Könönen M, Julkunen P. Repeatability of functional anisotropy in navigated  
 2212 transcranial magnetic stimulation--coil-orientation versus response. *Neuroreport* 2015;26(9):515-21.
- 2213 [155] Belardinelli P, Biabani M, Blumberger D, Bortoletto M, Casarotto S, David O, et al.  
 2214 Reproducibility in TMS-EEG studies: A call for data sharing, standard procedures and effective  
 2215 experimental control. *Brain Stimul* 2019;12(3):787-90.
- 2216 [156] Conde V, Tomasevic L, Akopian I, Stanek K, Saturnino G, Thielscher A, et al. The non-transcranial  
 2217 TMS-evoked potential is an inherent source of ambiguity in TMS-EEG studies. *Neuroimage* 2019;85:300-  
 2218 12.
- 2219 [157] Siebner H, Conde V, Tomasevic L, Thielscher A, Bergmann T. Distilling the essence of TMS-  
 2220 evoked EEG potentials (TEPs): A call for securing mechanistic specificity and experimental rigor. *Brain*  
 2221 *Stimul* 2019;12(4):1051-4.

- 2222 [158] de Graaf T, Sack A. Null results in TMS: from absence of evidence to evidence of absence.  
2223 *Neurosci Biobehav Rev* 2011;35(3):871-7.
- 2224 [159] Russo S, Sarasso S, Puglisi GE, Dal Palu D, Pigorini A, Casarotto S, et al. TAAC - TMS Adaptable  
2225 Auditory Control: A universal tool to mask TMS clicks. *J Neurosci Methods* 2022;370:109491.
- 2226 [160] Pellegrino G, Schuler AL, Arcara G, Di Pino G, Piccione F, Kobayashi E. Resting state network  
2227 connectivity is attenuated by fMRI acoustic noise. *Neuroimage* 2022;247:118791.
- 2228 [161] Sarasso S, D'Ambrosio S, Fecchio M, Casarotto S, Viganò A, Landi C, et al. Local sleep-like cortical  
2229 reactivity in the awake brain after focal injury. *Brain* 2020;143(12):3672-84.
- 2230 [162] ter Braack E, de Vos C, van Putten M. Masking the Auditory Evoked Potential in TMS-EEG: A  
2231 Comparison of Various Methods. *Brain Topogr* 2015;28(3):520-8.
- 2232 [163] Nikouline V, Ruohonen J, Ilmoniemi R. The role of the coil click in TMS assessed with  
2233 simultaneous EEG. *Clin Neurophysiol* 1999;110(8):1325-8.
- 2234 [164] Ohbayashi W, Kakigi R, Nakata H. Effects of white noise on event-related potentials in  
2235 somatosensory Go/No-go paradigms. *Neuroreport* 2017;28(13):788-92.
- 2236 [165] Koponen LM, Goetz SM, Tucci DL, Peterchev AV. Sound comparison of seven TMS coils at  
2237 matched stimulation strength. *Brain Stimul* 2020;13(3):873-80.
- 2238 [166] Ruohonen J, Ollikainen M, Nikouline V, Virtanen J, Ilmoniemi R. Coil design for real and sham  
2239 transcranial magnetic stimulation. *IEEE Trans Biomed Eng* 2000;47(2):145-8.
- 2240 [167] Gordon PC, Jovellar DB, Song Y, Zrenner C, Belardinelli P, Siebner HR, et al. Recording brain  
2241 responses to TMS of primary motor cortex by EEG - utility of an optimized sham procedure. *Neuroimage*  
2242 2021;245:118708.
- 2243 [168] Rossi S, Ferro M, Cincotta M, Ulivelli M, Bartalini S, Miniussi C, et al. A real electro-magnetic  
2244 placebo (REMP) device for sham transcranial magnetic stimulation (TMS). *Clin Neurophysiol*  
2245 2007;118(3):709-16.
- 2246 [169] Amaro E, Jr., Barker GJ. Study design in fMRI: basic principles. *Brain Cogn* 2006;60(3):220-32.
- 2247 [170] Premoli I, Castellanos N, Rivolta D, Belardinelli P, Bajo R, Zipser C, et al. TMS-EEG signatures of  
2248 GABAergic neurotransmission in the human cortex. *J Neurosci* 2014;34(16):5603-12.
- 2249 [171] Veniero D, Ponzio V, Koch G. Paired associative stimulation enforces the communication  
2250 between interconnected areas. *J Neurosci* 2013;33(34):13773-83.
- 2251 [172] Vernet M, Bashir S, Yoo W, Perez J, Najib U, Pascual-Leone A. Insights on the neural basis of  
2252 motor plasticity induced by theta burst stimulation from TMS-EEG. *Eur J Neurosci* 2013;37(4):598-606.
- 2253 [173] Leodori G, Fabbrini A, De Bartolo MI, Costanzo M, Ascì F, Palma V, et al. Cortical mechanisms  
2254 underlying variability in intermittent theta-burst stimulation-induced plasticity: A TMS-EEG study. *Clin*  
2255 *Neurophysiol* 2021;132(10):2519-31.
- 2256 [174] Rocchi L, Ibanez J, Benussi A, Hannah R, Rawji V, Casula E, et al. Variability and Predictors of  
2257 Response to Continuous Theta Burst Stimulation: A TMS-EEG Study. *Front Neurosci* 2018;12:400.
- 2258 [175] Morishima Y, Akaishi R, Yamada Y, Okuda J, Toma K, Sakai K. Task-specific signal transmission  
2259 from prefrontal cortex in visual selective attention. *Nat Neurosci* 2009;12(1):85-91.
- 2260 [176] Meteyard L, Holmes N. TMS SMART - Scalp mapping of annoyance ratings and twitches caused  
2261 by Transcranial Magnetic Stimulation. *J Neurosci Methods* 2018;299:34-44.
- 2262 [177] Bergmann T. Brain State-Dependent Brain Stimulation. *Front Psychol* 2018;9(2108):1-4.
- 2263 [178] Karabanov A, Thielscher A, Siebner HR. Transcranial brain stimulation: closing the loop between  
2264 brain and stimulation. *Curr Opin Neurol* 2016;29(4):397-404.
- 2265 [179] Esposito R, Bortoletto M, Miniussi C. Integrating TMS, EEG, and MRI as an Approach for Studying  
2266 Brain Connectivity. *Neuroscientist* 2020;26(5-6):471-86.
- 2267 [180] Bergmann TO, Lieb A, Zrenner C, Ziemann U. Pulsed Facilitation of Corticospinal Excitability by  
2268 the Sensorimotor mu-Alpha Rhythm. *J Neurosci* 2019;39(50):10034-43.

- 2269 [181] Zrenner C, Desideri D, Belardinelli P, Ziemann U. Real-time EEG-defined excitability states  
2270 determine efficacy of TMS-induced plasticity in human motor cortex. *Brain Stimul* 2018;11(2):374-89.
- 2271 [182] Karabanov AN, Madsen KH, Krohne LG, Siebner HR. Does pericentral mu-rhythm "power"  
2272 corticomotor excitability? - A matter of EEG perspective. *Brain Stimul* 2021;14(3):713-22.
- 2273 [183] Madsen KH, Karabanov AN, Krohne LG, Safeldt MG, Tomasevic L, Siebner HR. No trace of phase:  
2274 Corticomotor excitability is not tuned by phase of pericentral mu-rhythm. *Brain Stimul* 2019;12(5):1261-  
2275 70.
- 2276 [184] Bergmann TO, Born J. Phase-Amplitude Coupling: A General Mechanism for Memory Processing  
2277 and Synaptic Plasticity? *Neuron* 2018;97(1):10-3.
- 2278 [185] Schaworonkow N, Nikulin VV. Is sensor space analysis good enough? Spatial patterns as a tool  
2279 for assessing spatial mixing of EEG/MEG rhythms. *Neuroimage* 2022;253:119093.
- 2280 [186] Ilmoniemi R, Hernandez-Pavon J, Makela N, Metsomaa J, Mutanen T, Stenroos M, et al. Dealing  
2281 with artifacts in TMS-evoked EEG. *Conf Proc IEEE Eng Med Biol Soc* 2015;2015:230-3.
- 2282 [187] Rogasch N, Sullivan C, Thomson R, Rose N, Bailey N, Fitzgerald P, et al. Analysing concurrent  
2283 transcranial magnetic stimulation and electroencephalographic data: A review and introduction to the  
2284 open-source TESA software. *NeuroImage* 2017;147:934-51.
- 2285 [188] Vernet M, Thut G. Electroencephalography During Transcranial Magnetic Stimulation: Current  
2286 Modus Operandi. In: Rotenberg A, Horvath J, Pascual-Leone A, editors. *Transcranial Magnetic  
2287 Stimulation*. Neuromethods, New York, NY: Humana Press; 2014.
- 2288 [189] Litvak V, Komssi S, Scherg M, Hoehstetter K, Classen J, Zaaroor M, et al. Artifact correction and  
2289 source analysis of early electroencephalographic responses evoked by transcranial magnetic stimulation  
2290 over primary motor cortex. *Neuroimage* 2007;37(1):56-70.
- 2291 [190] Julkunen P, Pääkkönen A, Hukkanen T, Könönen M, Tiihonen P, Vanhatalo S, et al. Efficient  
2292 reduction of stimulus artefact in TMS-EEG by epithelial short-circuiting by mini-punctures. *Clin  
2293 Neurophysiol* 2008;119(2):475-81.
- 2294 [191] Picton T, Hillyard S. Cephalic skin potentials in electroencephalography. *Electroencephalogr Clin  
2295 Neurophysiol* 1972;33(4):419-24.
- 2296 [192] Johnson J. Thermal Agitation of Electricity in Conductors. *Nature* 1927(119):50-1.
- 2297 [193] Nyquist H. Thermal Agitation of Electric Charge in Conductors. *Physical Review* 1928(32):110-3.
- 2298 [194] Burbank D, Webster J. Reducing skin potential motion artefact by skin abrasion. *Med Biol Eng  
2299 Comput* 1978;16(1):31-8.
- 2300 [195] Li B, Virtanen J, Oeltermann A, Schwarz C, Giese M, Ziemann U, et al. Lifting the veil on the  
2301 dynamics of neuronal activities evoked by transcranial magnetic stimulation. *Elife* 2017;6(e30552):1-22.
- 2302 [196] de Talhouet H, Webster J. The origin of skin-stretch-caused motion artifacts under electrodes  
2303 *Physiol Meas* 1996;17(2):81-93.
- 2304 [197] Ruddy K, Woolley D, Mantini D, Balsters J, Enz N, Wenderoth N. Improving the quality of  
2305 combined EEG-TMS neural recordings: Introducing the coil spacer. *J Neurosci Methods* 2018;294:34-9.
- 2306 [198] Berg P, Scherg M. Dipole models of eye movements and blinks. *Electroencephalogr Clin  
2307 Neurophysiol* 1991;79(1):36-44.
- 2308 [199] Lins O, Picton T, Berg P, Scherg M. Ocular artifacts in recording EEGs and event-related  
2309 potentials. II: Source dipoles and source components. *Brain Topogr* 1993;6(1):65-78.
- 2310 [200] Korhonen R, Hernandez-Pavon J, Metsomaa J, Mäki H, Ilmoniemi R, Sarvas J. Removal of large  
2311 muscle artifacts from transcranial magnetic stimulation-evoked EEG by independent component  
2312 analysis. *Med Biol Eng Comput* 2011;49(4):397-407.
- 2313 [201] Paus T, Sipila P, Strafella A. Synchronization of neuronal activity in the human primary motor  
2314 cortex by transcranial magnetic stimulation: an EEG study. *J Neurophysiol* 2001;86(4):1983-90.
- 2315 [202] Friedman B, Thayer J. Facial muscle activity and EEG recordings: redundancy analysis.  
2316 *Electroencephalogr Clin Neurophysiol* 1991;79(5):358-60.

- 2317 [203] Hernandez-Pavon J, Metsomaa J, Mutanen T, Stenroos M, Mäki H, Ilmoniemi R, et al.  
2318 Uncovering neural independent components from highly artifactual TMS-evoked EEG data. *J Neurosci*  
2319 *Methods* 2012;209(1):144-57.
- 2320 [204] Tiitinen H, Virtanen J, Ilmoniemi R, Kampouri J, Ollikainen M, Ruohonen J, et al. Separation of  
2321 contamination caused by coil clicks from responses elicited by transcranial magnetic stimulation. *Clin*  
2322 *Neurophysiol* 1999;110(5):982-5.
- 2323 [205] Ross JM, Sarkar M, Keller CJ. Experimental suppression of transcranial magnetic stimulation-  
2324 electroencephalography sensory potentials. *Hum Brain Mapp* 2022.
- 2325 [206] Massimini M, Ferrarelli F, Esser SK, Riedner BA, Huber R, Murphy M, et al. Triggering sleep slow  
2326 waves by transcranial magnetic stimulation. *Proc Natl Acad Sci U S A* 2007;104(20):8496-501.
- 2327 [207] Mizukami H, Kakigi R, Nakata H. Effects of stimulus intensity and auditory white noise on human  
2328 somatosensory cognitive processing: a study using event-related potentials. *Exp Brain Res*  
2329 2019;237(2):521-30.
- 2330 [208] Koponen LM, Goetz SM, Peterchev AV. Double-Containment Coil With Enhanced Winding  
2331 Mounting for Transcranial Magnetic Stimulation With Reduced Acoustic Noise. *IEEE Trans Biomed Eng*  
2332 2021;68(7):2233-40.
- 2333 [209] Gordon P, Desideri D, Belardinelli P, Zrenner C, Ziemann U. Comparison of cortical EEG  
2334 responses to realistic sham versus real TMS of human motor cortex. *Brain Stimul* 2018;11(6):1322-30.
- 2335 [210] Kappenman ES, Luck SJ. The effects of electrode impedance on data quality and statistical  
2336 significance in ERP recordings. *Psychophysiology* 2010;47(5):888-904.
- 2337 [211] de Cheveigné A, Nelken I. Filters: When, Why, and How (Not) to Use Them. *Neuron*  
2338 2019;102(2):280-93.
- 2339 [212] de Cheveigné A, Arzounian D. Robust detrending, rereferencing, outlier detection, and  
2340 inpainting for multichannel data. *Neuroimage* 2018;172:903-12.
- 2341 [213] Hernandez-Pavon JC, Kugiumtzis D, Zrenner C, Kimiskidis VK, Metsomaa J. Removing artifacts  
2342 from TMS-evoked EEG: A methods review and a unifying theoretical framework. *J Neurosci Methods*  
2343 2022;376:109591.
- 2344 [214] Farrens J, Simmons A, Luck S, Kappenman E. Electroencephalogram (EEG) Recording Protocol for  
2345 Cognitive and Affective Human Neuroscience Research. *Research Square*; 2020:1-24.
- 2346 [215] Lioumis P, Zomorodi R, Hadas I, Daskalakis ZJ, Blumberger DM. Combined Transcranial  
2347 Magnetic Stimulation and Electroencephalography of the Dorsolateral Prefrontal Cortex. *J Vis Exp*  
2348 2018(138).
- 2349 [216] Hassan U, Pillen S, Zrenner C, Bergmann T. The Brain Electrophysiological recording &  
2350 STimulation (BEST) toolbox. *Brain Stimul* 2022;15(1):109-15.
- 2351 [217] Sekiguchi H, Takeuchi S, Kadota H, Kohno Y, Nakajima Y. TMS-induced artifacts on EEG can be  
2352 reduced by rearrangement of the electrode's lead wire before recording. *Clin Neurophysiol*  
2353 2011;122(5):984-90.
- 2354 [218] Mutanen T, Kukkonen M, Nieminen J, Stenroos M, Sarvas J, Ilmoniemi R. Recovering TMS-  
2355 evoked EEG responses masked by muscle artifacts. *Neuroimage* 2016;139:157-66.
- 2356 [219] Nunez PL, Srinivasan R. *Electric Fields of the Brain: The neurophysics of EEG*. Oxford University  
2357 Press; 2006.
- 2358 [220] Rogasch N, Biabani M, Mutanen T. Designing and comparing cleaning pipelines for TMS-EEG  
2359 data: a theoretical overview and practical example. *J Neurosci Methods* 2022; Under revision.
- 2360 [221] Mutanen T, Metsomaa J, Liljander S, Ilmoniemi R. Automatic and robust noise suppression in  
2361 EEG and MEG: The SOUND algorithm. *Neuroimage* 2018;166:135-51.
- 2362 [222] Ross JM, Ozdemir RA, Lian SJ, Fried PJ, Schmitt EM, Inouye SK, et al. A structured ICA-based  
2363 process for removing auditory evoked potentials. *Sci Rep* 2022;12(1):1391.

- 2364 [223] Biabani M, Fornito A, Mutanen T, Morrow J, Rogasch N. Characterizing and minimizing the  
2365 contribution of sensory inputs to TMS-evoked potentials. *Brain Stimul* 2019;12(6):1537-52.
- 2366 [224] Nieminen JO, Gosseries O, Massimini M, Saad E, Sheldon AD, Boly M, et al. Consciousness and  
2367 cortical responsiveness: a within-state study during non-rapid eye movement sleep. *Sci Rep*  
2368 2016;6:30932.
- 2369 [225] Onton J, Westerfield M, Townsend J, Makeig S. Imaging human EEG dynamics using independent  
2370 component analysis. *Neurosci Biobehav Rev* 2006;30(6):808-22.
- 2371 [226] Bell A, Sejnowski T. An information-maximization approach to blind separation and blind  
2372 deconvolution. *Neural Comput* 1995;7(6):1129-59.
- 2373 [227] Hyvärinen A, Oja E. Independent component analysis: algorithms and applications. *Neural Netw*  
2374 2000;13(4–5):411-30.
- 2375 [228] Iwahashi M, Arimatsu T, Ueno S, Iramina K. Differences in evoked EEG by transcranial magnetic  
2376 stimulation at various stimulus points on the head. *Conf Proc IEEE Eng Med Biol Soc* 2008;2008:2570-3.
- 2377 [229] Hamidi M, Slagter H, Tononi G, Postle B. Brain responses evoked by high-frequency repetitive  
2378 transcranial magnetic stimulation: an event-related potential study. *Brain Stimul* 2010;3(1):2-14.
- 2379 [230] Jolliffe I. *Principal Component Analysis*, Second Edition. Springer; 2002.
- 2380 [231] ter Braack E, de Jonge B, van Putten M. Reduction of TMS induced artifacts in EEG using  
2381 principal component analysis. *IEEE Trans Neural Syst Rehabil Eng* 2013;21:376-82.
- 2382 [232] Guzmán López J, Hernandez-Pavon J, Lioumis P, Mäkelä J, Silvanto J. State-dependent TMS  
2383 effects in the visual cortex after visual adaptation: A combined TMS–EEG study. *Clin Neurophysiol*  
2384 2021;134:129-36.
- 2385 [233] Uusitalo M, Ilmoniemi R. Signal-space projection method for separating MEG or EEG into  
2386 components. *Med Biol Eng Comput* 1997;35(2):135-40.
- 2387 [234] Mäki H, Ilmoniemi R. Projecting out muscle artifacts from TMS-evoked EEG. *Neuroimage*  
2388 2011;54(4):2706-10.
- 2389 [235] Mutanen T, Biabani M, Sarvas J, Ilmoniemi R, Rogasch N. Source-based artifact-rejection  
2390 techniques available in TESA, an open-source TMS-EEG toolbox. *Brain Stimul* 2020;13(5):1349-51.
- 2391 [236] Saturnino G, Puonti O, Nielsen J, Antonenko D, Madsen K, Thielscher A. SimNIBS 2.1: A  
2392 Comprehensive Pipeline for Individualized Electric Field Modelling for Transcranial Brain Stimulation. In:  
2393 Makarov S, Horner M, Noetscher G, editors. *Brain and Human Body Modeling: Computational Human*  
2394 *Modeling at EMBC 2018*: Cham (CH): Springer; 2019.
- 2395 [237] Stenroos M, Nummenmaa A. Incorporating and Compensating Cerebrospinal Fluid in Surface-  
2396 Based Forward Models of Magneto- and Electroencephalography. *PLoS One* 2016;11(7):1-23.
- 2397 [238] Plonsey R, Heppner D. Considerations of quasi-stationarity in electrophysiological systems. *Bull*  
2398 *Math Biophys* 1967;29(4):657-64.
- 2399 [239] Makkonen M, Mutanen T, Metsomaa J, Zrenner C, Souza V, Ilmoniemi R. Real-time artifact  
2400 detection and removal for closed-loop EEG-TMS. *International Journal of Bioelectromagnetism*  
2401 2021;23(2):1-4.
- 2402 [240] Metsomaa J, Sarvas J, Ilmoniemi R. Multi-trial evoked EEG and independent component analysis.  
2403 *J Neurosci Methods* 2014;228:15-26.
- 2404 [241] Metsomaa J, Sarvas J, Ilmoniemi R. Blind Source Separation of Event-Related EEG/MEG. *IEEE*  
2405 *Trans Biomed Eng* 2017;64(9):2054-64.
- 2406 [242] Oostenveld R, Fries P, Maris E, Schoffelen J. FieldTrip: Open source software for advanced  
2407 analysis of MEG, EEG, and invasive electrophysiological data. *Comput Intell Neurosci* 2011;2011:156869.
- 2408 [243] Atluri S, Frehlich M, Mei Y, Garcia Dominguez L, Rogasch N, Wong W, et al. TMSEEG: A MATLAB-  
2409 Based Graphical User Interface for Processing Electrophysiological Signals during Transcranial Magnetic  
2410 Stimulation. *Front Neural Circuits* 2016;10(78):1-20.

- 2411 [244] Wu W, Keller C, Rogasch N, Longwell P, Shpigel E, Rolle C, et al. ARTIST: A fully automated  
2412 artifact rejection algorithm for single-pulse TMS-EEG data. *Hum Brain Mapp* 2018;39(4):1607-25.
- 2413 [245] Delorme A, Makeig S. EEGLAB: an open source toolbox for analysis of single-trial EEG dynamics  
2414 including independent component analysis. *J Neurosci Methods* 2004;134(1):9-21.
- 2415 [246] Habibollahi Saatlou F, Rogasch N, McNair N, Biabani M, Pillen S, Marshall T, et al. MAGIC: An  
2416 open-source MATLAB toolbox for external control of transcranial magnetic stimulation devices. *Brain*  
2417 *Stimul* 2018;11(5):1189-91.
- 2418

Journal Pre-proof



**Highlights:**

- TMS–EEG is a powerful technique for basic research and clinical applications.
- The methodological combination of TMS–EEG is challenging.
- The lack of standardization may affect reproducibility and limit the comparability of results produced across groups.
- This article covers all aspects that should be considered in TMS–EEG experiments.
- We provide methodological recommendations for effective TMS–EEG recordings and analysis.

**Declaration of interests**

The authors declare that they have no known competing financial interests or personal relationships that could have appeared to influence the work reported in this paper.

The authors declare the following financial interests/personal relationships which may be considered as potential competing interests:

PJ has received consulting fees and shares a patent with Nexstim Oyj. PL has received consulting fees from Nexstim Oyj. Hartwig R. Siebner has received honoraria as speaker from Sanofi Genzyme, Denmark, Lundbeck AS, Denmark, and Novartis, Denmark, as consultant from Sanofi Genzyme, Denmark, Lophora, Denmark, and Lundbeck AS, Denmark, and as editor-in-chief (Neuroimage Clinical) and senior editor (NeuroImage) from Elsevier Publishers, Amsterdam, The Netherlands. He has received royalties as book editor from Springer Publishers, Stuttgart, Germany and from Gyldendal Publishers, Copenhagen, Denmark. TPM has successfully applied for funding for a collaborative research project (project not started at the time of the submission) with Bittium Biosignals Oy (Kuopio, Finland).